Final Report

FHWA/IN/JTRP – 2004/4

Evaluation and Repair of Wrought Iron and Steel Structures in Indiana

by

Mark D. Bowman
Professor of Civil Engineering

and

Amy M. Piskorowski
Graduate Research Assistant

School of Civil Engineering
Purdue University

Joint Transportation Research Program
Project No: C-36-SGJJJ
File No: 7-4-61
SPR-2655

Conducted in Cooperation with the
Indiana Department of Transportation
And the U.S. Department of Transportation
Federal Highway Administration

Purdue University
West Lafayette, Indiana
June 2004

TECHNICAL REPORT STANDARD TITLE PAGE

1. Report No.	2. Government Accession No.	3. Recipient's Catalog No.
FHWA/IN/JTRP-2004/4		

4. Title and Subtitle	5. Report Date
Evaluation and Repair of Wrought Iron and Steel Structures in Indiana	June 2004
	6. Performing Organization Code

7. Author(s)	8. Performing Organization Report No.
Mark D. Bowman, Amy M. Piskorowski	FHWA/IN/JTRP-2004/4

9. Performing Organization Name and Address	10. Work Unit No.
Joint Transportation Research Program 1284 Civil Engineering Building Purdue University West Lafayette, IN 47907-1284	
	11. Contract or Grant No. SPR-2655

12. Sponsoring Agency Name and Address	13. Type of Report and Period Covered
Indiana Department of Transportation State Office Building 100 North Senate Avenue Indianapolis, IN 46204	Final Report
	14. Sponsoring Agency Code

15. Supplementary Notes

Prepared in cooperation with the Indiana Department of Transportation and Federal Highway Administration.

16. Abstract

Throughout the state of Indiana, there a number of older, historical bridges which have been in service since the late 19th century. Many, although not all, of these bridges are truss structures comprised either partially or completely of wrought iron members. Moreover, most of them need some degree pf maintenance or rehabilitation. However, engineers who must recommend repair or rehab operations typically do not know the material properties and behavior of wrought iron members. Consequently, an investigation was initiated to review and classify typical material properties of wrought iron members. This investigation involved three phases that included a literature review of other research and bridge rehabilitation studies, a survey of many transportation agencies throughout Indiana and the United States, and fundamental material and mechanical testing in the laboratory. Based upon this research, rehabilitation and repair recommendations for wrought iron members in existing bridges were then developed.

.

17. Key Words	18. Distribution Statement
historic bridges, bridge rehabilitation, wrought iron, truss bridges, repair procedures, rehabilitation, welding.	No restrictions. This document is available to the public through the National Technical Information Service, Springfield, VA 22161

19. Security Classif. (of this report)	20. Security Classif. (of this page)	21. No. of Pages	22. Price
Unclassified	Unclassified	242	

Form DOT F 1700.7 (8-69)

TABLE OF CONTENTS

Page

Page

LIST OF FIGURES

Figure Page

Figure Page

Figure Page

Figure Page

Appendix Figure Page

Appendix Figure Page

Appendix Figure Page

LIST OF TABLES

Table Page

Appendix Table Page

Appendix Table Page

ACKNOWLEDGMENTS

The research project was financially supported by the Federal Highway Administration and the Indiana Department of Transportation through the auspices of the Joint Transportation Research Program and the Indiana Local Technical Assistance Program. The authors would like to express their grateful acknowledgment for sponsorship of this research.

The valuable suggestions and comments provided by the Study Advisory Committee and the staff of the Local Technical Assistance program are sincerely appreciated. The members of the Study Advisory Committee include Mr. Scott Newbolds and Mr. Tony McClellan from the Indiana Department of Transportation, and Mr. Matt Fuller from the Federal Highway Administration.

Sincere thanks are also due to Jim Barker, P.E. from J.A. Barker Engineering, Inc. for the bountiful donation of testing material and vast amount of knowledge, assistance and direction. The authors would also like to thank Dan McCain from the Wabash and Erie Canal Park in Delphi, Indiana for his helpful donation of testing material.

Steve Weintraut, James Cooper and Perry Green are thanked for their advice and expertise offered during the development and conduct of this project. Ross Brown, from the Village Blacksmith Ironworks, is also acknowledged for his assistance in heat straightening of the wrought iron members, delivering of testing material, and for his extensive knowledge of repair and reconstruction of historic bridges.

The authors would also like to thank Jeff Lynch of the Purdue University Central Machine Shop for his assistance in the development of the welding procedures utilized in this research and for performing the welding necessary in this project. Also, thanks are extended to Nick Humphrey of the Central Machine Shop for his advice on specimen preparation and for machining the specimens with such accuracy and excellence.

Those individuals that graciously gave time and knowledge to helped in the completion of this research, such as Harry Tidrick from the Kettelhut Structural Engineering Laboratory, Janet Lovell, Gerardo Aguiler, Yeliz Firat, and Ryan Huebschman from Civil Engineering are also thanked.

1. INTRODUCTION

Throughout the state of Indiana, there are numerous historical bridges that have been in service since the late 19th century and need to be either rehabilitated or replaced. Since the funds needed for replacement is often unattainable by the agencies owning these bridges, and the demolition of these historically significant bridges would be detrimental to preserving the history of the state, rehabilitation of these bridges is an option worth investigating.

Among the historical bridges existing in Indiana, many are older metal bridge structures comprised either partially or completely of wrought iron. Figure 1.1 depicts one of these existing bridges in Jackson County, Indiana. The properties and behavior of the wrought iron found in these bridges is unknown and varies considerably. It would be beneficial to determine the properties and behavior of the wrought iron to safely rehabilitate these existing historical structures.

1.1 Problem Statement

There are a number of existing historic metal truss bridges consisting of wrought iron members throughout the state of Indiana that need to be repaired or rehabilitated. Due to technological advances in material production during the late 19th century, the use of wrought iron diminished, along with a common knowledge of wrought iron material properties and behavior. When rehabilitating these bridges engineers often have a difficult time determining not only if the metal is wrought iron,

but also what material properties to utilize when designing repairs. This makes the repair and rehabilitation process extremely difficult.

The material behavior of the historical wrought iron is very different from that of common structural steel. The structure of historical wrought iron consists primarily of ferrite iron, along with numerous deposits of impurities, commonly known as slag, that are elongated throughout the metal. This creates a fibrous structure in historic wrought iron, as can be seen in Figure 1.2. Since the properties of the metal vary considerably due to the large deposits of impurities, it may be difficult to utilize typical repair procedures used in steel structures in these historical wrought iron structures.

1.2 Objective of Research

The research study involved three primary objectives: (1) collect information related to the performance and repair of wrought iron bridge structures, (2) initiate a database of sample material properties through data collection and experimental testing, and (3) develop a list of suggested repair techniques for joints and members typical of wrought iron bridge construction.

Upon the completion of these objectives, the historical properties of wrought iron were more fully understood and some typical repair procedures for historical wrought iron bridge members were developed. The properties of wrought iron were determined both by collecting data from previous studies and by performing experimental testing with wrought iron materials from two different bridges. The repair procedures were also developed from experimental testing and analysis of literary research.

1.3 Scope of Research

The scope of the research completed in this study consisted of a literature review / synthesis study, a survey of state Departments of Transportation and County Engineers, materials testing of historical wrought iron, analysis and evaluation of existing repair procedures and the development of repair recommendations.

In the literature review completed, an in-depth search of many databases such as TRIS, METADIX, and other engineering databases was completed along with an in-depth search of collections in the Purdue University library system, and many other library systems. In this search articles dealing with the repair and rehabilitation of specific bridges were found along with many articles dealing with the material properties and manufacturing processes of wrought iron. Also, many historic sources containing testing data on the material properties were discovered and the data were recorded. Although the literature search did find much information about wrought iron and rehabilitations in general, little information was found relating to actual repair procedures utilized in rehabilitating wrought iron bridge members.

A survey was distributed to State DOTs, State Local Technical Assistance Programs, Indiana County Engineers, and other engineering consultants to determine the number of existing historic iron bridges, and if there were any existing wrought iron repair procedures. The results from this survey did not lead to any existing wrought iron bridge member repair procedures, but it did lead to a better understanding of the need for more knowledge concerning the behavior of historic wrought iron.

Extensive material and mechanical testing was completed on wrought iron bridge members from two existing bridges in Indiana. This testing included: micrographs, chemical analysis, hardness testing, tensile coupon testing, charpy impact testing, tensile testing of eyebar end connection, and some limited fatigue testing. The micrographs that were taken helped to develop a better understanding of the

microstructure of the metal. The chemical analysis completed lead to a determination of particular elements that are commonly found in historic wrought iron. Hardness testing, tensile coupon testing, charpy impact testing, and fatigue testing helped to determine many common material properties. Eyebar end connection testing lead to a better understanding of particular bridge member's behavior.

Testing was also performed on different types of repairs that might exist in the field. These repairs included: member straightening with heat, straightening without heat, welding to join two members, and filler welding to restore section loss from corrosion. This testing, along with articles found in the literature search, helped lead to the development of some procedures and suggestions that could be used to repair historic wrought iron bridge members.

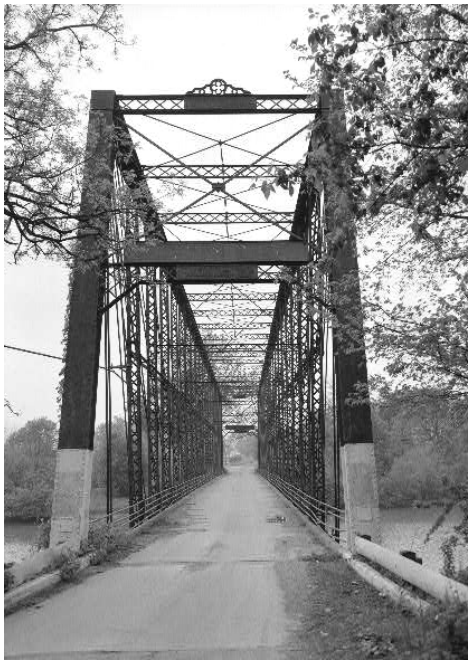

Figure 1.1 Historic Wrought Iron Bridge Spanning Laughery Creek, Aurora vicinity, Dearborn County, IN (Historic American Buildings Survey/Historic American Engineering Record)

Figure 1.2 Picture Showing Fibrous Nature of Wrought Iron. (Aston, 1949)

2. LITERATURE SEARCH

Before experimental testing began, an in depth literature review was conducted. This review had several goals which were to obtain an accurate description of, and historical background for, wrought iron as it was used as a structural material. Also from this review, historical tensile strength data of wrought iron was found, collected and analyzed. Through out the review, many articles dealing with repairs and rehabilitations of bridges that consisted of wrought iron members were located and summarized. Upon completing the review, a survey was created and distributed with the goal of determining if any such repair procedures are currently used throughout the country.

2.1 Background of Wrought Iron

2.1.1 Definition of Wrought Iron

Wrought iron was officially defined by the American Society for Testing Materials in 1930 as:

> "A ferrous material aggregated from a solidifying mass of pasty particles of highly refined metallic iron, with which, without subsequent fusion, is incorporated in a minutely and uniformly distributed quantity of slag."

Wrought iron is considered to be a material that consists of two main components: high-purity iron and iron silicate. Iron silicate, more commonly known as slag, is a glasslike substance that is mechanically intermingled with the iron. The addition of slag occurs during the manufacturing process for the wrought iron

This manufacturing process is dissimilar to common manufacturing processes because in this historic process, the metal is never completely molten. In modern manufacturing processes of metals, the ore is superheated until it is completely fluid and impurities rise to the surface and are discarded. During the process for making wrought iron, the metal exists in a red hot pasty condition and impurities are typically beaten and rolled out of the material. This creates many of the characteristic properties of wrought iron.

Structurally wrought iron is fibrous in nature. While in the red hot pasty condition after the iron ore has been heated, slag exists in pockets through out the material. When the material is rolled, the slag is "squeezed" out. Rolling causes the pockets of slag to become elongated and dispersed throughout the material. These elongated deposits of slag influence the iron so that it exists in fibers along one direction of the material. In some cases there may be more than 250,000 slag threads or fibers per one square inch of area (Mills, 1915). This creates a fibrous material structure that is similar to some types of wood, as can be seen in the fracture depicted in Figure 2.1.

Chemically, wrought iron consists of mostly iron with the addition of some elements. Chemical analysis of wrought iron shows that there is typically less than 0.15% carbon found in the material (Tiemann, 1919). Although a similar amount of carbon is commonly found in some steels, the other elements comprising wrought iron create the difference in the materials. Phosphorous and silicon are typically found in wrought iron and steel, but these elements usually exist in excess than what is typically found in steel. An excess of the element silicon is especially characteristic of wrought iron since it is the main constituent found in the slag which defines the metal.

The consistency and quality of wrought iron is difficult to asses simply because the manufacturing process utilized to make historic wrought iron was not capable of making wrought iron entirely structurally homogeneous in nature. Because of these

imperfections, the performance of the material will vary considerably. The properties of the material depend on the iron ore it was manufactured from and the individual that was manufacturing it. Since it is difficult to find consistency in both of these dependencies, it is also extremely difficult to find consistency in the material properties.

2.1.2 Manufacturing Process of Historic Wrought Iron

In 1784 Henry Cort patented a new process called the puddling process for producing wrought iron. In this process, a reverberatory type furnace was utilized in heating the iron ore. This furnace consisted of a “firebox”, where the fuel was burned, and was separated from the hearth, which contained the iron ore, by a bridge (Dennis, 1963).

After separating the iron ore, from the heat source, the iron ore was placed in a large hearth that was typically 6 feet by 4 feet in dimensions, which in Henry Cort’s original furnace was lined with fire-brick and sand. Unfortunately the iron ore would often oxidize with the sand creating extra iron-silicate slag and therefore reducing the amount of iron produced by 30% (Aston, 1949).

The amount of impurities in the wrought iron was reduced in 1830 when Joseph Hall modified Cort’s process, known as “dry puddling”, by lining the hearth with older hearth material such as iron silicate which contained iron oxide. This change increased the yield of wrought iron from iron ore, or pig iron, to 90% (Dennis, 1963). This new process became known as “wet puddling”.

Figure 2.2 shows a section of the puddling furnace as described above. The puddling furnace capacity ranged from 300 pounds to 1500 pounds of wrought iron per heat (Johnson, 1928). A single heat typically took about one and a half hours to complete. After heating, the wrought iron was shaped into a ball, commonly called a

bloom or sponge ball. Slag was dispersed through out the iron in small pockets at this stage and the structure of the hot wrought iron can then be compared to a common sponge.

The ball was then transported, while remaining at high temperatures, to a rotary squeezer. A photograph of a sponge ball being transported can be seen in Figure 2.3. In the squeezer, the iron was “squeezed” and “shingled” mechanically to remove most of the slag existing in the wrought iron. After being squeezed, the puddle ball was less than half the original size and then rolled into shape. The rolling process elongated the remaining existing slag deposits in one direction created a semi-fibrous structural state.

The rolling process began when the wrought iron sponge ball was transferred to the rolling mill where it would be rolled into needed shapes. First, the ball was rolled into small rectangular bars, known as “muck bars”. These muck bars were rolled to be a thickness of 2 to 4 inches and then cut into strips. The strips were then piled up and wired together, reheated to a welding temperature and then rolled again (Mills, 1915). The finished product, called a “merchant bar”, was then either sold or further rolled into different shapes.

The wrought iron manufactured from the puddling process has large deposits of impurities. The majority of these impurities are commonly known as “slag”. The term slag refers to a molten substance that is found in the furnace other than the iron ore being processed. This substance is mechanically intertwined in the material during processing (Tiemann, 1919). In historic wrought iron, slag consists mainly of iron silicate along with other miscellaneous oxides. The percent of slag found in the iron ranges from one to three percent by weight (Aston, 1949).

The wrought iron manufactured today is made from a process similar to that of steel. Iron is superheated to a liquid form, where most of the impurities are separated. Then a pre-produced molten slag is added to create the definitive slag deposits found in

wrought iron. Adding the slag after the iron has become molten and impurities have been separated creates a different microstructure in the modern day wrought iron than historic wrought iron. Modern day wrought iron differs from historic wrought iron because it contains fewer impurities and the slag deposits are of a different structure. These differences exist because the manufacturing processes are so dissimilar.

2.1.3 History of Wrought Iron Production

The history of wrought iron dates back to the primitive years of man, where iron was melted down in fires and used for tools. In this discussion of wrought iron, however we begin with the invention of the Catalan Furnace. This furnace can be marked as a starting point in the development of mass production of wrought iron.

The Catalan furnace was developed in the early 13th century in Northern Spain. It was one of the first furnaces to produce a large amount of iron at one time. This furnace consisted of an open hearth of which a trompe, or a large-scale air aspirator, was attached. The Catalan furnace could produce up to three times more iron than previous furnaces (Aitchison, 1960). For these reasons, he Catalan furnace was very popular and was used through out Europe for hundreds of years.

After the development of the Catalan furnace, other types of large furnaces such as the Osmund and the Stuckofen furnaces, which were larger versions of the Catalan, were developed. These furnaces used the basic concept of the Catalan furnace, and lead to the acceptance of the idea that producing large amounts of wrought iron at one time was possible. Therefore, it is evident that the Catalan Furnace was responsible for iron mass production.

From the time of American Colonization to the early twentieth century, the most common furnace used in the United States was the American Bloomery (Aston, 1949).

This furnace was named after the large balls of iron, or blooms, that would be produced in the furnace and then rolled into shapes. The American Bloomery was developed while America was still colonized by the British and was similar to a Catalan Forge except that it consisted of metal sides that were water cooled. Great Britain passed the Iron Act of 1750, which helped erect many furnaces, forges, and mills in communities throughout the colonies. It was intended that these communities would then produce colonial pig iron that was to be shipped to Great Britain (Fisher, 1963).

As a result of the Iron Act of 1750, the American colonials were able to develop the knowledge and tools to manufacture iron independently of Great Britain. This knowledge and manufacturing independence turned out to be invaluable during the Revolutionary War and it helped to facilitate industrial progress of the United States. In the mid 18th century an industrial revolution was also occurring in Great Britain. The processing and manufacturing of goods soon became the main source of stability for the economy, and iron was needed more than ever to support the booming industrial growth.

Before this time, production of wrought iron was very labor intensive. First the iron ore was heated and processed in a furnace such as the Bloomery. It would then be extracted in a large round ball, known as a bloom or sponge ball, and manually beaten to remove some of the slag and formed into bars. The resulting product was early wrought iron. Because of the rising need for wrought iron and the current processes for manufacture of iron being too labor-intensive, a more mechanical approach was needed for producing wrought iron.

In 1784, Henry Cort patented a new process called the puddling process for producing wrought iron. In this process a reverberatory type furnace was utilized in heating the iron ore. A reverberatory furnace utilizes air flow to turn the flames back over the iron in heating. This furnace was able to produce 20 times the amount of wrought iron produced using older methods in the same amount of time. The new

method for manufacturing wrought iron grew and many manufacturing plants were built through out the United States.

In the United States an industrial revolution occurred during the middle of the 19th century. Evidence of this can be seen in the development of new production processes, more industries being built, further development of the assembly line, growth of cities, and a decrease in the agricultural work force. The United States would later experience the civil war, which meant that much iron was needed for the war and for rebuilding after the war. During this time of industrialization and growth, wrought iron was used quite extensively through out the country as well as in the construction industry.

Many iron companies through out the region started manufacturing standardized shapes and sizes of iron to be used for construction purposes. Each iron company had a set of standardized shapes that were produced only by that company. The companies would print compilations of what they produced and from these booklets iron products could be purchased. The American Institute of Steel Construction (1953) compiled many of these standard shapes from larger companies throughout the country from the years 1873 to 1952. Some of these companies included Carnegie Brothers & Company, Limited, The Passaic Rolling Mill Company, and the Phoenix Iron Company.

In addition to producing standardized shapes for building construction, many of the iron manufacturers designed and produced bridges. One popular bridge company was the Wrought Iron Bridge Company of Canton Ohio. This company designed, patented, manufactured and constructed bridges. Most of the bridge companies published pamphlets describing the different types of bridges they built and their uses. For example, Figure 2.4 shows the front cover of a pamphlet published by the Wrought Iron Bridge Company. Many cities, counties and even farmers simply ordered bridges from bridge companies by using their pamphlets. This phenomenon lead to the existence of numerous wrought iron bridges through out the United States.

Since there was such a demand for wrought iron in the late 19th century, many mechanical processes were invented to increase the production and quality of wrought iron. These mechanical processes were needed to increase production capacity and reduce the amount of labor dependence that existed in the previous processes. Many new furnaces were introduced, but none were very successful in their attempts.

Concurrent with the attempts to improve the mechanical manufacture of wrought iron, Henry Bessemer developed a new process for making steel, which was introduced around 1855. Before this, the methods for making steel were very complex and tedious, therefore making steel was rare and more expensive to use for any sort of building purposes. These processes are known as the cementation and crucible processes. Developed many years before-hand, these steel-making processes involved the addition of carbon to iron by soaking iron in carbon and letting it set over time, or melting wrought iron and mixing it with a carbonaceous material (Stoughton, 1934).

The basic concept of the Bessemer process depends on the successful rapid oxidation of the impurities (Si, Mn and C) by keeping the iron ore in a fluid molten bath with extreme heat, thus forcing the slag to separate from the steel by floatation (Johnson 1928). This was done by subjecting molten pig iron to a superheated pressured blast for about twelve to fifteen minutes. Figure 2.5 depicts a picture of a Bessemer Converter during one of these blasts. After oxidizing all the impurities out of the molten iron, an aluminum and manganese alloy carrying several percent carbon was added. The introduction of this alloy resulted in the addition of carbon to the molten iron, making it steel. Then the molten steel is poured and solidified into ingots and castings which are then rolled into shapes (Johnson, 1928).

The original Bessemer process created a brittle steel that was not useful. Then in 1856 Robert Mushet discovered that by adding a compound containing manganese and iron to the molten iron in Bessemer's process, the resulting steel could be made more ductile and have superior strength (Fisher, 1963). Bessemer and Mushet received many

patents for their process and traveled the world promoting it and the manufacturing of steel.

While Bessemer and Mushet were developing the Bessemer Process, William Kelly from Pittsburgh was developing an idea to use a blast of air to oxidize out the impurities of iron. After many years of development he then created what is known as the pneumatic process for making mild steel and obtained an American Patent for this concept (Fisher, 1963). About ten years later, the Open Hearth process was developed. This process, like the Bessemer process, utilized a blast of air to oxidize out the impurities in pig iron.

In the beginning of the 19th century wrought iron was the most extensively produced metal in the United States. But by the end of the century, steel became the leader in the industry. The transfer between the two metals was not instantaneous, but rather a gradual transitional period of industrialization. Once the new processes for making steel were developed, wrought iron was not immediately neglected. Wrought iron was already being manufactured through out the United States, so it was easier and cheaper to construct with wrought iron even though it was found that steel was stronger. For example, the slow transition in the railroad industry from wrought iron rail to steel rail demonstrates and parallels the transition from wrought iron to steel throughout the rest of the country.

Originally in Great Britain, the rails for trains were made of wrought iron, but needed to be "turned" or replaced every six months. In an effort to promote mass produced steel, Henry Bessemer convinced the local authorities to try steel rails. The trial steel rails did not need to be replaced for two years and it was soon determined that steel was a stronger and more durable material (Fisher, 1963). This knowledge was spread to the United States and steel rails were slowly used throughout the populated east. Using steel rails in the western states was illogical since it was easier to straighten bent or damaged wrought iron rails then to wait several weeks for new steel rails. As

steel manufacturing mills began growing around the country, rails were eventually converted to steel across the country.

The transition from wrought iron to steel in the construction industry parallels that of the railroad industry. Just like any other structural building product, it took time to convince the design and construction community of the benefits from utilizing steel as a structural material and to build more manufacturing plants. Wrought iron was more familiar, cheaper, and more trusted from experience.

Not until Bessemer and his followers traveled the world trying to prove the superior quality of steel, did the industry begin to build manufacturing plants and start to use steel more in construction than wrought iron. This turn around in the United States could probably not be noticed until the 1890's or even the turn of the century. Since the quality of wrought iron was variable, and the process to make wrought iron was so labor intensive and time consuming compared to steel, it soon fell behind in use for building purposes.

2.2 Investigation of Research Completed on Historic Wrought Iron

By the middle of the nineteenth century experimental testing of metals was becoming a new phenomenon. Typically, before this time manufacturers and bridge designers used a method of trial and error to determine if a structure was to fail with certain loads. Examples of this can be seen in many instructional books written by such authors as Peter Barlow, William Fairbairn, and William Humber. In *The Application of Cast and Wrought Iron to Building Purposes* by Barlow (1845), a majority of the book was comprised of load testing beams that consisted of a variety of different rolled shapes and various configurations of plates that are riveted together. These beams would then be loaded in the center and the deflection noted. Typically the load would be increased slowly until failure.

This method of testing of structural elements worked well for this time period. Bridges typically were not designed by individual engineers, but rather were designed by an iron works company and then constructed. New methods in analyzing stresses and strains in structures were just being developed and not yet commonly used in engineering practice. Material behavior was also not yet fully understood.

In 1847, the Stephenson's bridge over the River Dee in Chester England which utilized cast iron beams, failed. This failure along with many other cast iron failures resulted in an increase in materials testing and research. Many books like *Experimental Researches on the Strength and other Properties of Cast Iron* by Eaton Hodgkinson (1850) investigated cast irons' material properties and determined that cast iron was not strong in tension.

By the 1860's wrought iron and steel were being produced and commonly used for construction purposes. The material properties of these metals were extensively investigated. One source that encompassed all aspects of iron bridge construction is *A Complete Treatise on Cast and Wrought Iron Bridge Construction* by William Humber (1870). This source describes methods to analyze and design iron bridges. Importantly, a section on material properties is included. In this section Humber tested the strength of wrought iron from different manufacturers throughout the country.

One of the most comprehensive sets of data acquired for the strength of wrought iron was completed by David Kirkaldy while he worked at Robert Napier's Vulcan Foundry Works in Glasgow. During this time period, the company was using wrought iron and steel to construct boilers and pressure vessels and was interested in ensuring the materials used were strong enough and well understood. Between 1858 and 1861, Kirkaldy completed a series of tensile load tests of common metals used during this time. He published *Results of an Experimental Inquiry into the Comparative Tensile Strength and other properties of various kinds of Wrought-Iron and Steel* in 1862.

In this testing, wrought iron bars, plates and other shapes were purchased from different merchants and makers to be tested. The origins of the testing samples were carefully recorded. The bars were then tested in the testing machine at the foundry where Kirkaldy worked. This testing machine consisted of a simple counter weight machine using a lever arm and lighter weights to load the specimens, as seen in Figure 2.6. Specimens were loaded slowly and observations of the maximum breaking weight, and percent elongation for the wrought iron bars were recorded during and after testing. The observations recorded did not include the yield stress of the wrought iron since at that time the idea of yield stress was not yet fully understood and was difficult to obtain.

Kirkaldy tested approximately 310 wrought iron bars while he was at Robert Napier's Vulcan Foundry Works in Glasgow. The results of these test results where copied and recorded from the paper he published in 1862, and can be found in Appendix A. The results show the average ultimate tensile stress that Kirkaldy found for the wrought iron bars was 55,420 psi. The standard deviation was 7,533 psi which was 13.6% of the mean. A plot of these results is shown in Figure 2.7.

Along with testing wrought iron bars, Kirkaldy also tested wrought iron plate and angle iron. The average ultimate strength found for angle iron, bar and plate were calculated and are shown in Table 2.1. As can be seen in this table, the bar had the highest ultimate strength while the plate had the lowest. The tensile stress results of the plate, angle iron, and bar were plotted together to achieve an average value for the ultimate tensile stress of 52,000 psi with a standard deviation of 7,240 psi. The standard deviation was 14% of the average found. A plot of all these results can be seen in Figure 2.8.

Kirkaldy also recorded the percent elongations for several wrought iron bars. To find the percent elongations Kirkaldy recorded the length of the specimen before and after testing and the compared these values to find the percent elongation. Figure 2.9 is a

plot of this percent elongation data, of which the average percent elongation was found to be 19.12% with a standard deviation of 6%. This standard deviation was 32% of the average found. Therefore, there was a large amount of variability in percent elongation of the wrought iron that Kirkaldy tested.

While Kirkaldy was testing iron in England, Knut Styffe a Swedish scientist was testing iron and steel that was manufactured in Sweden. His book *Elasticity, Extensilbility, and Tensile Strength of Iron and Steel* (1869) reported tensile strengths, or breaking weights, of the puddled iron that he tested. Due to the condition of the Styffe's book, some of Styffe's data is included in the combined tensile strength data collected for all historical testing results found, and can be seen in Figure 2.13. On a whole, the tensile strength of Swedish wrought iron was considerably higher than the values found from the testing in England.

The majority of the materials testing completed during the nineteenth century came from Europe. Since the iron ore and manufacturing processes were slightly different in the United States than in Europe, it was necessary to test material that was produced in the U.S. In 1875, President U. S. Grant of the United States appointed a board to:

> "…determine, by actual tests, the strength and value of all kinds of iron, steel, and other metals which may be submitted to them or by them procured, and to prepare tables which will exhibit the strength and value of said materials for construction and mechanical purposes, and to provide for the building of a suitable machine for establishing such tests, the machine to be set up and maintained at the Watertown arsenal.(Report of the United States Board, 1881)"

The board researched and tested several subjects which included the "examination and report upon the mechanical and physical properties of wrought iron." Commander L. A. Beardslee U.S.N. was the chairman in charge of the committee that completed the testing of wrought iron. The majority of the material tested was round bar material that could be forged into chain link. This material could also be used as tension rods in bridges.

The committee completed more than two thousand tests on wrought iron bar material from nineteen different manufacturers in the United States. Half of these tests were standard tensile tests where the bar specimens were pulled monolithically and resulted in a determination of the tensile strength and percent elongation of the material. The data from these tests was recorded and analyzed. The average ultimate tensile stress, based on 959 testing specimens, was 53700 psi with a standard deviation of 2680 psi, which was 5% of the average. This shows that there was little variation in the ultimate tensile stress. Figure 2.10 is a plot showing the tensile stresses found from this testing.

Besides determining the tensile stress of the wrought iron bars, the yield stress was also determined, but not accurately, through the use of the "first stretch" method. In this method, the yield stress, or elastic limit is determined when the amount of weight applied to the specimen produced the first perceptible change of form divided by the cross sectional area of the bar. Since the values for determining the yield stress are so coarse it can be presumed that they are not very accurate and most likely higher then the actual yield stress of the wrought iron bars tested. The average yield stress, or elastic limit, of the bars found from testing was 33,300 psi with a standard deviation of 2,990 psi, which was 9% of the average. This shows that there was little variation in the yield stress values determined. Figure 2.11 is a plot showing the yield stresses found from this testing.

Percent elongation was also observed by Beardslee and his committee for majority of the wrought iron bars. The method in acquiring the percent elongation consisted of measuring the length of each specimen before and after testing and then determining the amount that the specimen had stretched. This amount was then divided by the original length and the percent elongation was determined. The average percent elongation from the testing completed by the committee was 19.12% with a standard deviation of 12.19%, which was 32% of the average. This shows that there was

significant variation in the percent elongations of the wrought iron tested. Figure 2.12 is a plot showing the percent elongations found from this testing.

All of the data collected from the historic sources previously described was complied together and compared. Figure 2.13 shows a plot of the tensile stress values found for every type of wrought iron. This plot shows that majority of the tensile strength values collected fall into a one-standard-deviation range, with the exception of the data collected from Sweden. The average ultimate tensile stress for the entire set of data collected was 54,000 psi with a standard deviation was 9,000 psi which is 16.71% of the average.

The wrought iron bar data was also collected and compared to get a better estimate of the strength of the material that would be typically used for bridge applications. The average of all the wrought iron bar tensile strengths was 53,300 psi with a standard deviation of 5,800 psi, which was 11% of the average tensile strength. The standard deviation of just the bars was smaller than the standard deviation for all of the material, which indicates that separating the ultimate tensile stress values by product type (angle iron, bar, plate, etc) is more accurate. Figure 2.14 shows a plot of the bar tensile strengths. In this plot, majority of the tensile strength values fall between plus and minus one standard deviation from the mean.

A comparison of the percent elongation data was also completed. It is important to note that all this data consists of testing samples with different lengths used to calculate the percent elongation which could increase the variability of the data. In this comparison, all the data collected for percent elongation of wrought iron was from bar material. Figure 2.15 is a plot showing this data. In this plot it can be seen that there is a wide variation in the data. The average for this data was 23.2% with a standard deviation of 7.6%, which was 33% of the mean. This shows that the percent elongation data varies considerably.

2.3 Case Studies of Rehabilitated Wrought Iron Bridges

2.3.1 Walnut Street Bridge, Pennsylvania, 1860

Through out the country there are a number of common types of truss bridges. These types are usually denoted by the engineer that patented their design, such as the Whipple Trusses and Pratt Trusses. The Walnut Street Bridge is one of these types of bridges, which is a cast and wrought iron Pratt through truss bridge that was built in Hellertown, PA in 1860. This combination of materials, such as cast and wrought iron is common in bridges from this time period. Like many other historic wrought iron bridges, the bridge was removed from vehicular service in 1970 and then stored by the state.

In 1994, graduate students at Lehigh University performed a detailed visual inspection of the Walnut Street bridge to determine if the bridge was salvageable. There was moderate corrosion and it was determined that a further investigation into the structural integrity of the bridge was necessary. Mechanical testing was completed to determine the structural properties of the materials. This testing included tensile, flexure, compression and Charpy impact tests on the materials acquired from the bridge. From these tests, the strength of the various materials including wrought iron were determined.

The tensile strength and charpy impact strength of wrought iron was found to be comparable to that of mild steel. However, the results of the material testing still concluded that it would be beneficial to restore the bridge for pedestrian use only. The Walnut Street Bridge was rebuilt in a historical park near where it was originally constructed. Significant corrosion damage was found on several of the wrought iron tensile members during the visual inspection of the bridge. These members were replaced with A36 steel during restoration. A more detailed account of the rehabilitation can be found in *Rehabilitation of a Nineteenth Century Cast and Wrought Iron Bridge* written by Perry S. Green, Robert J. Connor, and Christopher Higgins (1999).

The practice of restoring historic bridges for pedestrian use is very common through out the country. This practice is viewed by many as an effective compromise between keeping the historical validity of a bridge and keeping it structurally safe to use. Francis E. Griggs, Jr is the director of Historic Bridge Programs at Clough, Harbour & Associates LLP. He has rehabilitated and reconstructed many historic bridges in this manner. One bridge in particular is an 1864 Moseley Wrought Iron Bridge that was moved to the Campus of Merrimack College in N. Andover, MA (Griggs, 1997).

2.3.2 Carroll Road Bridge, Maryland, 1879

The Carroll Road Bridge was a wrought iron Pratt through bridge that spanned 92 feet and was constructed in Baltimore County, Maryland in 1879. This bridge consisted of two wrought iron trusses with a wooden deck supported by stringers. The upper and lower chords of the trusses are made up of eyebars with pin connections. Pin connections are a typical type connection found in many historical truss type bridges.

The Baltimore County Department of Public Works decided to rehabilitate the Carroll Road Bridge in order to preserve the historic character and upgrade the live load capacity of the bridge to modern vehicle standards. This preservation project is explained in the paper *Upgrading and Recycling of Pin-Connected Truss Bridge by Pin Replacement* by Shahin Taavoni (1994).

In the initial phase of the study, a visual inspection of the bridge was completed. Also material shavings where taken from the bridge to determine the type of metal in the bridge. Chemical analysis results determined that the material was wrought iron. During the visual bridge investigation it was found that the pin connections on the bridge were not acting symmetrically.

The lack in symmetry found at the pin connections was a result of dynamic effects of the live load and past repairs. Corrosion and fatigue could also lead to movement in the eyebars but was not considered to be an issue for this bridge. An analysis of the lack of symmetry and resultant effects determined that the pins needed to be replaced with a higher strength material and the eyebars moved back to a symmetrical position. This would ensure that the pins would not experience an unsafe amount of shear, that the eyebars would all carry the load equally.

The rehabilitation of the bridge consisted of taking apart the trusses and reassembling them with higher strength pins. Members added during past repairs were also removed. Many of these past repairs involved the addition of a third component in a previous two component member. To sustain the higher load the third component would be removed and the two component member would be replaced with a stronger two component material. Finally, spacers were added to the pin connection to ensure that symmetry would be maintained in the future.

Rehabilitation using the pin replacement method turned out to be efficient, expeditious and economical according to Taavoni. It could also be easily adapted to many other historic truss bridges that have similar pin connections.

2.3.3 Chestnut Ford Bridge and Hubby Bridge, Iowa, circa 1900

Construction on the Des Moines River in Iowa lead to the removal of five iron pin connected truss bridges in that area. The first of these bridges, the Chestnut Ford Bridge, was subjected to service load testing, and supplementary static and fatigue tests of tension eyebars taken from the bridge. The second bridge, the Hubby Bridge, was also subjected to service load testing and eyebar laboratory testing, but also went through an ultimate load test. The paper *Service Load and Fatigue Tests on Truss Bridges* by Hotten A.

Elleby, Wallace W. Sanders, F. Wayne Klaiber, and Douglas Reeves (1976) discusses the testing that was performed on the eyebars from both of the bridges.

The eyebars of the bridges were tested both cyclically and statically. The majority of the testing concentrated on the fatigue testing of the wrought iron eyebars. Both fatigue and static type tests were performed on both undamaged and damaged eyebars. The damaged eyebars were actually undamaged eyebars that had been purposefully damaged in the laboratory and then repaired. Three types of repair were simulated on the eyebars and investigated. The first type was repair of a fracture in the forging area near a turnbuckle. The second was a fracture at the neck of an eye that had been welded together with splice bars. The third was a fracture in the eye where the entire eye was removed and a new eye was formed out of cold rolled bar stock.

Of the fatigue tests performed, it was found that the repairs made to the eyes did not significantly affect the fatigue life of the eye. Instead, the life of the eye connection was governed by the characteristics of the eye. For the static testing, the repair procedures affected the resulting tensile strength of the eye. This is especially true when adding a new eye with a welded splice plate connection. Failures in these tests were governed by the quality of the forges in the eye connection. From both the fatigue and static testing it can be concluded that the repair procedures used on the eyes are acceptable when repairing the eyebar members of a bridge.

2.3.4 Norfolk and Western Railway Bridge, Wabash Railroad, 1888

The Norfolk and Western Railway Bridge spans the Mississippi river between Illinois and Missouri and consists of seven truss spans and one continuous swing span for a total length of 1,580ft. The bridge consists of riveted built up compression members and tension eyebars. It has undergone many repairs during its service life. These repairs included shortening of the spans and tightening of the eyebars. To tighten the eyebars, a

piece was cut out from the center of the eyebar. The two cut ends were then drawn closer to each other and splice plates were welded on either side. The splice plates used were a mild steel material.

The paper Fatigue Behavior of Welded Wrought-Iron Bridge Hangers by Peter B. Keating, John W. Fisher, Ben T. Yen, and William J. Frank (1984) investigates the splice plate repair in detail. While doing a visual inspection of these splice plate repairs fatigue cracking was found across the toe of the transverse welds of the detail. Fatigue cracking was also found in the welded gap at the center of the lap splice. To further investigate this repair procedure, laboratory fatigue tests were completed on both actual spliced details from the bridge and fabricated details.

Similar to the splice plate details on the bridge, the details that were tested developed surface cracks at the toe of the splice plates that were welded to the surface of the wrought iron eyebars. These cracks developed at cyclic lives that were comparable to the lives of the steel components. The cracks in the wrought iron were arrested by the slag deposits dispersed throughout the metal. Therefore, they did not have an adverse effect on the fatigue resistance of the wrought iron. The investigation of this repair demonstrates that using a splice plate method to shorten or tighten eyebars in a bridge could be an acceptable method of repair.

2.4 Survey Results

To determine if there were any existing maintenance and repair procedures that existed through out the country, a survey was created and distributed to all fifty State Departments of Transportation and Local Technical Assistant Programs. To determine if there were any formal repair procedures in the state of Indiana, a survey was distributed and sent to the engineer or highway supervisor in all ninety-two county highway departments in Indiana and some various bridge engineering design consultants.

From all the surveys that were distributed 59 were received. Of the surveys sent out to the DOTs 35 were received, and 2 were received from other state's LTAPs. A total of 19 surveys were received from the local county engineers of Indiana, and 3 more surveys were received from various bridge engineering consultants. An example of the survey that was completed and distributed can be seen Appendix B.

Of the 59 received state DOT completed surveys, 16 reported that there were historic wrought iron bridges in their state. Of these 16 states, 1 state had over 101 bridges, 1 state had between 41 and 100 bridges, 2 had between 21 and 40 bridges, 2 had between 11 and 20 bridges, and 10 had between 1 and 10 bridges. A plot showing the distribution of historic bridges is shown in Figure 2.16. Of all the state DOTs that reported that there were historic wrought iron bridges in their state, 7 states reported that they maintained a number of the bridges.

From all received surveys completed by the state DOTs none reported that there were formal repair and maintenance procedures established for historic wrought iron bridges. Five of the DOTs surveyed said they allowed heat straightening in these types of bridges and three allowed welding. The inspection procedures reported for most historic bridges included only visual inspection, except for two states that also included dye-penetrant and ultrasonic testing to detect suspect cracking.

For load rating, the majority of the states reported that they used the procedures outlined in the AASHTO Manual for the Condition Evaluation of Bridges (1994). Five DOTs specifically reported that they either determined the actual material properties of the wrought iron bridge material or used predetermined material properties of wrought iron from literature in evaluating the load capacity of the bridges. Two DOTs stated they used the same material properties as steel to evaluate the load capacity of the historic wrought iron bridges.

Of the nineteen Indiana county engineers that completed the survey, 13 stated that there were historic wrought iron bridges in their county. Of the 13 counties with these bridges, 2 had between 11 and 20 bridges, while 11 counties had between 1 and 10 bridges. None of the counties had available any formal repair and maintenance procedures, but 3 allowed heat straightening of members and 6 allowed welding. One county engineer referred to *Restoring Historic Metal Truss Bridges,* a source written by James L. Cooper (2001), for repair procedures. All reported that inspection procedures consisted of typical visual inspections that were completed as part of the mandatory two year inspection cycle. Moreover, it was also reported that the majority of the load rating for these bridges was completed by hired consultants.

Table 2.1 Average Ultimate Strength and Standard Deviation for Angle Iron, Bar, and Plate Material Tested by Kirkaldy (1862).

Type of Material Tested	**Average Tensile Strength**	**Standard Deviation of Tensile Strength**
Angle Iron	53,190 psi	4,910 psi (9.2%)
Bar	55,420 psi	7,530 psi (13.6%)
Plate	48,500 psi	5,580 psi (11.5%)

Figure 2.1 Fracture Showing Fibrous Nature of Wrought Iron. (Aston, 1949)

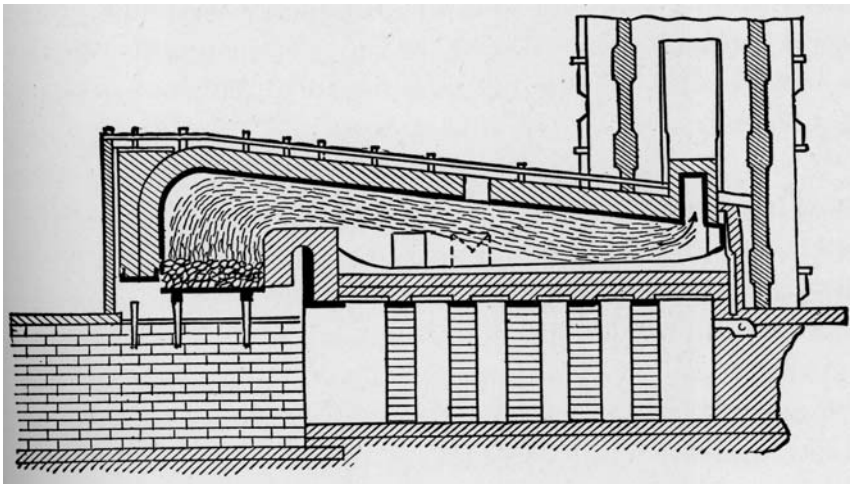

Figure 2.2 Cross Section of Puddling Furnace (Johnson, 1928)

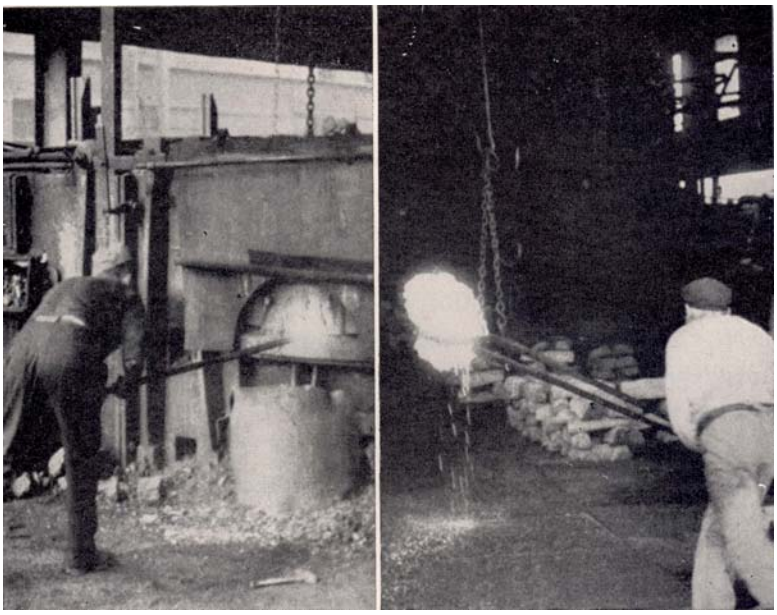

Figure 2.3 Wrought Iron “Sponge Balls” being transported after firing (Aston, 1949)

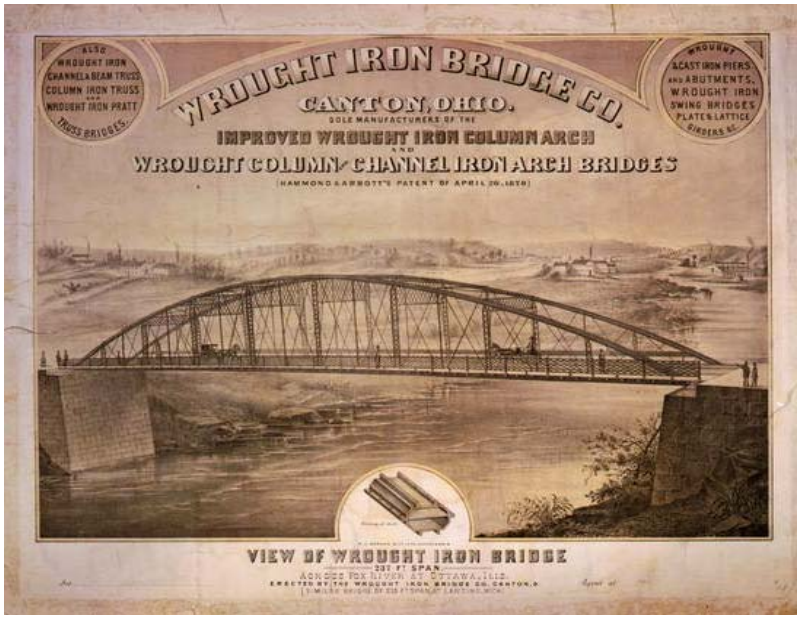

Figure 2.4 Front page of Pamphlet from Wrought Iron Bridge Co. Canton OH

Figure 2.5 Picture of Bessemer Converter (Aston, 1949)

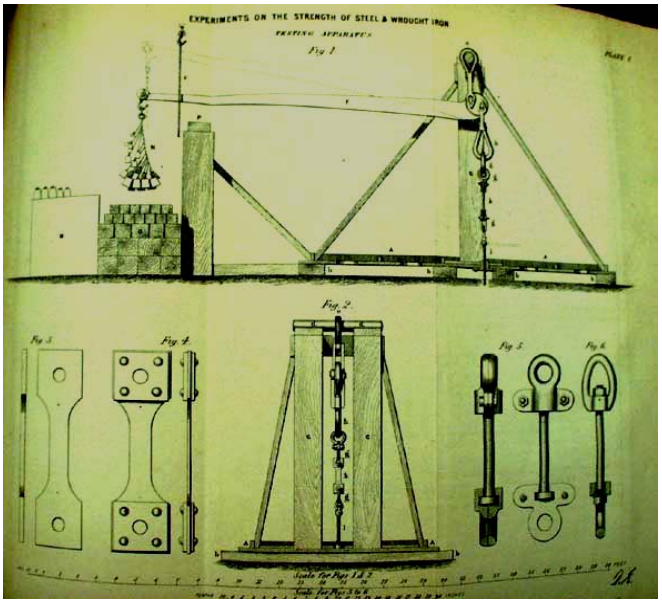

Figure 2.6 Drawing of Testing machine at Robert Napier's Vulcan Foundry Works in Glasgow (Kirkaldy 1962)

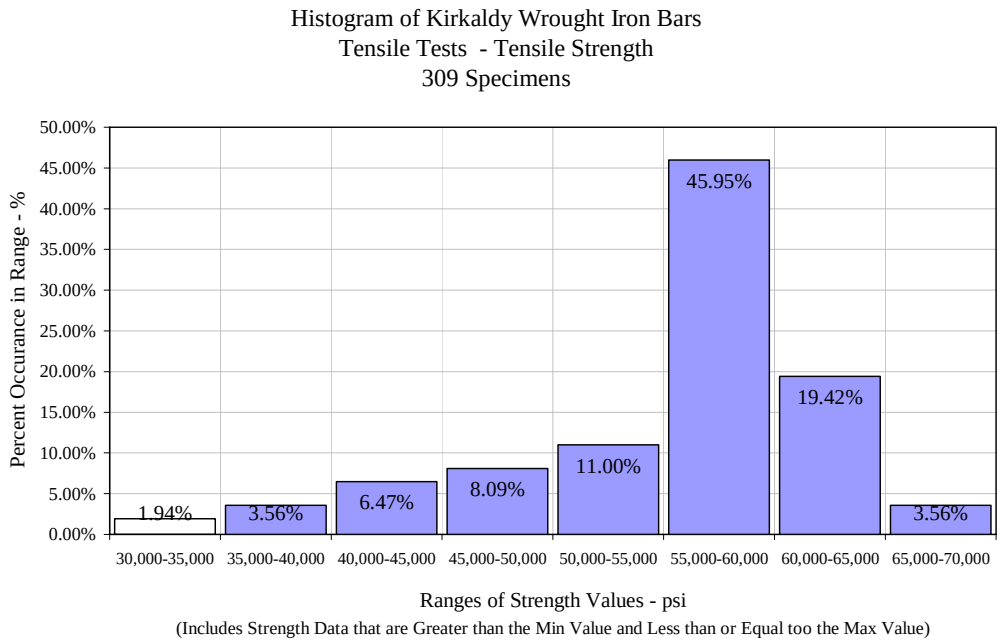

Figure 2.7 Tensile Strength of Wrought Iron Bars Tested by Kirkaldy

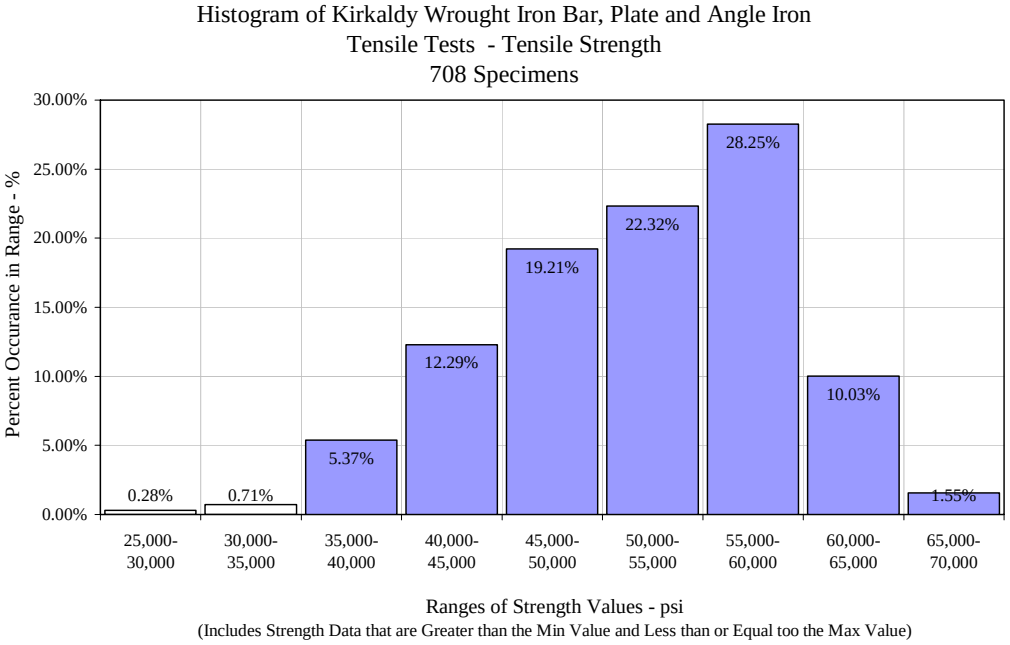

Figure 2.8 Tensile Strength of all Wrought Iron Shapes Tested by Kirkaldy

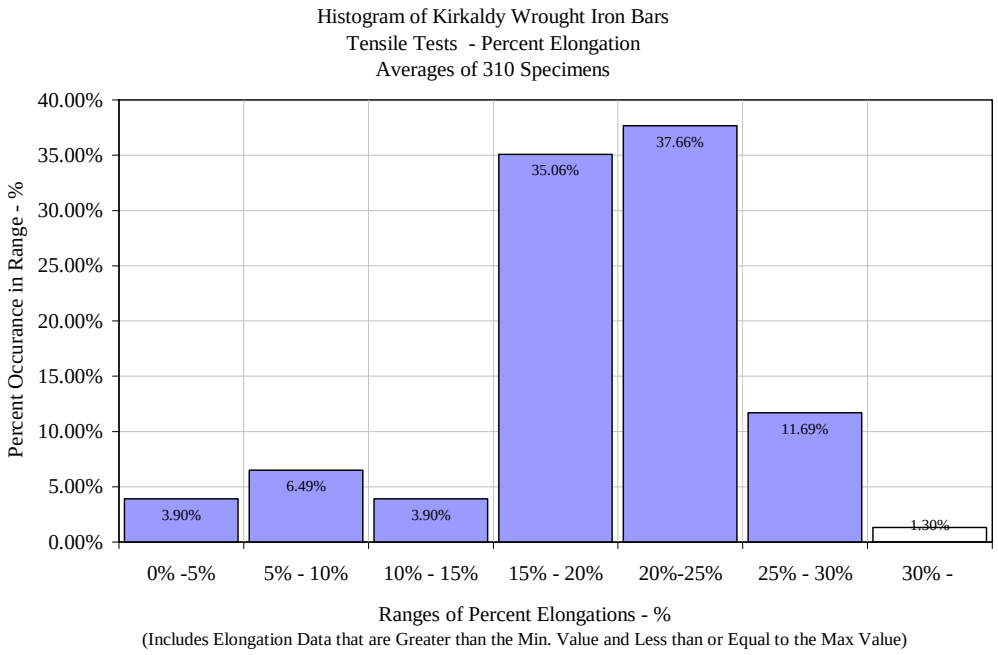

Figure 2.9 Percent Elongation of Wrought Iron Bars Tested by Kirkaldy

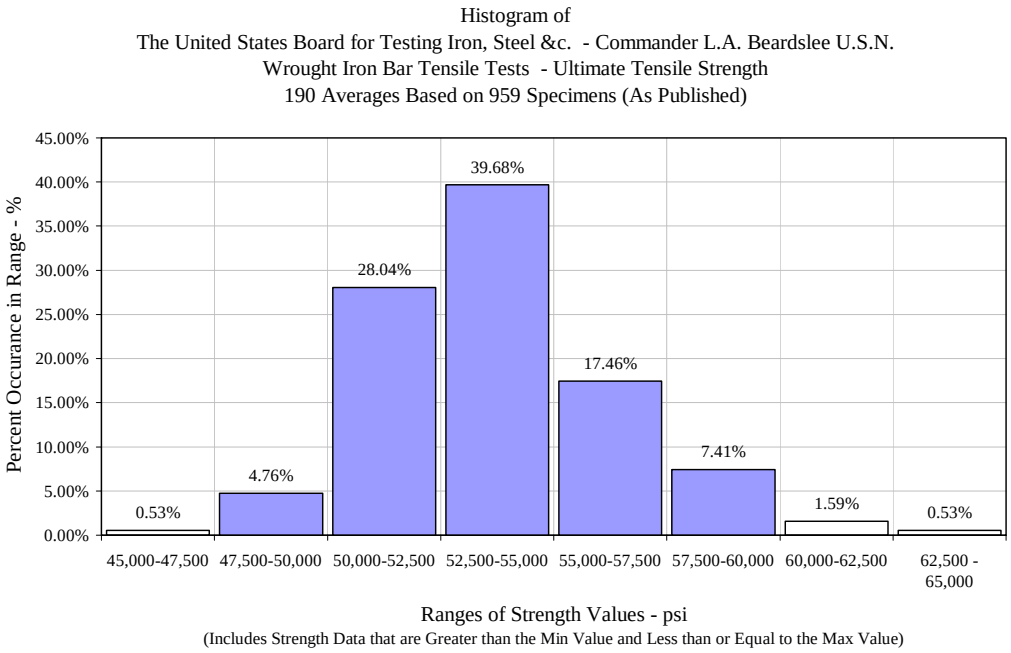

Figure 2.10 Tensile Strength of Wrought Iron Bars Tested by Beardslee

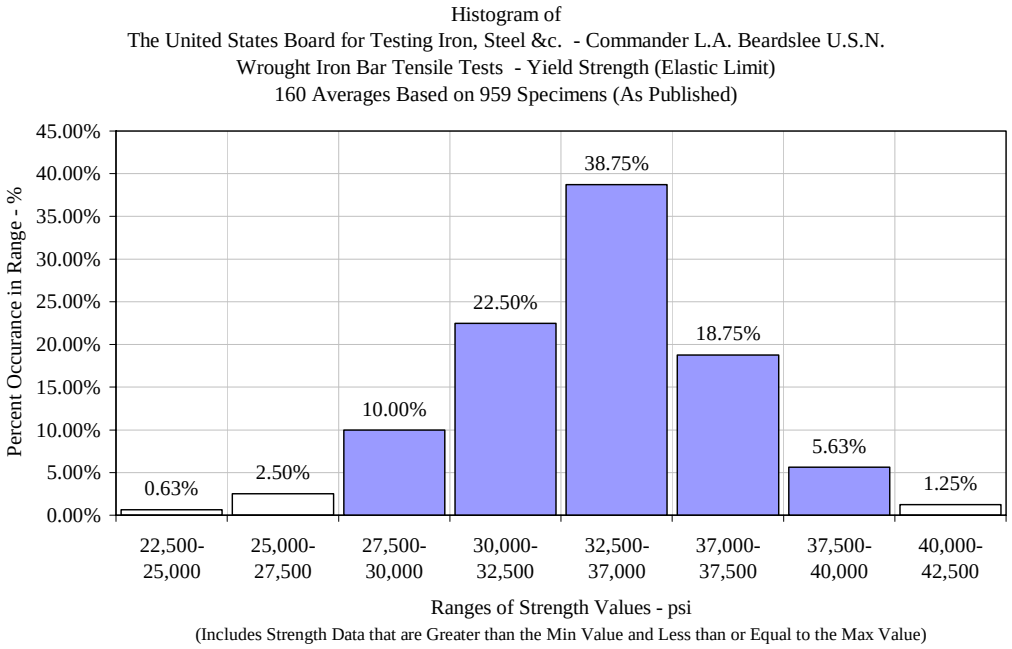

Figure 2.11 Yield Strength of Wrought Iron Bars Tested by Beardslee

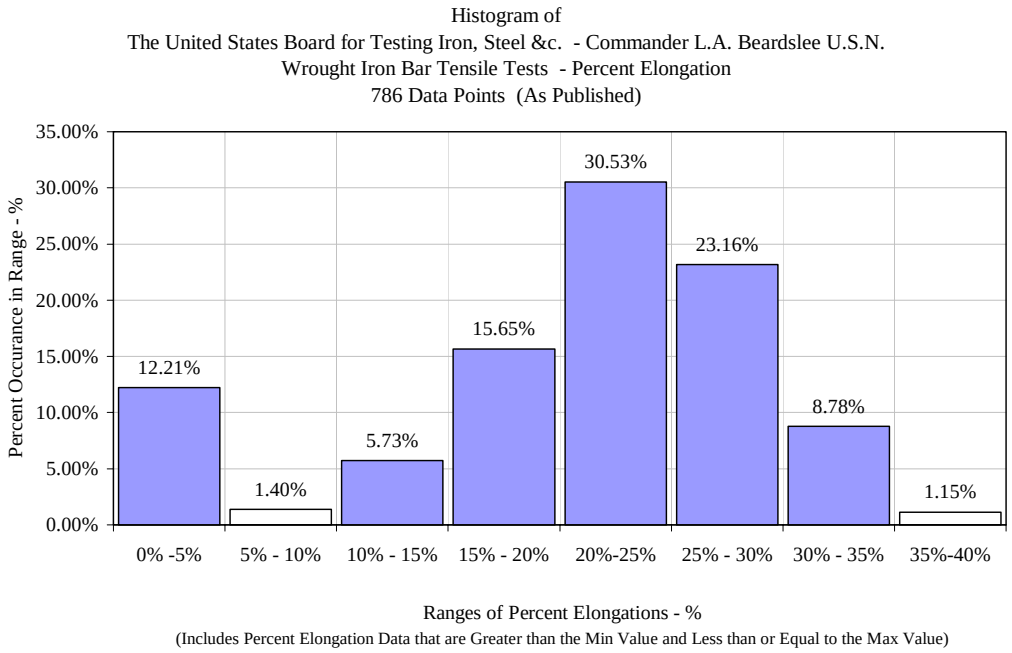

Figure 2.12 Percent Elongation of Wrought Iron Bars Tested by Beardslee

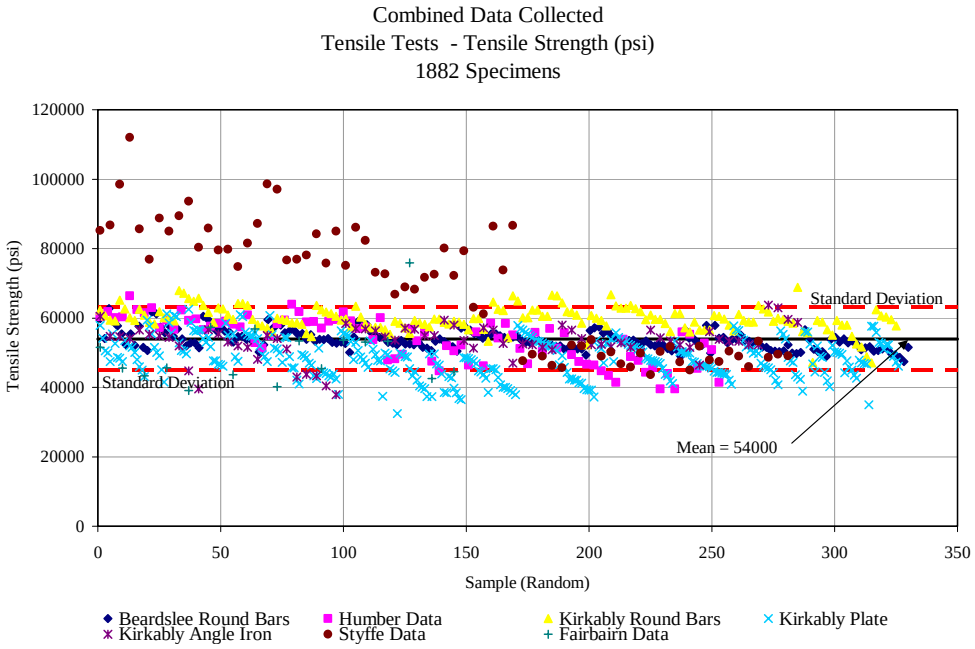

Figure 2.13 Tensile Strength of all the Data Combined

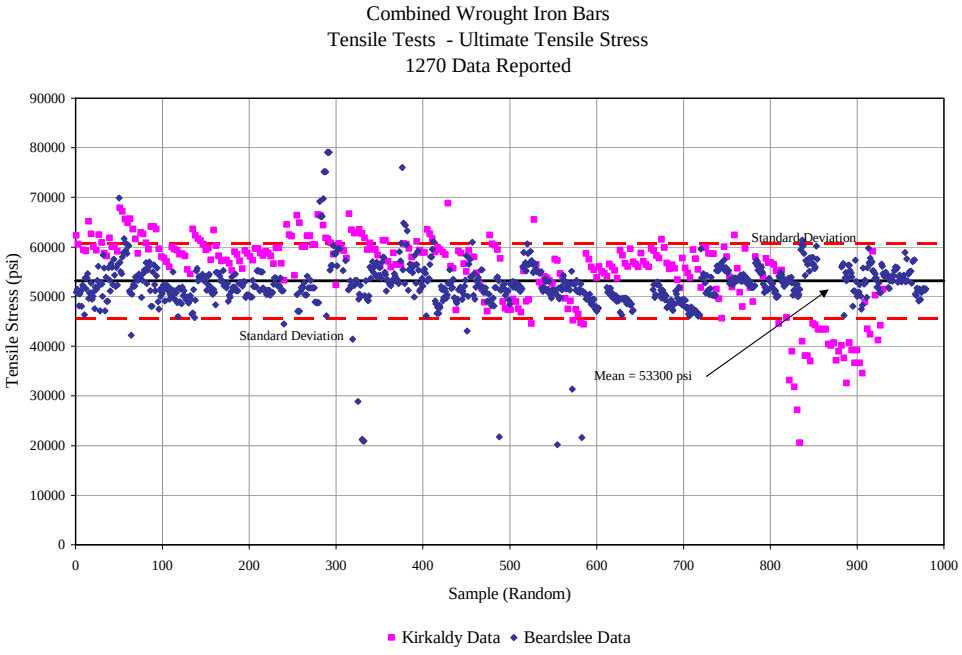

Figure 2.14 Tensile Strength of all the Bar Data Combined

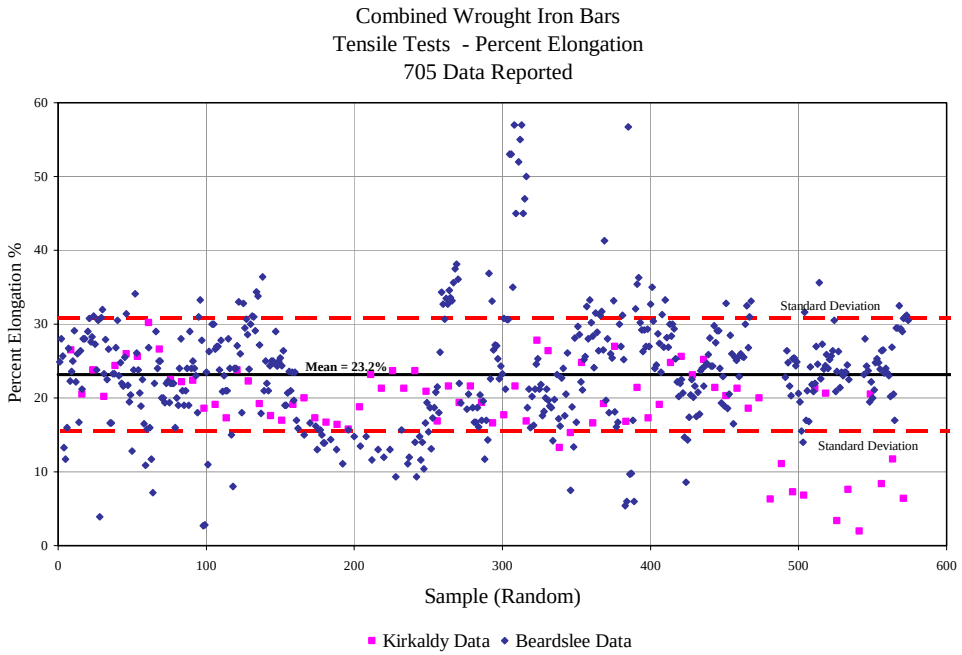

Figure 2.15 Percent Elongation of all the Bar Data Combined

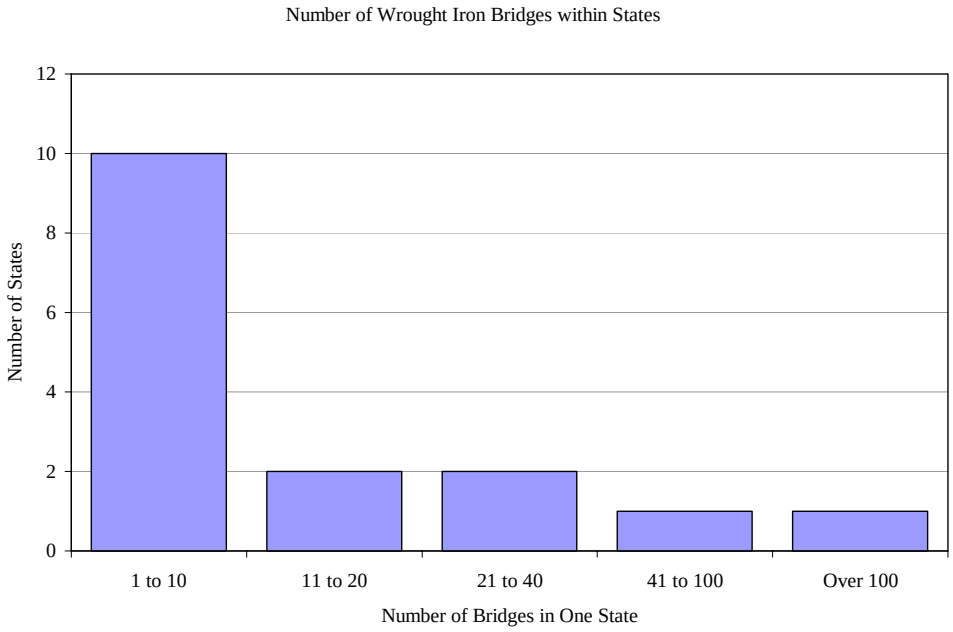

Figure 2.16 Bar Chart Showing the Number of Wrought Iron Bridges Located within a State

3. TEST PROCEDURES FOR MECHANICAL AND CONNECTION TESTS

To adequately determine the properties of wrought iron, several different tests are necessary. For this study, the following tests were completed: micrographs, chemical analysis, hardness tests, tensile coupon tests, fatigue tests, charpy impact tests, and eyebar connection tests of wrought iron members from historical bridges. This chapter describes the materials utilized, specimen descriptions, procedures followed, and data collected for all of the testing that was completed during this research.

3.1 Material Utilized in Testing

The material and structural differences between modern day wrought iron and historic wrought iron makes it necessary for only historic wrought iron to be tested and evaluated. A portion of the historic wrought iron used in the testing completed was donated by Mr. Jim Barker P.E. from J. A. Barker Engineering Inc. This material was once part of a covered bridge built in 1869 by the Seymour Bridge Company. The bridge, known as the Jackson County Bell Ford Covered Bridge, partially collapsed during a storm in February of 1999. Figure 3.1 shows a photograph of the collapsed portion of this bridge. To rebuild the bridge, members were recovered and a plan for reconstruction of the bridge was developed. J.A. Barker Engineering Inc. was hired to reconstruct and rehabilitate the Bell Ford Covered bridge. In the first phases of the reconstruction process, the wrought iron from this bridge was recovered and stored for later refurbishing. During this reconstruction process, Mr. Barker decided to donate a portion of this historic wrought iron to this research project.

The Bell Ford Bridge consisted of timber compression members and wrought iron tension members. The wrought iron tension members were the same size and shape as each other and made of the same material found in many wrought iron truss bridges. It was believed that testing these tension members would provide a reasonable estimate of the material properties of the wrought iron used in other historic wrought iron bridges.

The wrought iron tension members donated to this research project consisted of five bottom tension bars, also known as eyebars. Figure 3.2 is a photograph of eyebars, arbitrarily labeled one, two and three. These eyebars had been severely damaged in the collapse of the bridge. Two of them had been heat straightened in some areas while the third had only been heat straightened on the far end and was still disfigured. Figure 3.3 is a photograph which includes eyebars four and five. These eyebars had not encountered as much visible damage as eyebars one, two and three.

Other material that was tested in this study came from the Adams Mill Covered Bridge in Carroll County, Indiana. This bridge was built in 1873 by the Wheelock Bridge Company. Similarly to the Bell Ford Bridge, it is also a covered bridge that utilizes wrought iron members in tension. The pieces utilized for testing from this bridge, however, consisted of round tension rods that were the diagonal members of the Adams Mill Covered bridge. These tension rods were replaced with steel tension rods and the wrought iron was then stored. This stored wrought iron was donated for research. Figure 3.4 shows the round wrought iron tension rods from the bridge.

3.2 Microstructure

The specimens used to determine the microstructure of wrought iron were machined from two of the eyebars of the Bell Ford Bridge. Eyebar one and two were heat straightened and had some visible damage. From each eyebar, a piece about one inch square was cut from an area that had not been heat treated or visibly damaged. The

surfaces of these pieces were then ground smooth to remove the outer corrosive surfaces. Once the corrosion was removed, the pieces were then polished.

This was done using a range of metallic grit paper of varying roughness. Initially a very coarse paper was used to polish the specimens. Then finer grains of papers were used to polish the specimens until finally a diamond powder and polishing wheel was used to make the surfaces as smooth as possible. After polishing, a 2% Nitol solution was applied to the surface of the specimens to etch and make the microstructure visible. This same specimen preparation procedure was used to prepare a piece of carbon steel from the testing laboratory. The steel and wrought iron specimens were then compared so that the differences in the microstructures of the two metals could be observed.

To view the microstructure of the wrought iron, a microscope with a light source was used to magnify the microstructure of the metal. A digital camera was attached to this microscope and was used to photograph the magnified microstructure. To accurately determine the magnification of the pictures, a magnifying ruler was placed on photographs at various magnifications. The magnification of each photograph was then found by measuring the distance between the ruler marks on the photographs and comparing that distance to the known distance between the marks of the ruler.

The data acquired from the micrographs consisted of photographs taken of the wrought iron and steel. These photographs were magnified to approximately 100 times and accurately showed the microstructure of both wrought iron and steel. An example of the photographs acquired can be seen in Figure 3.5.

3.3 Chemical Analysis

The specimens for the chemical analysis of wrought iron were taken from members of the Bell Ford Bridge. Two separate samples were cut from Eyebars One and

Two. These samples were taken from areas on the eyebars that had not been heat treated or visibly damaged, and were approximately a half inch square in size. These samples were then sent to a commercial testing laboratory (Sherry Laboratories in Muncie, IN) which determined the chemical composition of the material. The laboratory then returned a listing of the elements found in the wrought iron. The quantity of each element was determined by finding the percent by weight for each element.

3.4 Hardness Testing

Pieces from Eyebars One, Two and Three of the Bell Ford Bridge were used for hardness testing. The Rockwell B hardness test (ASTM 370) was performed on these pieces. This procedure utilized a hardness testing machine and a 1/16 inch diameter ball to determine the hardness values of the metal. A calibration disk was used to check the results provided by the hardness machine. Hardness values were found at multiple locations of the specimens and then recorded with reference to their location. Figure 3.6 is a drawing of the hardness values determined from this testing for one piece of wrought iron.

3.5 Tensile Coupon Testing

3.5.1 Specimens Used in Tensile Coupon Testing

Tensile testing coupons were machined from all five eyebars of the Bell Ford Bridge. Eyebars 1, 2 and 3 were visibly damaged in the collapse of the bridge and had been heat straightened or mechanically straightened. Tensile testing coupons from the heat straightened areas, and mechanically straightened areas were machined from these eyebars along with non-repaired tensile testing coupons. Eyebar 4 had not experienced

visible damage and non-repaired tensile testing coupons were also machined from this eyebar. Welded tensile testing coupons were machined from Eyebar 5 which also had not experienced much visible damage.

Eyebars 1 and 2 were partially heat straightened to help the machinist prepare the testing samples. To heat straighten the eyebars, a blacksmith heated the damaged and bent areas until they were bright red hot in color. Once the material was heated to this color, the pieces were then hammered until they were straightened. The heat straightening created a blue area that was easily noticeable on the wrought iron eyebars after cooling to room temperature. Figure 3.7 is a photograph demonstrating the color variation in the wrought iron eyebar after heat straightening.

To more accurately determine the temperature of the wrought iron during heat straightening, a sample from Eyebar 3 was heated until it was the same cherry red color used when areas on Eyebars 1 and 2 were heat straightened. A pyrometer was then used to record the temperature at various locations on the red hot piece of wrought iron. The temperatures ranged from 1160 to 1270 degrees F. Figure 3.8 illustrates the test piece when it was the cherry red color immediately before the temperature was taken.

All of the heat straightened areas were measured and recorded. Then an appropriate labeling scheme that noted which specimens had been heat treated was developed. This labeling scheme was marked on the eyebars in sections where the corresponding specimens were to be removed and machined. The sections of the eyebars were carefully measured and then cut for tension coupon testing specimens.

Eyebar 1 and 2 contained sections of both heated and non-heated areas. These two eyebars were split into appropriate sections and then machined into standard tension testing coupons. To meet ASTM A370 standards, the eyebar sections were surface ground and then milled to the adequate dimensions. It was essential to ensure that the

specimens were of constant cross sectional area. Figure 3.9 is a drawing of the tensile coupon dimensions that were used for the testing samples.

Eyebar 3 from the Bell Ford Bridge was too disfigured and bent from the collapse to be used without further straightening. It was decided that mechanically straightening a specimen from this eyebar would be beneficial to evaluate the effects from straightening without heat. A section from the eyebar of the same length as the test coupon (18") was removed and measured to determine the amount of curvature and deflection in the piece. The piece was then bent in the center with a deflection of a half inch compared to the ends.

A three point method was used to straighten the piece. Figure 3.10 is a drawing of the method used to straighten the bent piece. In this method, two vertically fixed supports hold the piece in place while a plunger pushes the piece past a neutral position. This force counters the residual stresses holding the piece in its original curved shape. The force then creates new residual stresses that again change the shape of the piece. After deforming the piece originally, it was again slightly deformed in the other direction. The piece was then turned over and the three point method was repeated to straighten the piece even more. This process was repeated until the piece was completely flat. Once the piece was bent into a flat shape it was then machined into the standardized tensile coupon shape.

Eyebar 4 from the Bell Ford Bridge had not been heat straightened and had not experienced much visible damage from the collapse. Therefore, standard non-treated tensile specimens where machined from this eyebar. These specimens were used to compare with the other specimens that experienced more damage and repair procedures.

Eyebar 5 was similar to Eyebar 4 because it was not damaged as significantly as the first three eyebars. From Eyebar 5, welded tensile coupons were machined for testing. The eyebar was cut into sections from which the specimens would be machined.

The sections of the eyebars where labeled on either side and then cut directly into half. These halves were then beveled and joined together using the shielded metal arc welding process.

The joint used for these groove welded specimens was a double V butt joint with a sixty degree incline and a one sixteenth inch land. Figure 3.11 is a detail of the connection used for welding the specimen. Weld passes were alternated on either side to ensure that heat distortion in the piece was minimized.

After the initial root pass was completed, the surface of the weld pass was cleaned with a chisel hammer and wire brush and then back ground on the opposite side where the second weld pass was to be placed. This was to ensure the second weld pass fully penetrated the wrought iron and the initial pass. Figure 3.12 is a photograph of the welded connection after the initial root pass had been deposited and ground back to the weld metal. After the second weld pass, the specimen was again cleaned with a chisel hammer and wire brush and the piece was turned over and slightly back ground for the following pass. This process continued until the final weld passes were above the surface of the specimen on either side. A more detailed description of the welding procedure utilized for this testing is provided in Appendix D.

Once the joint was completely welded, the surface of the piece was then ground flush so the piece was completely flat. From this smooth piece the tensile coupon specimen was then cut out of the center of the piece. Cutting the specimen out of the center of the piece helped to ensure that only an adequate weld would be tested. This is because the ending and starting points of the weld, which usually include impurities and air pockets, were removed during machining. To evaluate the effect of weld metal on the wrought iron, two different weld metals, E6010 and E7018 SMAW, were used to weld different specimens together.

Along with rectangular tensile coupons taken from eyebars of the Bell Ford Bridge, round tensile coupons were also tested from the Adams Mill Covered bridge. The members from this bridge consisted of round diagonal tension rods. Similar to the eyebars, these rods were measured and sectioned into pieces. The pieces where then labeled and test specimens were removed and machined from these pieces. The dimensions of these specimens can be seen in Figure 3.9. The tensile coupon specimens used in testing were considered to be non-treated standard specimens. Figure 3.13 is a photograph of a typical round tension testing coupon.

3.5.2 Testing Procedure for Tensile Coupon Testing

After the tension coupon specimens had been machined, the coupons were then prepared for testing. To begin, a gauge length was marked at the center eight inches along the coupon sample with a ruler and some scribes, so the markings were permanent. The center point of the sample was also scribed along with the two-inch placement of the extensometer along the edge of the sample. These scribe indentations were then intensified with a black marker for ease of viewing. Once the sample was scribed, the width and thickness of the sample was measured using a micrometer at nine different points along the gage length. These values were then averaged and multiplied together to obtain the average area along the gage length of the sample to nearest thousandth of a square inch.

Measurements Group CEA-06-250UN-350 type strain gages were applied to both faces in the center of the testing coupons. These strain gages were used to measure very small changes in length while testing the tensile testing coupons. They were applied using the appropriate methods described by Measurements Group, Inc. The manufacturer’s specifications were followed when installing these gages to ensure that an adequate bond of the gage to the metal was obtained.

With the strain gages attached, the sample was ready to be loaded in the testing machine. The testing was performed in the Kettelhut Structural Engineering Laboratory using a 220-kip MTS servo-hydraulic testing machine. A level was used when placing the coupon in the grips of the machine. This was done to ensure that the specimen was vertical and that only tension in one direction would occur in the coupon. A two inch extensometer was then attached to the specimen using very tight and strong elastic bands in the center two inches of the coupon. Figure 3.14 is a photograph of the specimen after it had been marked, the strain gages had been applied, the extensometer attached, and placed in the testing machine grips.

The strain gages, extensometer, load cell, and stroke readings were all transferred to a Measurements Group System 5000, Model 5100 data acquisition scanner and computer where they were interpreted and recorded using Strain Smart software. The function generator and controller of the MTS testing machine were used to control either the loading rate or the (stroke) crosshead rate, depending on the type of test conducted. For each coupon, two different tests were completed.

In the initial test, the specimen was loaded only in the elastic region of the stress-strain curve. In this test, the rate of increase in load being applied was controlled while the amount of strain in the specimen was recorded. The readings from the strain gages, extensometer, load cell and stroke LVDT of the MTS machine were recorded during this test. This test was conducted at a rate of five thousand pounds per minute.

The sample was only stressed until 15 ksi or less was reached in the specimen. The reason for such a low stress limit during the initial loading was to ensure that the specimen was never taken out the elastic region for wrought iron and thus permanent deformations were never created. Using the strain gages, and load cell readings, the stress-strain elastic linear relationship could be plotted for each sample.

After the initial test loading was completed, the coupon was then tested until failure. This was done with the amount of stroke movement in the MTS machine being controlled; in stroke control the rate of crosshead movement in the sample is controlled rather than the loading rate. The testing coupon was then loaded at a rate of 1/32 inch per minute until specimen yielding, and was then stretched 1/8 inch per minute in the plastic region until failure. Similarly, as in the initial test, the readings from the strain gages, extensometer, load cell and stroke LVDT were recorded using Strain Smart Software.

Once both tests were completed, the readings in Strain Smart were then transferred into a spreadsheet so that the results could be plotted and evaluated. The modulus of elasticity, yield stress, ultimate tensile stress, and strain hardening exponent and coefficient where then determined from these data. The markings from the original measured eight inch gauge length were measured again and compared to the original length to obtain the percent elongation.

3.5.3 Type of Data Collected from Tensile Coupon Testing

For both coupon tests, the strain gage readings, extensometer, load cell and crosshead stroke of the MTS machine, were recorded using the data acquisition unit. These recordings were then transferred into engineering units using Strain Smart Software. The values recorded from the strain gages were recorded in micro strains, which indicates that the actual strains in the specimens were $1x\ 10^{-6}$ times the micro-strains reported. Strain is simply the amount of stretch in the specimen divided by the original length; therefore it is a unit-less quantity.

The extensometer recorded values in terms of inches. These values were then converted into micro strains to correlate with the strain gages. This was done in a spreadsheet after the Strain Smart software had transferred the data. The extensometer readings were converted by dividing the actual recordings by the extensometer gage

length of two inches. This value was then multiplied by $1x10^6$. The final extensometer readings were then displayed in micro strains. The values recorded from the stroke, or the amount the MTS machine moved, were used to verify other readings.

The load cell in the MTS testing machine's output was in pounds. This value was converted to stress (psi) using the average area determined before testing. This was done by dividing the output of force in units of lbs, from the load cell, by the average net section area of the test coupon.

After all the units were converted, the stress strain diagram could then be created by using a spreadsheet package. For the initial test, the average output from the two strain gages were plotted against the load cell's output to create a plot of the elastic region of the stress strain curve for the metal. A plot of this initial elastic region for one of the test specimens can be seen in Figure 3.15.

The average output of the two strain gages was also used along with the extensometer when creating the full stress-strain curve from the second test. In the initial elastic area of the stress-strain curve, the strain found from the output from the strain gages was plotted against the stress found from the output from the load cell. Once the specimen yielded, the strain found using the output from the extensometer was plotted against the stress found from the output of the load cell. This plotted the inelastic non-linear curved section of the stress-strain curve. An example of a full stress-strain curve found from full testing of one of the test specimens can be seen in Figure 3.16.

Along with the stress verses strain curves, the amount of stretch at failure was also recorded. This deformation, which is a measure of the material ductility, is the amount that the eight inch gauge length (for the eyebar) had stretched at the onset of failure. This was found using a ruler and measuring the distance between the original scribed eight inch gauge marks. The amount that the gauge length distance had changed was then divided by the original gauge length to determine the percent elongation.

3.6 Fatigue Testing

To develop a better understanding of the fatigue behavior of wrought iron found in many historic bridges, some limited fatigue testing was completed during this study. Four un-notched, smooth tensile coupon specimens were prepared from round bars of the Adams Mill Bridge. The larger diameter round bar material was machined to a reduced half inch diameter coupon, the same as tensile coupons as seen in Figure 3.9.

The specimens were tested under constant-amplitude alternating stress until either failure or three million cycles occurred. The stress ranges utilized in testing were 20 ksi, 30 ksi, and 35 ksi (two specimens). The R value, which is the ratio of minimum to maximum stress, was maintained at 0.05; hence, compressive loading was never placed on the specimens during testing. This simulates the type of loading that an actual wrought iron bridge tension member would experience throughout its life, since the member is typically under some tension stress to support the dead load of the bridge.

The fatigue specimens were tested using a 220-kip MTS four-pole servo-hydraulic testing machine in the Kettelhut Structural Engineering Laboratory at Purdue University. Each specimen was cycled at a rate of 2.5 Hz, in a sinusoidal pattern. A mechanical counter attached to the MTS testing machine was utilized to record the number of cycles each specimen had undergone. The amount of time passed was also recorded to serve as a back-up check of the counter accuracy. For each fatigue test performed, the alternating stress and number of cycles were recorded.

3.7 Charpy Impact Testing

Material from the Bell Ford Bridge and Adams Mill Bridge were used to create specimens for Charpy impact testing completed during this study. The specimens machined from the eyebars in the Bell Ford Bridge where orientated in different

directions. This was done to determine the fracture toughness in various directions of the material.

The first type of orientation and specimen category is the Longitudinal Notched to the Side specimen (LS). The long direction of this specimen type runs along the length of the eyebar. This direction is parallel to the direction in which the eyebar was “rolled”, and is the same direction in which the slag particles in the material are elongated. The notch of the LS specimens was orientated to the side of the eyebar, as shown in Figure 3.17. This orientation of the notch evaluates the fracture toughness of the material to resist a crack if it was running against the longitudinal grain-like structure of the wrought iron and propagating across the width of the eyebar.

The second type of orientation and specimen category is the Longitudinal Notched to the Top specimen (LU). The long direction of these specimens, like the LS specimens, runs along the length of the eyebar. The notch of the LU specimens was faced upward, toward the top or front of the eyebar, as seen in Figure 3.17. This orientation of the notch evaluates the material fracture toughness to resist a crack if it was running through the thickness of the eyebar and against the longitudinal grain-like structure of the wrought iron. LU specimens are similar to LS specimens, although the direction of crack growth differs.

The third type of orientation and specimen category is the Transverse Notched specimens (T). The long direction of this specimen type is perpendicular to the longitudinal direction of the eyebar. The T specimens are therefore perpendicular to the other LU and LS specimens and the slag deposits that are deposited along the length of the eyebar. The notch of the T specimens was orientated to the side of the specimen, -see Figure 3.17. This orientation of the notch evaluates the fracture toughness of the material to resist a crack that runs along the longitudinal direction of the eyebar.

The final specimen category consists of charpy impact specimens machined from the round tensile rods from the Adams Mill Bridge. Only one orientation of the specimens was possible to be machined from the original bridge pieces due to the size and shape of the members. The longitudinal direction of the Charpy V-notch specimen was parallel to the direction of rolling, similar to the LS and LU specimens. The orientation of the notch on these specimens evaluated the fracture toughness of the material to resist a crack that runs through the cross section of the round bars.

The specimens used in the Charpy impact test to determine the fracture toughness of the material were Charpy V-notch specimens. Figure 3.18 shows the standard dimensions provided in the ASTM E23 (2001) Specification for these specimens. This standard was used when machining the Charpy V-notch specimens.

The Charpy impact test determines the impact energy of the specimens at different temperatures. The procedure (ASTM E23) calls for the specimens to be cooled to a specified temperature before being placed in the impact testing machine. Once in the impact testing machine, a swinging weight strikes and breaks the specimen and the impact energy is determined. Figure 3.19 is a photograph of the SATEC impact testing machine used for this testing, which was installed and verified to national testing standards.

A number of different test temperatures were used to evaluate the fracture toughness of the wrought iron over a wide range of temperatures. The specimens were tested at room temperature, forty degrees Fahrenheit, ten degrees Fahrenheit, negative ten degrees Fahrenheit, and negative thirty degrees Fahrenheit. To cool the specimens to the desired temperatures, they were suspended in a liquid bath consisting of either ice and water or ice, water, and alcohol.

The specimens were suspended by placing them on a chicken wire platform that was inside of a Styrofoam cooler. A photograph of this setup can be seen in Figure 3.20.

Depending upon the desired temperature different liquid and ice combinations were used. To achieve a constant temperature of forty degrees Fahrenheit, for example, a combination of ice and water was used. To achieve constant temperatures of ten degrees Fahrenheit or below, a combination of dry ice, water and alcohol was used.

Once the liquid cooling bath used for cooling the Charpy V-notch specimens reached the desired temperature, the specimens remained suspended in the bath for a minimum of five minutes. Then they where transferred to the anvil of the impact testing machine and the weighted lever arm and was released and the specimen broken. As per ASTM E23, this step was to be completed in 5 seconds or less to ensure the temperature of the sample did not increase notably. A dial on the impact testing machine read the impact energy needed to break the specimen.

The data acquired from performing this test consisted of the temperature of the specimen and the correlating impact energy. Also, the characteristics of the fracture plane on the Charpy V-notch samples were noted.

3.5 Eyebar Connection Testing

The eyebars that were received from the Bell Ford Bridge were composed of a middle or “shank” section and one or two end connections – see Figure 3.2 and Figure 3.3. These end connections consist of one large hole in a wider and thicker cross section, where the eyebar would be attached to the bridge using a large pin. The diameter of the holes in these connections were 2 ¼ inch. The material around the hole was wider than the shank to decrease the possibility of failure in the connection and not the shank. To more fully understand the behavior of these connections a finite element analysis and experimental evaluation of the eyebar connection was completed.

This analysis was completed using the computer software ANSYS. To use this software, an accurate model of the connection detail was drawn. This was done by carefully measuring the dimensions of the connection and then accurately drawing them in a CAD software package. This model was then imported into ANSYS. While using the computer analysis software, an accurate loading model was applied to the connection detail. This model consisted of pulling a constant force of 30,000 psi over the shank of the connection and holding one side of the connection hole in place by preventing the nodes around the inside of the hole, where contact with the pin would occur, from displacing. A combination of quadrilateral 4 node elements with two degrees of freedom at each node (Q4) that were ¼ inch in size were meshed into the connection detail. The loading effects on the connection were then analyzed.

The connections at the end of the eyebars were experimentally tested also. It should be noted that the entire eyebar was not tested, but rather only a portion of the eyebar at the end of the member. Enough material was retained, after removal of the tensile coupons, so that the eyebar connection could be tested. Consequently, the length of the test piece was usually between eighteen to twenty-five inches in length, as can be noted in Figure 3.2, which shows the eyebar markings for removal of the tensile coupons.

The eyebar connection was loaded in tension using the 220-kip servo hydraulic MTS testing machine. Before placing the eye connection into the testing machine, strain gages were applied to the surface at ten locations on both faces of the connection. All gages were oriented in the longitudinal (loading) direction.

Two Measurements Group CEA-06-250UN-350 type strain gages were placed in the bottom shank of the eyebar connection on either side – Gages 1 and 2 in Figure 3.21. Measurements Group CEA-06-125UN-350 type strain gages were placed on each edge of the hole on both faces of the connection – Gages 3 thru 6 in Figure 3.21. Measurements Group CEA-06-125UN-350 type strain gages were then placed on one face away from one of the gages on the edge of the hole to the end of the eye connection – Gages 9 and

10 in Figure 3.21. Two Measurements Group CEA-06-125UN-350 type strain gages were also placed on the side (thickness) of the eyebar connection – Gages 7 and 8 in Figure 3.21. Figure 3.22 shows one of the eyebar connections after the strain gages were attached.

A fixture was manufactured to load the eyebar connection test sample. This fixture consisted of three thick steel plates that were bolted together. The dimensions of the plates were determined so that yielding would not occur in the plates prior to failure occurring in the eyebar connection. The middle plate was inserted into the MTS machine while the other two plates extended down to the eye connection detail. These two plates had holes that were 2 ¼ inch in diameter, similar to the eye connection detail.

A large pin, 2 $^{3}/_{16}$ inch diameter steel rod, was inserted through all three holes and the eyebar connection was therefore connected to the test fixture. The shank of the eye connection was then placed in the second lower grip of the MTS testing machine. Figure 3.23 is a photograph of the test fixture and eyebar connection in place in the MTS testing machine. After the eyebar connection was placed into the MTS testing machine a two inch extensometer was attached to the shank of the eyebar above the lower grips of the MTS testing machine with some very tight elastic bands. Then the strain gages, load cell, stroke crosshead, and extensometer were attached to the data acquisition scanner for recording.

Similar to the tensile coupon testing procedure, two tests were completed on the eye connection. In the initial test, the specimen was loaded only in the elastic region of the stress strain curve with the load applied at a fixed rate of five thousand pounds per minute. The readings from the strain gages, extensometer, load cell and stroke were continuously recorded during this test. The sample was only stressed until a stress of 12 ksi or less was reached in the shank of the specimen. Again, the low stress limit used for this test was to ensure that the specimen was never taken out the elastic region for wrought iron and permanent deformations were never created.

After the initial test was completed, the sample was then tested until failure. This was done with the amount of stroke movement in the MTS machine being controlled. This means that the amount of strain placed on the sample was controlled rather than the amount of load that was placed on the sample. The testing coupon was first pulled at a rate of 1/32 inch per minute until after the yielding, and was then stretched 1/8 inch per minute in the plastic region until failure. As in the initial test, the readings from the strain gages, extensometer, load cell and stroke control were recorded using the Strain Smart software. Once the test was completed, measurements were taken of the eye hole using a micrometer parallel and perpendicular to the direction of loading. This was done to determine the amount of elongation of the hole in the connection.

From the initial test, the data collected were the linear strains that occurred during the elastic testing. The strains that occurred for all ten gages were then depicted on the same plot so that they could be compared to each other. From this plot it can be seen where the stresses are greater on the eye connection. A plot of the strains that occurred at the various strain gages for one eyebar connection test can be seen in Figure 3.24. This data was then compared to the results generated from the ANSYS computer model of the eye connection. The second test to full failure was completed to see if the connection would fail in the eye detail or in the shank.

3.9 Eyebar Connection Testing with Filler Weld

A common problem that occurs when repairing historic iron truss bridges is excessive corrosion of these eyebar end connections. Often it is too costly to replace the entire eyebar, so a less expensive repair method is preferred. Therefore, along with investigating the behavior of a typical eyebar end connection, the behavior of a damaged and repaired eyebar end connection was also investigated. One repair method that was investigated during this study was filling the corroded area of the eyebar with weld material to reduce the loss of section. Two eyebar end connections were tested in tension

using the 220-kip servo hydraulic MTS testing machine in the Kettelhut Structural Engineering Laboratory, each with different patterns of corrosion and repair modeled.

The first eyebar connection, Eyebar A had material removed to simulate a common corrosion pattern found on the lower chord eyebars of historic iron truss bridges. In this pattern, excessive corrosion was typically prevalent in an arched area on the bottom edge of one surface of an eyebar end connection. This corrosion is most likely the result of condensation that collects at the edge on one side of a bottom chord eyebar member. Figure 3.25 is a picture of Eyebar A, after some of the material was removed to model this corrosion pattern. Half of the thickness of the original eyebar was removed in the area of which the eyebar was machined to resemble corrosion.

Once this material was removed, the area simulating corrosion needed to be filled with weld material. To do this an E7024 SMAW 1/8” diameter welding rod was utilized with a DC reverse polarity electric source. The welding rod used is only permitted for welding in the flat and horizontal direction but is a very good filler welding rod and reduces the number of passes needed to fill the area.

Welding passes were added in the long direction of the treated area to reduce heat distortion in the eyebar. The initial root pass was placed in the far corner of the area that was removed with the bar lying flat on a surface. Figure 3.26 shows the eyebar after the initial pass had been placed, and illustrates the direction in which the welds were deposited.

Additional weld passes were added first along the base of the removed section and then on top of the previous welds using the same procedure between passes. This procedure consisted of checking the temperature of the metal to ensure that it had not exceeded approximately 280 deg F to ensure that the filler weld would not be too fluid and the metal to hot to weld. The weld was also cleaned with a chisel hammer and wire brush. Figure 3.27 shows the eyebar end connection after the filler welding was

completed, but before the surface was ground flush to make the welds blend into the original eyebar connection.

Eyebar B was modeled to be a worst case scenario of section loss due to corrosion in an eyebar end connection. In this eyebar, half the thickness of the original eyebar's material was removed from the center two and a half inches around the hole and perpendicular to the direction of loading. Figure 3.28 shows Eyebar B after this material was removed and prepared for welding.

Once this material was removed, the area simulating corrosion needed to be filled with weld material. To do this an E7024 SMAW 1/8" diameter welding rod was utilized with a DC reverse polarity electric source, similar to Eyebar A. An initial pass around the hole in the eyebar and along the open edges were placed to create a dam for the filler material, as can been seen in Figure 3.29.

Once the initial passes were placed, filler passes were then placed in the open area in the direction of loading of the eyebar to reduce heat distortion. In between passes the temperature of the base metal was also monitored to ensure the metal was not to hot to weld and to reduce the amount of heat distortion in the metal. It was necessary to take breaks and allow the metal cool between sets of passes. The welds were also cleaned using a chisel hammer and wire brush in between each pass. Figures 3.30 and 3.31 show the eyebar end connection after all the welding was completed.

As can been seen in Figure 3.31 there was a slight amount of heat distortion and curvature in the wrought iron eyebar connection from the filler weld. To straighten this piece, the eyebar was heated until it was red hot, as seen in Figure 3.32, and then straightened by striking the eyebar with large hammer. The color of the eyebar was similar to the color of the iron that was heat straightened in the tension testing coupons and therefore at the adequate temperature to straighten the iron without inducing

significant strain damage in the metal. The eyebar was then allowed to cool slowly and then surface ground to make the filler weld blend into the original eyebar.

After surface grinding to a flush condition, Measurements Group CEA-06-250UN-350 type strain gages were placed on both faces of the shank of the eyebar connections of Eyebars A and B. Figures 3.33 and 3.34 are photographs of the eyebars after being surface ground and directly before testing. The same fixture that was utilized with the MTS testing machine when testing the eyebar connection that had not been repaired was also used in testing Eyebar A and B.

This fixture, which consisted of three thick plates that were bolted together, was placed in the upper grip of the testing machine. A $2\ ^{3}/_{16}$ inch steel pin was placed through two of these plates and hole in the eyebars. The bottom of the eyebar was then placed in the bottom grip of the MTS testing machine. A two inch extensometer was then attached at the shank of the eyebar connection above the lower grip with strong elastic bands. Figures 3.35 and 3.36 are front and side view photographs of Eyebar A immediately before testing.

The eyebar connections were then tested in the same manner than the eye connections that had not experienced any repair. The eye connections were initially loaded only in the elastic region of the stress-strain curve. In this test, load was applied at a fixed rate while the amount of strain in the specimen was recorded. The readings from the strain gages, extensometer, load cell and stroke were recorded during this test. This test was done at a rate of five thousand pounds per minute. The sample was only stressed until a stress of 10 ksi or less was reached in the shank of the specimen. This test was completed to ensure that the testing and data recording equipment was working properly.

After the initial test, both Eyebar A and B were loaded completely until failure. The eye connections were pulled at a constant rate of 1/12 inch per minute until failure. The failure location of the eye connections was recorded along with the strain gage

readings, load cell readings and extensometer readings that were recorded during testing. Once the test was completed, measurements were taken of the eye hole using a micrometer parallel and perpendicular to the direction of loading to determine the amount of elongation of the hole.

Figure 3.1 Bell Ford Bridge After Collapse of One Span

Figure 3.2 Donated Eyebars 1 thru 3

Figure 3.3 Donated Eyebars 4 and 5 Along With a Similar Eyebar that Was Straightened and Used in the Reconstruction of the Bell Ford Bridge

Figure 3.4 Round Diagonal Tensile Rods

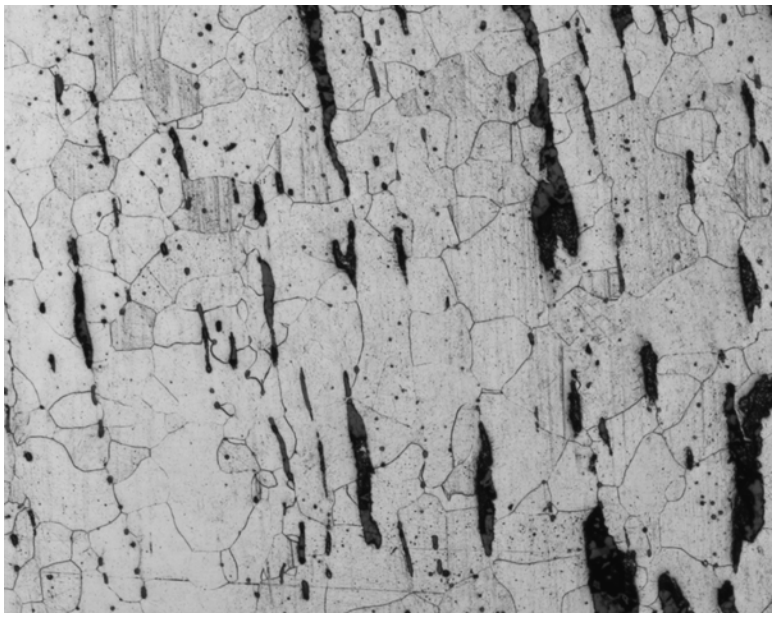

Figure 3.5 Micrograph of Wrought Iron (100 x magnification)

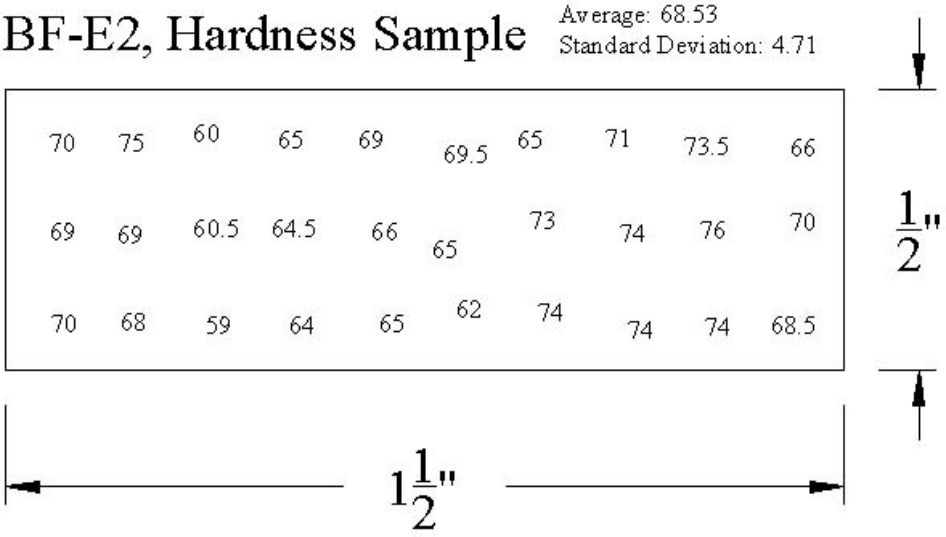

Figure 3.6 Hardness Values for One Sample of Wrought Iron

Figure 3.7 Heated Areas in Blue on Eyebar 2

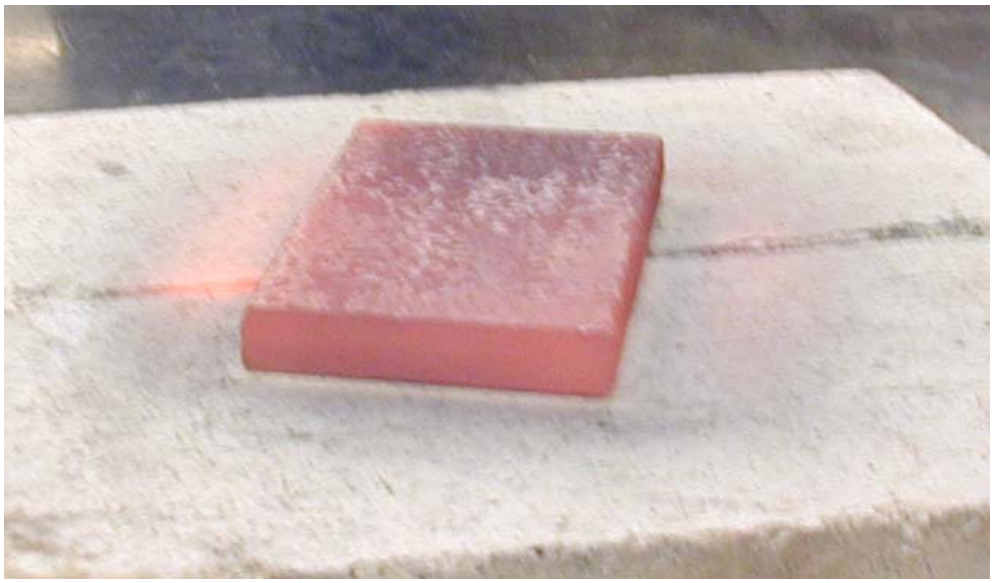

Figure 3.8 Piece of Historic Wrought Iron From Eyebar 3 Heated Till it is Cherry Red In Color

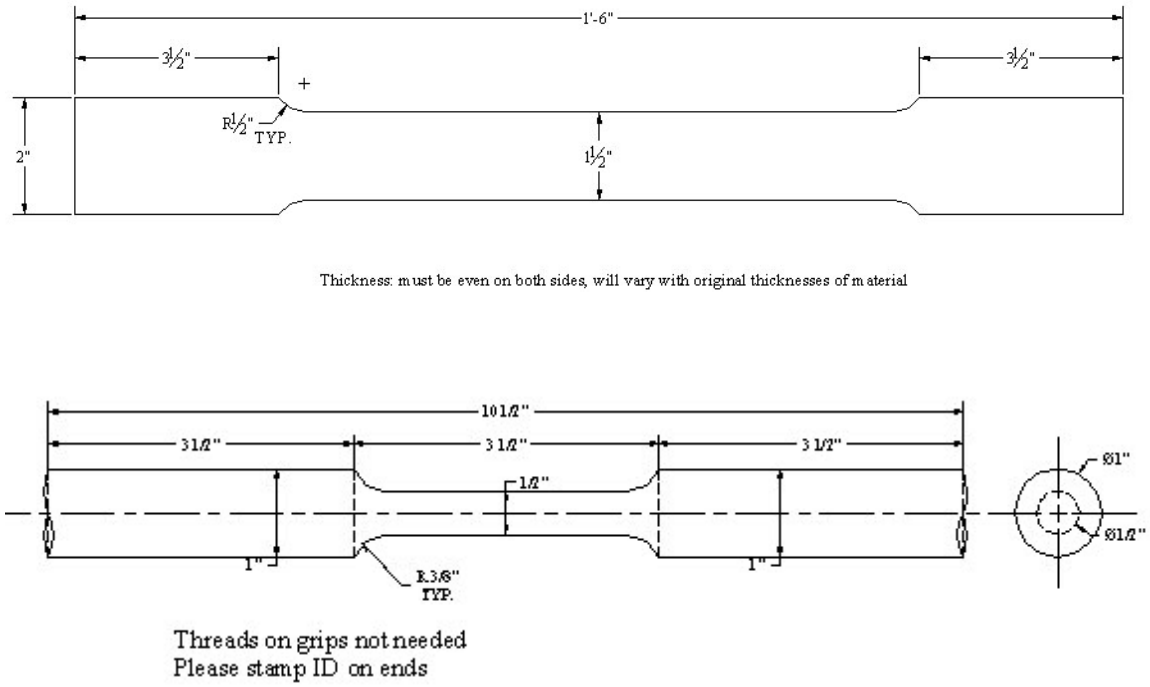

Figure 3.9 Tensile Coupon Dimensions per ASTM 370

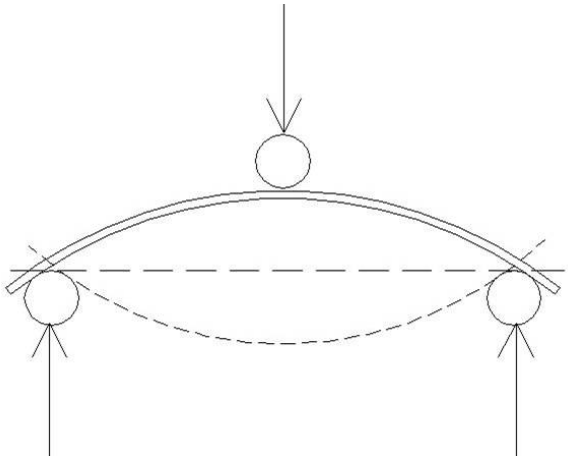

Figure 3.10 Method used to Mechanically Straighten a Bar

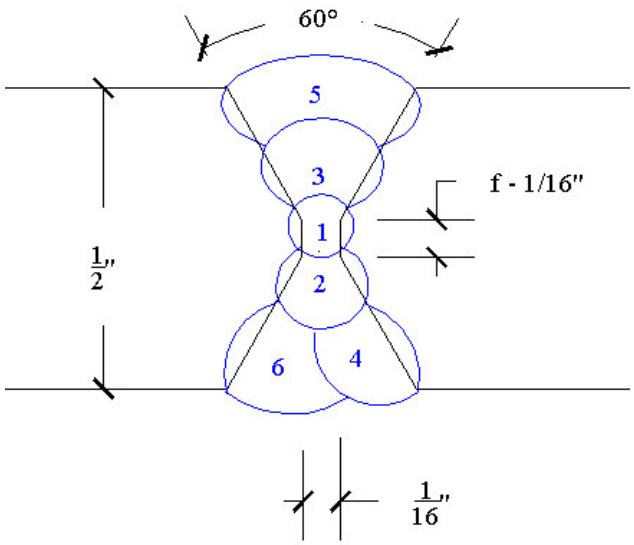

Figure 3.11 Detail Used in Groove Weld Test Specimens

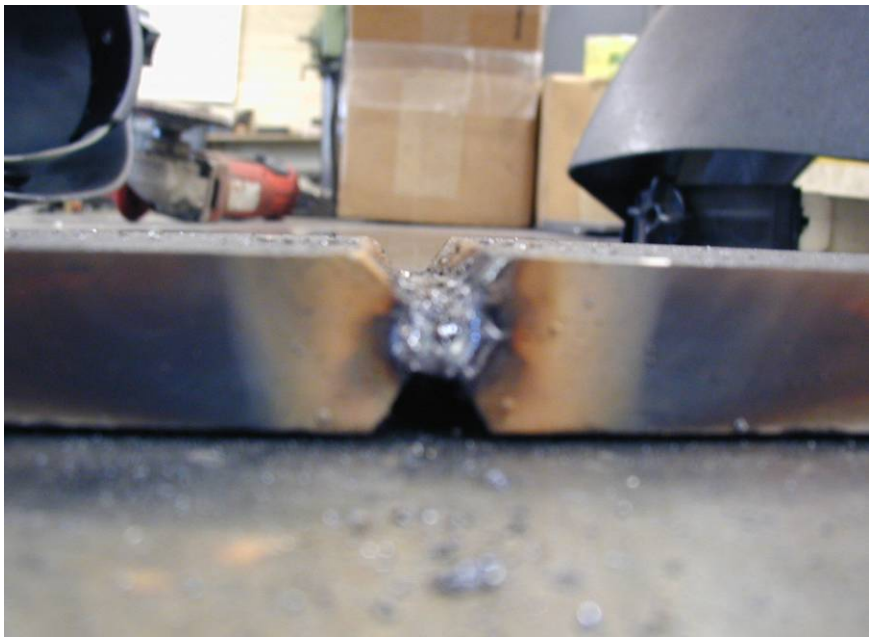

Figure 3.12 Weld Detail after Initial Root Pass on Testing Specimen

Figure 3.13 Round Tensile Testing Specimen

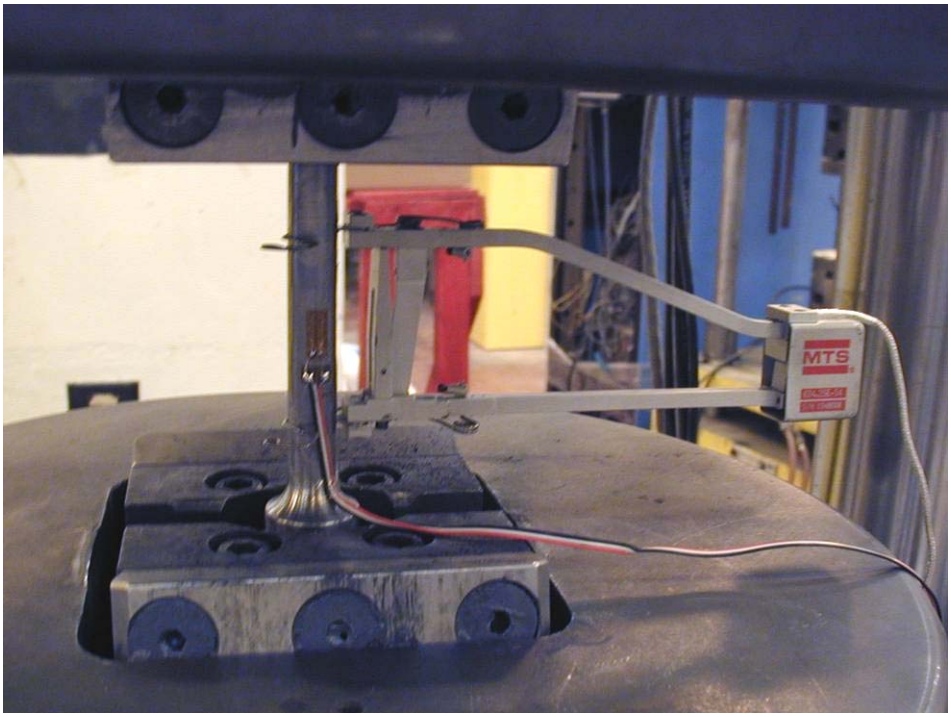

Figure 3.14 Specimen in Testing Machine Ready to be tested

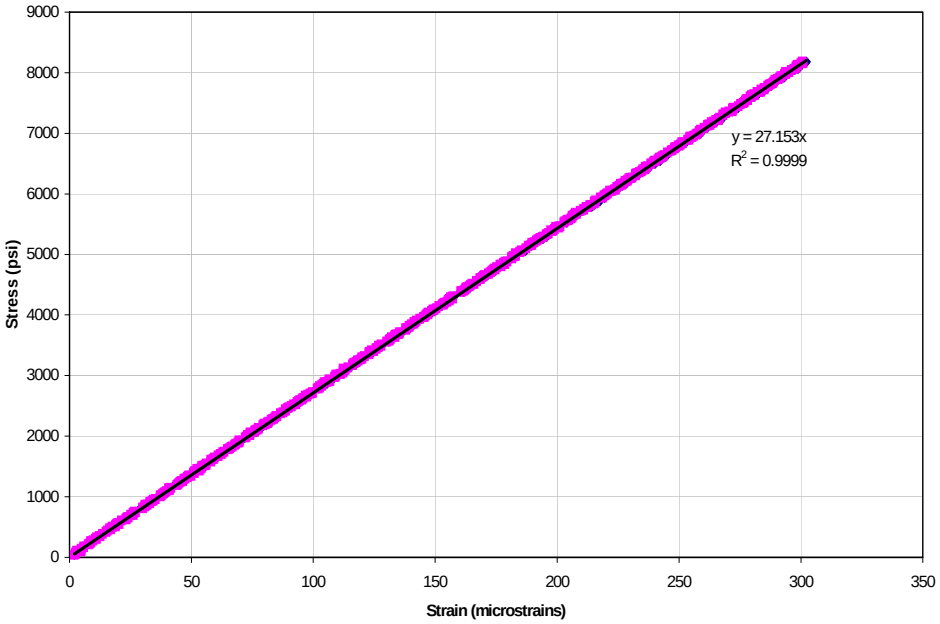

Figure 3.15 Typical Plot of Stress vs. Strain from Elastic Test

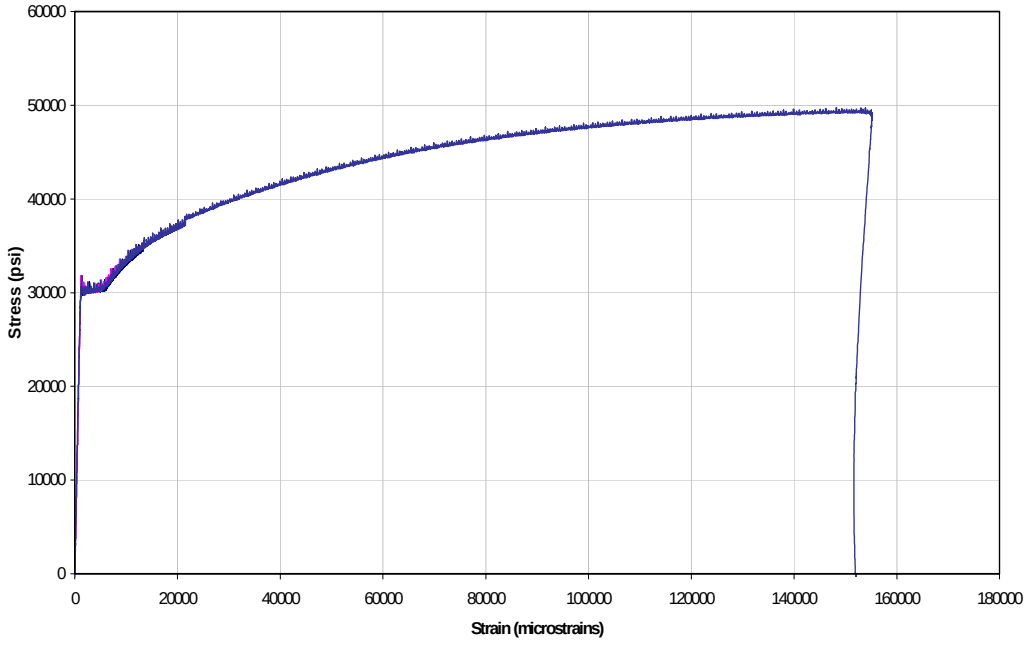

Figure 3.16 Typical Plot of Stress vs. Strain from Test to Full Failure

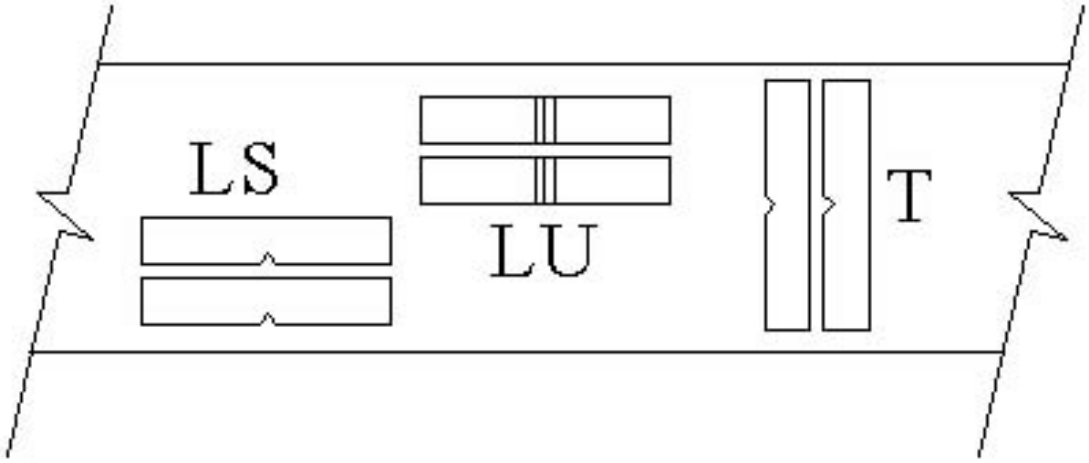

Figure 3.17 Orientation of Different Charpy Specimens

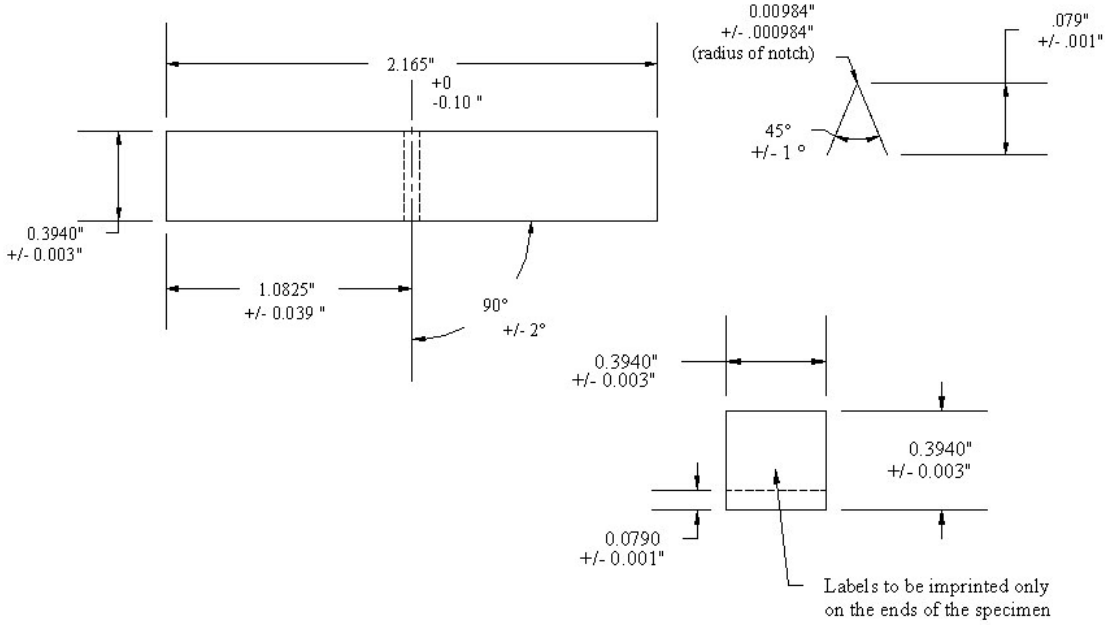

Figure 3.18 Dimensions of Charpy Specimens per ASTM E23

Figure 3.19 Charpy Impact Testing Machine

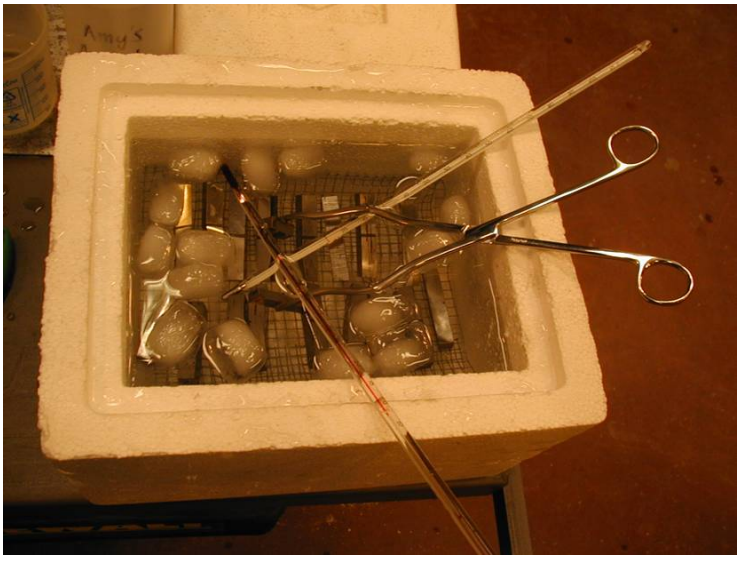

Figure 3.20 Liquid Bath Setup used for Cooling Charpy Specimens

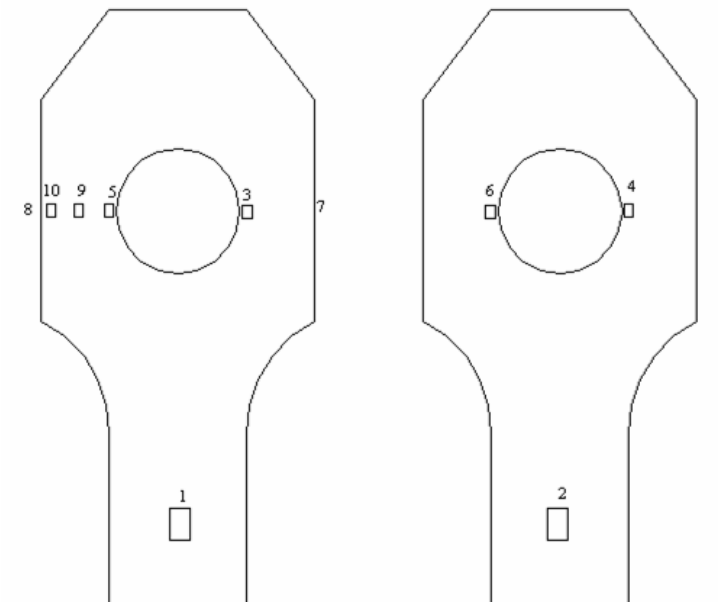

Figure 3.21 Placement of Strain Gages on Eyebar Connections

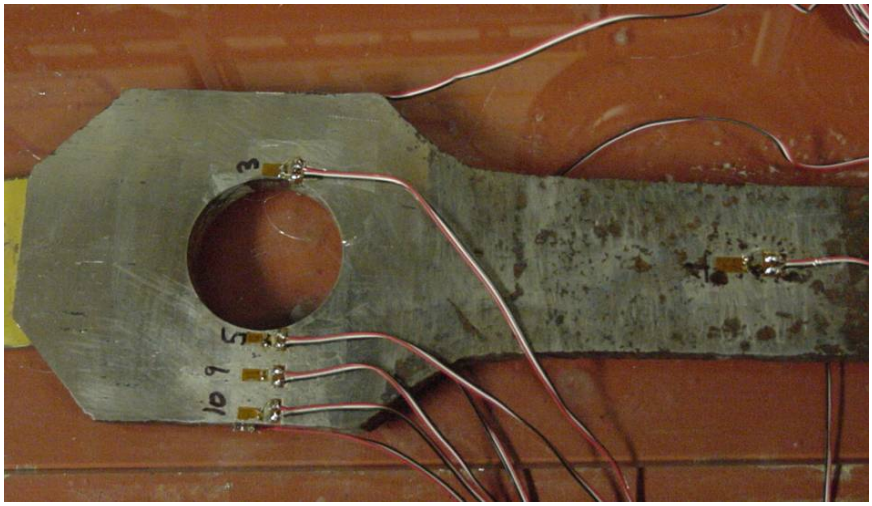

Figure 3.22 Eyebar Connection After Strain Gages were Applied

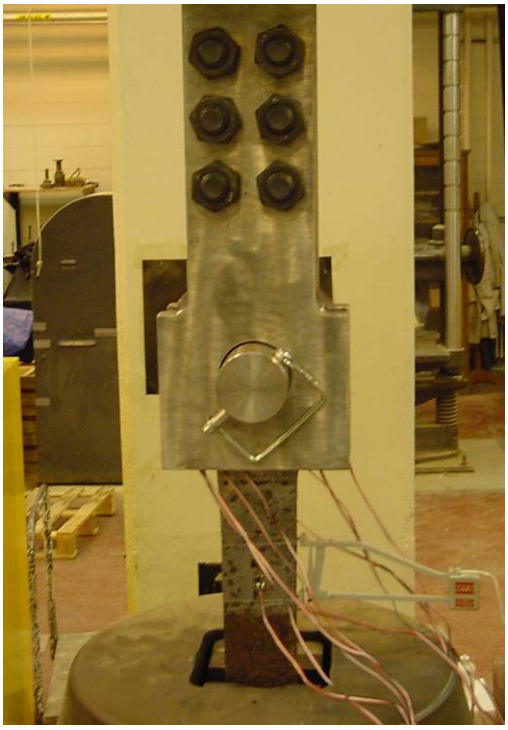

Figure 3.23 Eyebar Connection in MTS Machine with Added Setup before Testing

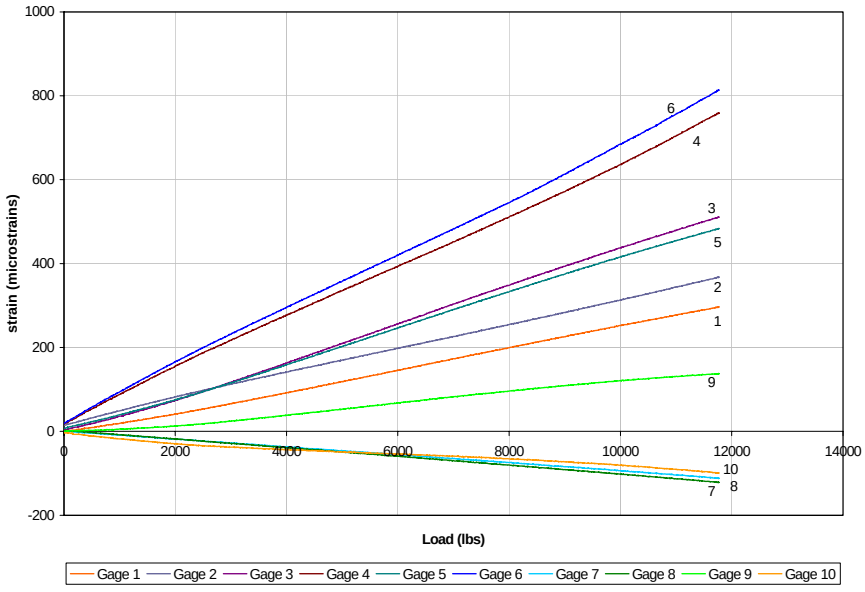

Figure 3.24 Plot of Linear Strain Readings from Strain Gages on Eye Connection

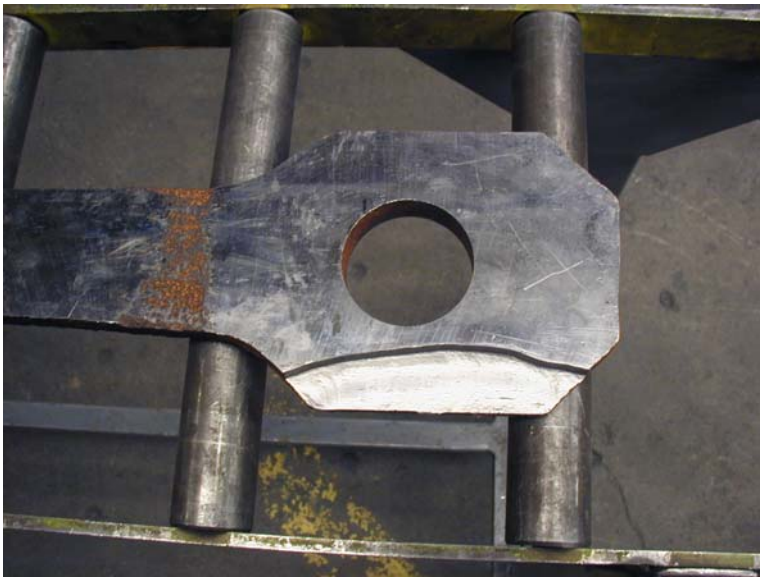

Figure 3.25 Eyebar Connection A After Material Was Removed to Simulate Corrosion

Figure 3.26 Initial Filler Weld Pass on Eyebar Connection A

Figure 3.27 Eyebar A After Filler Weld was Completed and Before Surface Grinding

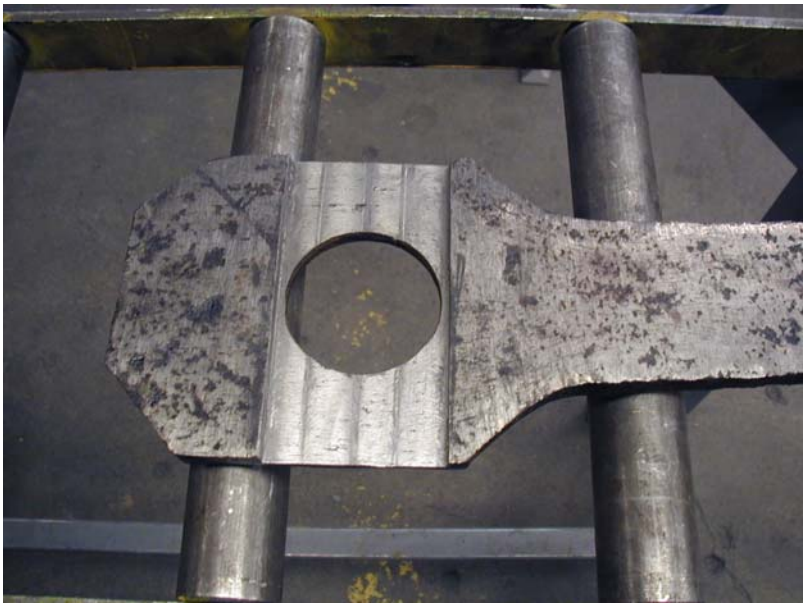

Figure 3.28 Eyebar B After Material Was Removed to Simulate Worst Case Corrosion

Figure 3.29 Initial Filler Weld Passes on Eyebar Connection B

Figure 3.30 Top View of Finished Filler Weld in Eyebar Connection B

Figure 3.31 Side View of Finished Filler Weld in Eyebar Connection B Showing Heat Distortion

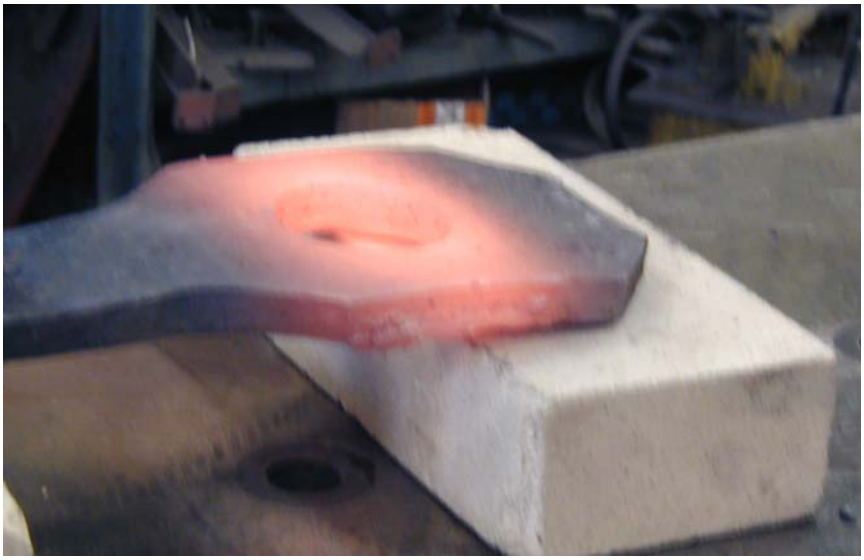

Figure 3.32 Eyebar Connection B Cherry Red Hot Before Being Straightened

Figure 3.33 Eyebar A Before Testing and After Surface Ground and Strain Gages had been Attached

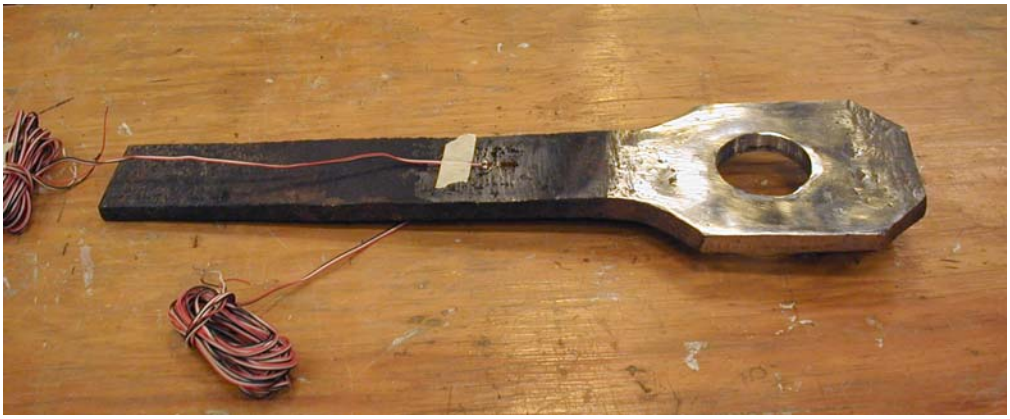

Figure 3.34 Eyebar B Before Testing and After Surface Ground and Strain Gages had been Attached

Figure 3.35 Front View of Eyebar B in Testing Machine with Extensometer Attached

Figure 3.36 View of Eyebar B in Testing Machine with Extensometer Attached Showing Slight Amount of Distortion in Eyebar

4. PRESENTATION OF TEST RESULTS

In addition to the mechanical and material testing completed, an in depth investigation of the results from this testing was also conducted. From these results, the mechanical properties of historic wrought iron were evaluated and compared with historical data. An improved understanding of these mechanical properties will assist bridge engineers when they need to conduct a condition assessment of structures consisting of historic wrought iron. This is especially true for wrought iron truss bridges consisting of wrought iron eyebars, since mechanical testing was completed on a number of eyebar coupons and connection eyes.

4.1 Microstructure

To determine the microstructure of historic wrought iron, an investigation of the micrographs that were taken during testing was completed. This investigation determined that the microstructure consisted of ferrite particles intermixed with many large inclusions that are typically elongated in one direction. Figure 4.1 is a photograph of a typical micrograph taken during testing.

The lighter areas in Figure 4.1 consist of mostly ferrite particles with some sparse deposits of pearlite particles. These ferrite particles were larger and coarser than ferrite particles commonly found in steel. Patches of pearlite were also found amongst the ferrite particles in the microstructure of wrought iron. Pearlite is commonly found in structural steel and is the product that is formed from the infusion of carbon with iron. Pearlite is not as prevalent in wrought iron as in steel and is typically so sparse that any

strength from the existence of pearlite is negligible. Carbon in wrought iron typically exists as fine precipitates of iron carbide, or cementite intermixed with the ferrite (Gordon,1988). This is because the wrought iron was never fully heated to a liquid form during the manufacturing process, and so the carbon is not heated fully enough to form pearlite.

The dark, elongated areas in the micrograph in Figure 4.1 are inclusions which consist of a variety of impurities like phosphorous, sulfur or silicon. The majority of these impurities are iron silicate and other oxides which are commonly grouped together and known as slag. The slag was intertwined into the microstructure of the wrought iron during the manufacturing process where the molten slag was used to help heat the iron ore. Most of the molten slag was squeezed out of the material during rolling of the wrought iron into the eyebar shape.

The slag inclusions that remained in the material were typically elongated and extended along only one direction in the material. These inclusions were larger than inclusions that are typically found in other metals such as steel. Some of these inclusions are large enough to be seen with the naked eye. Figure 4.2 shows a typical large inclusion found throughout the material.

Figure 4.3 is a photograph of a micrograph taken of the scrap piece of steel. This micrograph was used to compare the microstructure of the historic wrought iron to that of a common structural steel. The micrograph of the steel indicated that steel consisted of a smaller grain structure than wrought iron. It also shows a mixture of ferrite, pearlite and impurities that create the microstructure of steel. The impurities, or inclusions in the steel were much smaller and more distributed, unlike the inclusions in wrought iron.

The addition of carbon in the form of pearlite increases the strength and ductility of pure iron to form steel. Since the composition of wrought iron consists mainly of ferrite with widely dispersed areas of cementite and impurities, the mechanical properties

are not similar to that of steel and indicate the wrought iron has lower strength and ductility.

The non-uniform nature of the microstructure of the wrought iron caused by the amount and irregular distribution of impurities and inclusions in the material create points of higher stresses that initiate crack growth through out the material. This reduces the strength and ductility of the material. The lack of uniformity also makes it difficult to accurately determine a definite yield and ultimate strength, since the amount of inclusions found in wrought iron varies considerably. This variation in microstructure is the reason why a significant variation in mechanical properties was observed in the historical data gathered for wrought iron.

4.2 Chemical Analysis

A chemical analysis of the wrought iron test material was completed to determine the elements present. Table 4.1 shows the results from this chemical analysis. The elements that were found to be prevalent in Eyebars E1 and E2 included carbon, phosphorous, sulfur, and most importantly, silicon.

The amount of silicon present in the wrought iron and was between 0.12 and 0.15 percent by weight. In steel, silicon amounts exceeding 0.3% are sometimes used in certain heat-treatable alloy steels and electrical steels (Linnert, 1994). Silicon typically promotes the fluidity of the metal while it is being processed into shapes and it also promotes hardenability. In wrought iron, silicon can be found mainly in the slag that is dispersed in pockets through out the metal. This slag causes an overall decrease in strength, but also helps to prevent corrosion. Since slag is a major component in the definition of wrought iron, the presence of silicon in excess of what is typically found in steel would be a crucial step in identifying an unknown metal as wrought iron.

The carbon content present in the wrought iron was similar to the carbon content in some, low carbon steels. Even though the wrought iron contained the same amount of carbon as some low carbon steel, the properties of wrought iron are much different to that of steel. This is due to the manufacturing process of wrought iron. In this manufacturing process the iron ore is not completely heated until it is fluid in nature and completely above the eutectoid transition temperature needed for pearlite to form and impurities to separate. Instead, the iron is heated until it achieves a pasty condition at a lower temperature; at this temperature pearlite is not able to be formed and impurities are not easily or fully removed. Therefore, wrought iron consists mainly of ferrite which has body-centered cubic (BCC) structure and a low solubility for carbon. Because of this and the existence of many impurities throughout the iron, the strength of the wrought iron is lower than common steel.

A greater amount of phosphorous and sulfur was found in the wrought iron than what is found in common steels. The amount of phosphorous in the wrought iron was between 0.25 and 0.36 percent by weight and the amount of sulfur in the material was between 0.062 and 0.072 percent by weight. The high amounts of phosphorous and sulfur in the wrought iron decreases the overall strength of the material.

Ferrite iron can hold approximately 0.1 percent phosphorous in solution at room temperature. Phosphorous in excess of this amount exists as Fe_3P particles embedded in the structure of ferrite. Phosphorous tends to decrease the fracture toughness in steel especially if the steel is to be heat treated, where the amount of phosphorous is usually limited to 0.04% (Linnert, 1994). The addition of phosphorous increases the machinability of iron and was commonly added in low carbon steels for this reason.

The presence of sulfur in the metal also affects the overall tensile strength of the metal. Sulfur creates hot shortness which creates cracks dispersed though out the metal. Sulfur has a relatively low melting point and is insoluble in molten iron. When present in molten iron, sulfur creates iron sulfide which also solidifies at a lower temperature than

the rest of the molten iron. This leads to separation of the iron sulfide and the creation of inclusions, which decrease the overall strength of the wrought iron.

4.3 Hardness Test Results

Hardness is a measurement of the resistance to permanent indentation of a material. The resulting values from hardness testing depend directly upon the test that was performed and, therefore, is not a fundamental property and can be arbitrary. Even so, hardness is still determined for many materials because of its relationship with other fundamental properties, such as tensile stress.

In the material testing that was completed for this research, the Rockwell B hardness test was performed on wrought iron samples from the Bell Ford Bridge. The average of all the resulting hardness values was 70 with a standard deviation of 6.5. To correlate this value to the tensile strength of the metal, Table 3, of ASTM A370 (1997a) which contained the approximate hardness conversions for nonaustenitic steels was utilized. The average hardness corresponded to a tensile strength of 61 ksi if the material was a nonaustenitic steel. This value is considerably higher than the tensile results found from other mechanical material testing on wrought iron. Therefore, the hardness conversion charts for steel are not an accurate method to relate the hardness of wrought iron to its tensile strength. The hardness of the wrought iron may be higher than structural steel for a certain tensile strength.

A comparison of the tensile strength data from experimental testing to the hardness data was completed for wrought iron. In this comparison it was determined that if the hardness for the wrought iron is linearly related to the tensile strength, the tensile strength may be roughly estimated by multiplying the hardness value (from Rockwell B Hardness Test) by 655. Due to the lack of more hardness data from other sources, this

value may not be very accurate but could lead to an approximate estimate of the tensile strength.

4.4 Tensile Coupon Test Results

4.4.1 Resulting Fracture Surfaces

All of the fractures of the historic wrought iron tensile coupon testing were somewhat brittle in nature. The fractured surfaces were very jagged and uneven. These fractured surfaces, as seen in Figure 4.4, clearly show the "grain-like" characteristic of the wrought iron. The long deposits of iron silicate, known as slag, separated the iron into fibers that appear to have torn during testing.

Before any of the specimens were about to fail during testing, there was no visible necking or any typical pre-failure behavior that is typically found in structural steel. Figure 4.5 shows a typical ductile steel failure for a sample of steel tested with the same procedures as the wrought iron. As the photograph demonstrates, the steel failure consisted of a considerable amount of necking, followed by an inclined failure plane that is typical of ductile failures.

The failure of wrought iron was more brittle in nature than the aforementioned steel. During tensile testing, a slow tearing or ripping of what could be called the grains of the wrought iron would start to occur and then the specimen would fail almost instantaneously. In some cases, a crack would occur at the edge of the specimen in the middle of testing and would remain until the specimen failed in a different area after undergoing a considerable amount of strain. Figure 4.6 shows a typical failure of a wrought iron tensile test coupon immediately after it occurred.

4.4.2 Overall Results from Tensile Testing

A total of thirty-five tensile coupon tests were completed for this study. Of the thirty five tensile testing coupons, four had been heat straightened, five had been welded, and one had been mechanically straightened. Initially, all the specimens were compared without differentiating between specimens that had been treated. In each tension coupon test the modulus of elasticity, yield strength, ultimate tensile strength, percent elongation, and strain hardening coefficient and exponent were determined. Tables 4.2 and 4.3 show the results from the tensile coupon tests for the eyebar and round specimens.

The first result determined from testing was the modulus of elasticity. This modulus is the slope of the elastic region of the stress strain curve for wrought iron. The slope was found using linear regression methods, as performed with common spreadsheet software, with the data found from the initial test of the tension coupons, as discussed in Chapter 3.

Figure 4.7 is a plot of the resulting modulus of elasticity from each tensile testing coupon. In this plot, the results from the rectangular (eyebar) tensile coupons were compared to the results from the round tensile coupons. The values for the modulus of elasticity for all the tensile tests had very little variation between the square and round tensile coupons. The average modulus of elasticity found from testing was 27,870,000 psi with a standard deviation of 590,000 psi, which is only 2% of the average value.

The second result determined from testing was the yield strength, which is the stress at which permanent deformations start to occur in the specimen. The yield strength was determined by offsetting a line, with the same slope as the Modulus of Elasticity, at a strain of 0.002 and determining where this line intersects the stress-strain curve. Figure 4.8 is a plot showing the resulting yield strengths determined from testing for both the rectangular and round tensile coupons. As seen in the plot, the yield strength values all fall between 25,000 psi and 35,000 psi, with little variation. The average of all the yield

strengths was found to be 29,940 psi with a standard deviation of 2,400 psi, which is 8% of the average. The average yield strength of the rectangular specimens was 31,600 psi with a standard deviation of 1,280 psi, which is 4.05% of the average. The average yield strength of the round specimens was 28,000 psi with a standard deviation of 1,790 psi which was 6.39% of the average.

Tensile strength, or ultimate stress, is the stress at which failure occurs. This point of failure was well defined and easy to determine from the stress strain curves developed from testing. Figure 4.9 is a plot showing the tensile strength results from all tensile testing coupons for both the rectangular and round specimens. The plot indicates that, with some exceptions, there is little variation between the tensile strengths obtained from testing. The average tensile strength of the wrought iron was 47,000 psi with a standard deviation of 3,000 psi, which was 6.5% of the average. The average tensile strength of the rectangular specimens was 47,200 psi with a standard deviation of 3,380 psi which was 7.16% of the average. The average tensile strength of the round specimens was 46,800 psi with a standard deviation of 2,470 psi which was 5.28% of the average.

The percent elongation results from testing were determined by measuring the change in length of the predetermined 8” gauge length for the rectangular specimens from the eyebars and a 2” gauge length from the round specimens, and dividing that value by the original gage length. This variable was also compared to the total strain that occurred in the specimen to check the results obtained. Figure 4.10 is a plot of the percent elongation values determined from the rectangular and round tensile testing coupons. The plot indicates that the percent elongation values of the rectangular specimens were considerably lower than the resulting percent elongations for the round specimens. The average percent elongation for the round specimens was 25% with a standard deviation of 6%, while the average percent elongation for the rectangular specimens was 12% with a standard deviation of 5%.

It is believed that the percent elongation values from the rectangular specimens were lower than those of the round specimens as a result of the loading history of the material. The rectangular specimens were manufactured from eyebars taken from the Bell Ford bridge. This bridge experienced extensive damage in its collapse during a winter storm. From this collapse, eyebars experienced visual damage which indicated that they had been stretched past yielding and some permanent deformations may have developed in the material. The onset of permanent deformations in the wrought iron would reduce the ductility or plastic strain that otherwise the wrought iron would have exhibited. Therefore, when the strained wrought iron was tested, the percent elongation and ductility of the material was lower than expected.

The strain hardening coefficient (K) and exponent (n) are variables that are used to describe the inelastic region of the stress-strain curve. These variables are determined by taking the log of the true strain versus the log of the true stress and fitting a line to the data. The intercept of this line is the strain hardening coefficient and the slope is the strain hardening exponent. The stress in the plastic region of the stress-strain curve is equal to the strain hardening coefficient multiplied by the strain in the plastic region to the strain hardening exponent.

The strain hardening exponent and coefficient was determined for every testing specimen. The average strain hardening exponent was found to be 0.21 and the average strain hardening coefficient was found to be 82 ksi. These values along with the average modulus of elasticity were used to determine a theoretical stress strain curve for historic wrought iron. Figure 4.11 is a plot of this theoretical stress strain curve.

4.4.3 Comparison of Overall Results to Historical Data

A comparison of the tensile testing results to the tensile testing data collected from historical sources was conducted. In this comparison, only the data from historic

wrought iron bars were investigated, because this material was commonly used for bridge construction.

The tensile strengths from the testing and historical data can be seen in the plot in Figure 4.12. In the plot, the results from the tensile testing conducted for this study fall below the mean found for the historical data and mostly are near the lower standard deviation of this data. All of the testing results except for one, were above the second standard deviation from the mean of the historical data. For a set of data, sixty-eight percent of the data falls within one standard deviation of the mean and ninety-five percent falls within the second standard deviation. This second standard deviation of 40,000 psi could be used as a conservative estimate of the tensile strength of historic wrought iron.

The percent elongation values collected from historic data were also compared to the percent elongation values found in this study. Figure 4.13 is a plot of these two data sets. In this plot, the data collected from the round test specimens taken from the Adams Mill Bridge were plotted separate from the rectangular eyebar test specimens taken from the Bell Ford Bridge. The percent elongations from the round specimens were generally greater than the average percent elongation of the historical data. All of the percent elongations of the round samples, except one, were greater than one standard deviation less than then mean of the percent elongations for the historical data.

The percent elongation results for the rectangular specimens were considerably lower than for the round specimens. Most of the rectangular specimen percent elongation results were less than one standard deviation lower than the mean of the historical data, and a few were less than the second standard deviation. As previously mentioned, it is believed that these low percent elongations are the result of damage that these specimens endured during the collapse of the Bell Ford Bridge. Since many bridge members endure damage and are repaired and reused, the second standard deviation could be used as a possible minimum value of percent elongation for historic wrought iron.

4.4.4 Results of the Heat Straightened Specimens

Four of the rectangular tensile testing specimens were heat straightened before they were tested. The procedure that was used to heat straighten these tensile coupon specimens was outlined in Chapter 3. These specimens were machined from the Bell Ford Bridge material and, therefore, were compared to the tensile specimens taken from the same bridge that were not heat straightened.

When comparing the tensile strength and yield strength of the heat straightened specimens to the regular (not heat straightened) specimens, little difference in the values was observed. Figure 4.14, for example, illustrates the tensile strength values. Moreover, if the percent elongations of the heat straightened specimens is compared to the regular specimens, there is again very little effect on the specimen ductility, as Figure 4.15 demonstrates.

4.4.5 Results of the Mechanically Straightened Specimen

One of the tensile coupon specimens from the Bell Ford bridge was mechanically straightened. The procedure utilized in straightening this bar without heat was presented in Chapter 3. The properties of the mechanically straighten bar were compared to the other non treated bars from the Bell Ford bridge. The tensile strength of the mechanically straightened bar was only 37,500 psi and the percent elongation was only 3.1%. Figure 4.16 is a plot of the percent elongations from all the tensile coupons with the result from the mechanically straightened bar highlighted. As the plot indicates, the percent elongation for this specimen is considerably lower than any other specimen results.

The lack of ductility and tensile strength in this specimen is directly related to the effects induced from mechanically straightening the bar. When straightening the bar, the cold metal is forced past the yield stress until permanent deformations and residual

stresses are induced. These permanent deformations clearly removed some of the ductility available in the material, thus making it less ductile. This parallels the hypothesis that the rectangular testing coupons have less ductility than the round testing coupons as a result of damage that effectively reduced the amount of plastic strain that was available in the material. Therefore, significantly straightening a damaged specimen without heat reduces the plastic strain ductility of the specimen, and thus reduces the percent elongation exhibited by the material.

4.4.6 Results of Welded Specimens

Five tensile coupon specimens were cut in half and then welded before testing. The procedure that was used in welding these specimens was discussed in Chapter 3. Before testing, a macrograph was taken of the welded material to determine if the weld fully penetrated the wrought iron material. Figure 4.17 shows this macrograph and indicates that there was full penetration of the weld material. The macrograph also indicates that only a slight inclusion was created.

During testing none of the welded specimens failed within the region of the weld. Therefore, the weld demonstrated to be was stronger than the wrought iron material and could be considered a satisfactory weld detail. When comparing the tensile strength of the welded specimens to the other tensile coupons from the Bell Ford bridge that had not been welded, there is little variation between them, as shown in Figure 4.18. There was also little variation of the yield strength between the welded and non-welded specimens.

When investigating the percent elongation of the welded and non-welded specimens, the welded specimens consistently had a lower percent elongation, as shown in Figure 4.19. Even though the percent elongation values of the welded samples were found to be lower, the reduction in ductility was not large enough to question the validity of the weld detail.

4.5 Fatigue Test Results

To develop a better understanding of the fatigue behavior of wrought iron found in many historic bridges, some limited fatigue testing was completed during this study. Four un-notched smooth tensile coupon specimens, from the Adams Mill bridge, were cycled at a constant-amplitude stress range (R=0.05) until either failure or three million cycles occurred.

The first specimen was cycled at a stress range of 20 ksi. It never failed and the test was considered a run-out when the specimen reached three million cycles. The second specimen was cycled at a stress range of 30 ksi and it also never failed and the test was stopped at three million cycles. Two additional fatigue tests were completed at a stress range of 35 ksi. These specimens failed at 639,200 cycles and 713,900 cycles, respectively. Although the database is very limited, this may suggest that the endurance limit for smooth wrought iron specimens is somewhere between 30 and 35 ksi.

Other fatigue testing that was reported during the literature search consisted of testing completed on certain truss members such as eyebars (Elleby, 1976). Since these members were not smooth specimens and have localized notch and stress effects their fatigue lives were much lower than the fatigue lives found during experimental testing reported herein.

4.6 Charpy Impact Test Results

To evaluate the notch toughness of the wrought iron material, the Charpy impact test was performed on specimens from both the Bell Ford Bridge and the bridge near Delphi, IN. The Charpy impact test determines the impact energy needed to fracture a notched specimen of the material. The greater the impact energy, the greater the fracture

toughness the material. The test is also used as a method to determine the ductile / brittle transition temperature that occurs in metals.

The Charpy impact testing consisted of four different types of Charpy V notch specimens. Three of these specimen types were machined from eyebars taken from the Bell Ford Bridge. These specimen types were the longitudinal notched to the side (LS) type, longitudinal notched to the top (LU) type, and Transverse (T) type. The fourth specimen type consisted of Charpy V notch specimens that were machined from the round diagonals of the bridge near Delphi, IN. The differences between the charpy specimen types are explained in more detail in Chapter 3.

Figure 4.20 is a plot of the impact energy needed to fracture the charpy impact specimens versus the test temperature for every specimen type. In the plot, the impact energy for the LU specimens was the greatest, while the T specimens had the lowest impact energies. For all impact charpy specimens it was difficult to determine a transition temperature between ductile and brittle failure since there was not a significant change in Charpy impact energy for any of the temperatures tested. Tables 4.5 and 4.6 show the results from the Charpy impact tests for each specimen type.

According to AASHTO, Indiana is in a Zone 2 since the lowest anticipated service temperature is between 0 and -30^{o}F. The base metal Charpy V-notch requirements for fracture critical members for ASTM A36 steel is 25 ft lbs at 40^{o}F in this zone. Since the A36 steel has the closest material properties to wrought iron, the Charpy impact energy values should equal or exceed 25 ft lbs. However, for the orientation tested, only the LU specimens were above this minimum.

An additional observation from Figure 4.20 is the extremely low impact energy for the transverse specimen type. The resulting impact energy of this specimen type was never greater than 3 ft lbs. This is extremely dangerous if any cracks are running along the direction of rolling, which is due to the fibrous nature of wrought iron. Fortunately,

the stress is generally oriented in the direction of rolling, so cracks will usually not be present to initiate a fracture in this direction. However, if stresses do occur perpendicular to the longitudinal direction then extreme caution should be used.

The fracture surfaces of the charpy impact specimens were also examined. For the longitudinal specimens (LS and LU), the fractured surfaces were typical cleavage type. The transverse specimens had a fracture surface unique to wrought iron which had an appearance of a slipping or sliding of the grains of the wrought iron again each other. Figure 4.21and Figure 4.22 illustrate these two different types of fracture surfaces.

Very few charpy impact data on historic wrought iron were located during the literature search completed in this study. Green et al. (1999) reported charpy impact strength data for temperatures ranging 68^{o}F to 208^{o}F, which were much higher than the temperatures used in the testing that was completed in this study. The average charpy impact strength at room temperature (68^{o}F) for the data reported by Greeen et al. (1999) was 9.7 ft lbs, which is lower than the average found during testing (16.7 for the LS Specimens). Other charpy impact strength data and requirements for wrought iron that were found during the literature search were based on wrought iron that was produced using a modern Aston process, which creates a different microstructure and, therefore, should not be compared to the historic wrought iron being evaluated in this study.

4.7 Typical Eyebar Connection Testing Results

Both finite element analysis and experimental testing were undertaken to evaluate the end connections of the eyebars from the Bell Ford Bridge. The procedures that were used for both the analytical and experimental approaches were described in Chapter 3. In both methods the stress patterns that arose in the eyebars upon loading were determined.

From the finite element analysis, it was determined that upon loading the eyebar connection, the largest stress that occurs in the eyebar was directly on either edge of the pin hole. The stress then decreased across the width of the connection till it turned into a compressive stress on the outer edge. The second highest stress occurred in the shank of the eyebar. Not surprisingly, the stresses above pin hole were compressive. Figure 4.23 depicts of the resulting stresses in the eyebar connection as predicted using the finite element analysis model.

In the experimental testing that was completed, strain gages were applied to both faces of the eyebar connection. A detailed description of the strain gage pattern can be found in Chapter 3. For each eyebar end connection, the specimen was first loaded only in the elastic region for wrought iron. During this initial testing, the strains from all the gages that were attached to both faces of the eyebar were recorded continuously. These strains were then compared to the strains found in the shank of the eyebar to get a better understanding of the behavior of the eyebar end connection.

Figure 3.24 is a plot of the normalized stresses (strains) for the gages in the eye region of the eyebar. The strains measured in the shank gages were essentially constant and, thereby, were used to normalize the strains in the eye gages. From this plot it can be seen that higher stresses occurred directly outside of the hole in the center of the connection. The stresses then decreased as they were further away from the edge of the hole, until they became compressive on the outside edge – see Figure 4.24 and Table 4.7. The finite element analysis and the experimental testing results directly agree with each other.

After experimentally testing the eyebar connections in the elastic region only, the eyebars were then loaded until failure. The results of the eyebar tests are given in Table 4.8. All of the connections failed in the shank of the eyebar connection. There was some elongation of the pin holes in the eyebar connection from being loaded to failure. A photograph of the pin hole elongation for specimen E5L can be seen in Figure 4.25. Two

measurements were taken of the holes to determine the amount of elongation: one measured the diameter of the pin hole parallel to the direction of loading, the second measured the diameter of the hole perpendicular to the direction of loading. These pin diameter measurements are provided in Table 4.9. The average pin hole elongation parallel to the direction of loading was 5.6%, while the average contraction perpendicular to the loading direction was 1.3%.

4.8 Repaired Eyebar Connection Testing Results

Two eyebar connections were machined to model severe corrosion that might be found on a typical member from an existing historic wrought iron bridge and then repaired. These eyebar connections were repaired by filling in the modeled corroded area with filler weld material. Eyebar A was modeled after typical corrosion along the edge of an eyebar connection, while Eyebar B was modeled after severe corrosion across the face of the eyebar connection. The procedure utilized for this repair is further explained in Chapter 3.

To determine if the repair was adequate, these eyebars were tested using a similar method as the testing method utilized for the non-repaired eyebar connections. The main difference in the testing methods was that the strains around the face of the eyebar connection were not recorded for the repaired eyebar connections.

Both repaired eyebar connections were loaded until failure. Both connection specimens fractured in the shank of the eyebar connection, proving that the repair was suitable. The first eyebar connection, Eyebar A failed at a higher stress than the second (Eyebar B). Similar to the non-repaired eyebar connections, the elongation of the pin holes were measured and recorded. The results from these two tests can be seen in Tables 4.8 and 4.9.

Table 4.1 Chemical Analysis of Eyebars 1 and 2

Chemistry Results, Weight %

Element	**Sample, E1**	**Sample, E2**
Carbon	0.008	0.030
Manganese	0.02	<0.01
Phosphorus	0.36	0.25
Sulfur	0.072	0.062
Silicon	0.12	0.15
Nickel	0.02	0.02
Chromium	<0.01	<0.01
Molybdenum	<0.01	<0.01
Copper	0.02	0.02
Magnesium	0.005	0.005

Table 4.2 Tensile Coupon Test Results for Eyebars

Coupon ID	Avg. Area (in^2)	Tensile Load (lbs)	Modulus of Elasticity (ksi)	Yield Strength (psi) (.002 offset)	Tensile Strength (psi)	Percent Elong. (%) 8" Gauge Length	Strain Harden. Exp.	Strength Coeff. (ksi)
BF-E1-NR1	0.598	26,939	27,554	30,500	44,000	8.59	0.19	78.24
BF-E1-NR2	0.595	25,720	27,154	31,000	42,500	7.81	0.20	76.69
BF-E1-NR3	0.595	27,300	27,034	32,000	45,500	21.09	0.20	80.12
BF-E1-H1	0.612	29,700	27,605	31,500	48,500	10.15	0.21	90.30
BF-E2-NR1	0.609	30,400	27,884	33,000	48,000	10.94	0.15	70.88
BF-E2-NR2	0.607	31,200	28,695	35,000	50,000	16.41	0.21	88.58
BF-E2-H1	0.613	29,100	27,586	32,000	47,500	8.59	0.20	80.12
BF-E2-H2	0.562	29,300	28,641	33,000	52,000	17.18	0.20	86.80
BF-E2-H3	0.594	30,300	28,397	32,000	50,500	15.625	0.19	82.65
BF-E3-M1	0.538	21,000	26,731	31,000	37,500	3.125	0.13	65.26
BF-E4-NR1	0.991	47,500	27,811	32,500	47,500	12.5	0.15	68.45
BF-E4-NR2	0.988	49,000	27,575	32,000	49,000	17.19	0.19	81.50
BF-E4-NR3	0.993	49,400	27,153	30,000	49,000	15.625	0.19	81.66
BF-E4-NR4	1.000	50,300	27,590	32,500	50,000	15.625	0.22	89.77
BF-E5-W1	0.936	42,100	27,732	30,000	44,500	7.032	0.18	78.89
BF-E5-W2	0.937	42,600	27,836	30,000	45,000	7.8125	0.19	82.21
BF-E5-W3	0.933	43,100	27,618	30,000	46,000	7.8125	0.21	85.15
BF-E5-W4	0.934	46,800	27,991	30,500	50,000	10.16	0.20	86.97
BF-E5-W5	0.907	45,900	27,855	32,000	50,000	9.375	0.18	81.52
Average	**0.765**	**36,711**	**27,707**	**31,605**	**47,211**	**11.72**	**0.19**	**80.83**
Standard Deviation	**0.185**	**9,548**	**492**	**1,283**	**3,381**	**4.52**	**0.02**	**6.70**

Note: Non-Repaired Coupons have a Coupon ID ending with – NR#
Heat Straightened Coupons have a Coupon ID ending with –H#
Mechanically Straightened Coupon has a Coupon ID ending with – M1
Welded Coupons have a Coupon ID ending with -W#

Table 4.3 Tensile Coupon Test Results for Round Bars

Coupon ID	Avg. Area (in^2)	Tensile Load (lbs)	Modulus of Elasticity (ksi)	Yield Strength (psi) (.002 offset)	Tensile Strength (psi)	Percent Elong. (%) 8" Gauge Length	Strain Harden. Exp.	Strength Coeff. (ksi)
A4	0.197	10,600	28,061	32,000	53,000	21.05	0.19	86.23
B1	0.196	9,600	29,008	29,000	49,000	32.4	0.23	83.37
B2	0.197	9,400	27,289	28,000	48,000	31.07	0.22	83.92
B3	0.197	9,300	27,443	28,000	47,500	29.1	0.25	88.43
B4	0.196	8,400	29,259	24,900	42,500	25.2	0.27	83.38
B5	0.197	9,100	28,512	26,000	45,500	24.83	0.24	83.72
B6	0.199	9,000	27,756	26,000	45,000	33.7	0.25	84.84
C1	0.196	9,300	28,535	28,000	46,000	26.37	0.24	85.82
C4	0.195	9,100	28,500	27,500	46,500	20.42	0.25	86.83
D1	0.196	8,600	26,860	29,000	44,000	28.77	0.24	79.79
D2	0.196	9,000	28,279	26,000	45,250	24.53	0.25	85.57
D3	0.194	9,100	27,650	26,500	46,000	28.96	0.25	85.56
D4	0.196	9,200	27,730	29,000	46,500	24.56	0.23	85.08
D5	0.197	9,700	27,745	30,000	49,000	16.05	0.20	82.07
D6	0.196	8,900	28,350	30,000	50,000	13.7	0.20	78.27
D7	0.195	9,000	27,960	27,500	45,300	30.93	0.23	80.19
Average	**0.196**	**9,206**	**27,995**	**27,963**	**46,816**	**25.73**	**0.23**	**83.94**
Standard Deviation	**0.001**	**495**	**579**	**1,791**	**2,471**	**5.52**	**0.02**	**2.65**

Table 4.4 Average and Standard Deviation of Tensile Coupon Test Results

	Modulus of Elasticity (ksi)	**Yield Strength (psi) (.002 offset)**	**Tensile Strength (psi)**	**Percent Elongation (%)**	**Strain Hardening Exponent**	**Strength Coeff. (ksi)**
Eyebars						
Average	**27,700**	**31,600**	**47,200**	**11.7**	**0.19**	**81**
St. Dev.	500	1,280	3,380	4.5	0.02	6.70
% of Avg.	1.8%	4.1%	7.2%	38.6%	11.7%	8.3%
Rounds						
Average	**28,000**	**28,000**	**46,800**	**25.7**	**0.23**	**84**
St. Dev.	620	1,790	2,470	5.5	0.02	2.65
% of Avg.	2.2%	6.4%	5.3%	21.5%	8.5%	3.2%
All Tests						
Average	**27,900**	**29,900**	**47,000**	**18.1**	**0.21**	**82**
St. Dev.	590	2,410	3,050	8.7	0.03	5.55
% of Avg.	2.1%	8.1%	6.5%	48.1%	14.6%	6.8%
Heat Straightened						
Average	**28,057**	**32,125**	**49,625**	**12.9**	**0.20**	**85**
St. Dev.	542	629	2,016	8.8	0.09	45.95
% of Avg.	1.9%	2.0%	4.1%	68.5%	45.3%	54.1%
Mech. Straightened						
Average	**26,731**	**31,000**	**37,500**	**3.1**	**0.13**	**65**
Welded						
Average	**27,806**	**30,500**	**47,100**	**8.4**	**0.19**	**83**
St. Dev.	140	866	2,702	1.3	0.01	3.17
% of Avg.	0.5%	2.8%	5.7%	15.2%	5.2%	3.8%
Historic						
Average	**NA**	**33,300**	**54,000**	**23.2**	**NA**	**NA**
St. Dev.		2,990	9,000	7.6		
% of Avg.		9.0%	16.7%	32.9%		

Table 4.5 Charpy Impact Test Results

Longitudinal Notched to the Side (LS)					
Spec. Descriptor	**Spec. ID**	**Estimated Temp F**	**Actual Temp**	**Impact Energy (ft lbs)**	**Description of Specimen**
BF-E1-NH-LS5	**1E**	10	10.2	**6.5**	Broken into 2 pieces
BF-E1-NH-LS6	**1F**	10	10.2	**6**	Broken into 2 pieces
BF-E1-NH-LS7	**1G**	10	10.2	**11.5**	Broken into 2 pieces
BF-E4-NH-LS5	**4E**	10	10.2	**14**	Broken into 2 pieces
BF-E4-NH-LS6	**4F**	10	10.2	**6**	Broken into 2 pieces
BF-E4-NH-LS7	**4G**	10	10.2	**29**	Broken into 2 pieces
BF-E1-NH-LS9	**1I**	40	39	**9.5**	Broken into 2 pieces
BF-E1-NH-LS10	**1J**	40	39	**10**	Broken into 2 pieces
BF-E1-NH-LS11	**1K**	40	39	**17**	Broken into 2 pieces
BF-E4-NH-LS10	**4J**	40	39	**10**	Broken into 2 pieces
BF-E4-NH-LS11	**4K**	40	39	**13.5**	Not Broken
BF-E4-NH-LS12	**4L**	40	39	**14.5**	Broken into 2 pieces
BF-E1-NH-LS13	**1M**	RT	68.5	**20**	Broken into 2 pieces
BF-E1-NH-LS14	**1N**	RT	68.5	**18**	Broken into 2 pieces
BF-E1-NH-LS15	**1O**	RT	68.5	**13**	Broken into 2 pieces
BF-E1-NH-LS16	**1P**	RT	68.5	**13**	Broken into 2 pieces
BF-E4-NH-LS2	**4B**	RT	68.5	**11**	Broken into 2 pieces
BF-E4-NH-LS8	**4H**	RT	68.5	**19.5**	Broken into 2 pieces
BF-E4-NH-LS9	**4I**	RT	68.5	**27**	Broken into 2 pieces
BF-E1-NH-LS12	**1L**	RT	68.5	**12**	Broken into 2 pieces
BF-E1-NH-LS8	**1H**	RT	68.5	**17**	Not Broken
BF-E1-NH-LS1	**1A**	-30	-30	**3.5**	Broken into 2 pieces
BF-E1-NH-LS2	**1B**	-30	-30	**5.5**	Very Unique Fracture surface
BF-E1-NH-LS3	**1C**	-30	-30	**8.5**	Broken into 2 pieces
BF-E4-NH-LS1	**4A**	-30	-30	**6.5**	Broken into 2 pieces
BF-E4-NH-LS3	**4C**	-30	-30	**4.5**	Broken into 2 pieces
BF-E4-NH-LS4	**4D**	-30	-30	**5**	Broken into 2 pieces
BF-E1-NH-LS4	**1D**	-30	-30	**4**	Broken into 2 pieces

Longitudinal Notched to the Top (LU)					
Spec. Descriptor	**Spec. ID**	**Estimated Temp F**	**Actual Temp**	**Impact Energy (ft lbs)**	**Description of Specimen**
BF-E4-NH-LU5	**4Q**	10	10	**18**	Broken into 2 pieces
BF-E4-NH-LU6	**4R**	10	10	**9**	Broken into 2 pieces
BF-E4-NH-LU7	**4S**	10	10	**17**	Broken into 2 pieces
BF-E4-NH-LU8	**4T**	10	10	**19**	Not Broken
BF-E4-NH-LU9	**4U**	40	40	**30**	Not Broken
BF-E4-NH-LU10	**4V**	40	40	**16.5**	Not Broken
BF-E4-NH-LU11	**4W**	40	40	**40**	Not Broken
BF-E4-NH-LU12	**4X**	40	40	**28**	Not Broken
BF-E4-NH-LU13	**4Y**	68.5	68.5	**41**	Not Broken
BF-E4-NH-LU14	**4Z**	68.5	68.5	**20.5**	Not Broken
BF-E4-NH-LU15	**4AA**	68.5	68.5	**42**	Not Broken
BF-E4-NH-LU16	**4BB**	68.5	68.5	**43**	Not Broken
BF-E4-NH-LU1	**4M**	-30	-30	**12**	Not Broken
BF-E4-NH-LU2	**4N**	-30	-30	**4.5**	Almost Broken
BF-E4-NH-LU3	**4O**	-30	-30	**8**	Almost Broken
BF-E4-NH-LU4	**4P**	-30	-30	**6**	Not Broken

Table 4.5 (continued) Charpy Impact Test Results

Transversed Notched to the Side (T)					
Spec. Descriptor	**Spec. ID**	**Estimated Temp F**	**Actual Temp**	**Impact Energy (ft lbs)**	**Description of Specimen**
BF-E3-NH-T4	**D**	10	10.2	**3**	Broken into 2 pieces
BF-E3-NH-T5	**E**	10	10.2	**2**	Brittle - odd fracture
BF-E3-NH-T7	**G**	10	10.2	**2**	Broken into 2 pieces
BF-E3-NH-T1	**A**	40	39	**2**	Broken into 2 pieces
BF-E3-NH-T2	**B**	40	39	**2**	Broken into 2 pieces
BF-E3-NH-T3	**C**	40	39	**3**	Broken into 2 pieces
BF-E3-NH-T6	**F**	68.5	68.5	**3**	Broken into 2 pieces
BF-E3-NH-T8	**H**	68.5	68.5	**2**	Broken into 2 pieces

Charpy Specimen from Round Bars (-charpy)					
Spec. Descriptor	**Spec. ID**	**Estimated Temp F**	**Actual Temp**	**Impact Energy (ft lbs)**	**Description of Specimen**
D1-NH-Charpy	**A2**	10	10.2	**10**	Not Broken
D2-NH-Charpy	**B2**	10	10.2	**13.5**	Not Broken
D4-NH-Charpy	**D2**	10	10.2	**5.5**	Not Broken
D1-NH-Charpy	**A3**	40	39	**7**	Not Broken
D2-NH-Charpy	**B3**	40	39	**45**	Not Broken
D3-NH-Charpy	**C1**	40	39	**12.5**	Not Broken
D4-NH-Charpy	**D1**	40	39	**9**	Not Broken
D1-NH-Charpy	**A4**	68.5	68.5	**18.5**	Not Broken-close
D2-NH-Charpy	**B4**	68.5	68.5	**41**	Not Broken
D2-NH-Charpy	**B5**	68.5	68.5	**53**	Not Broken
D1-NH-Charpy	**A1**	-30	-30	**4.5**	Broken into 2 pieces - brittle
D1-NH-Charpy	**A5**	-30	-30	**4.5**	Broken into 2 pieces - brittle
D2-NH-Charpy	**B1**	-30	-30	**4**	Broken into 2 pieces - brittle

Table 4.6 Average Charpy Impact Strength from Testing and Literature for Certain Temperatures

Source		**Temperature (^{o}F)**				
	Orientation	*-30*	*10*	*40*	*68 (RT)*	*102-105*
Experimental Testing (Piskorowski)	Longitudinal Notched to the Side (LS)	5.4	12.2	12.4	16.7	-
	Longitudinal Notched to the Top (LU)	7.6	15.8	28.0	36.6	-
	Transverse Notched to the Side (T)	-	2.3	2.3	2.5	
	Round Bars	4.3	9.7	18.4	37.5	-
Green et al.		-	-	-	9.7	23.3

Table 4.7 Comparison of Strain Gage Readings at Various Locations During Elastic Loading for Eyebar Connection Testing

Eyebar Connection Specimen	**Avg. 1&2, ε_{12}** (microstrain)	**Strain from Gage 5, ε_5** (microstrain)	**Strain from Gage 9, ε_9** (microstrain)	**Strain from Gage 10, ε_{10}** (microstrain)	**Strain from Gage 8, ε_8** (microstrain)
E2	285	418	122	-81	-103
$\varepsilon/\varepsilon_{12} = \sigma/\sigma_{12}$	*1.00*	*1.47*	*0.43*	*-0.28*	*-0.36*
E4L	282	767	292	73	-49
$\varepsilon/\varepsilon_{12} = \sigma/\sigma_{12}$	*1.00*	*2.72*	*1.03*	*0.26*	*-0.17*
E4R	288	469	128	-58	-96
$\varepsilon/\varepsilon_{12} = \sigma/\sigma_{12}$	*1.00*	*1.63*	*0.44*	*-0.20*	*-0.33*
E5L	286	841	430	175	-111
$\varepsilon/\varepsilon_{12} = \sigma/\sigma_{12}$	*1.00*	*2.94*	*1.50*	*0.61*	*-0.39*
Average	**285**	**624**	**243**	**27**	**-90**
$\varepsilon/\varepsilon_{12} = \sigma/\sigma_{12}$	***1.00***	***2.19***	***0.85***	***0.10***	***-0.31***

Table 4.8 Eyebar Connection Results (Regular and Repaired)

Eyebar Connection Specimen	Pu (lbs)	Tensile Strength (psi)	Failure Location
E2	55,742	50,559	Shank
E4L	79,074	47,068	Shank
E4R	78,544	42,745	Shank
E5L	88,827	48,341	Shank
E5R, Eyebar A	89,887	46,441	Shank
E1, Eyebar B	46,378	37,103	Shank

Table 4.9 Elongation of Pin Holes in Eyebar Connections

Eyebar Connection Specimen	Original Diameter (in)	Diameter 1 (in)	Diameter 2 (in)	Elongation of Diameter 1
E2	2.25	2.48	2.21	10.22%
E4L	2.25	2.3	2.25	2.22%
E4R	2.25	2.39	2.2	6.22%
E5L	2.25	2.45	2.2	8.89%
E5R, Eyebar A	2.25	2.36	2.21	4.89%
E1, Eyebar B	2.25	2.28	2.25	1.33%

Diameter 1: Measurement of Diameter Parallel to Direction of Testing
Diameter 2: Measurement of Diameter Perpendicular to the Direction of Testing

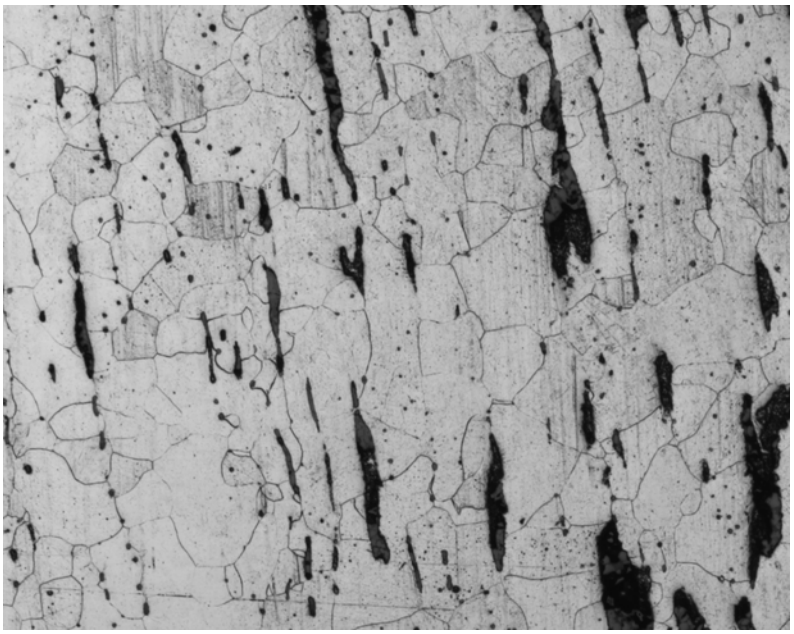

Figure 4.1 Typical Micrograph of Wrought Iron (100x Magnification)

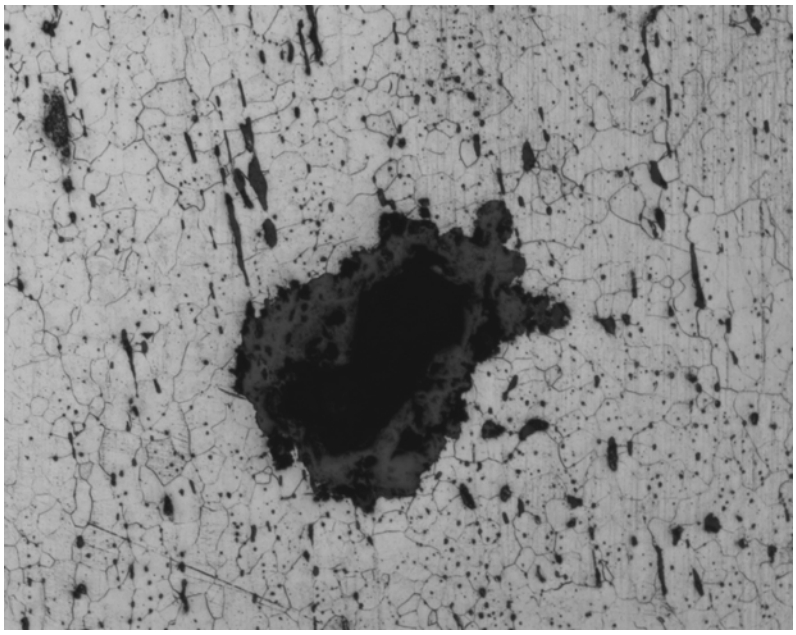

Figure 4.2 Micrograph of Wrought Iron with Large Inclusion (100x magnification)

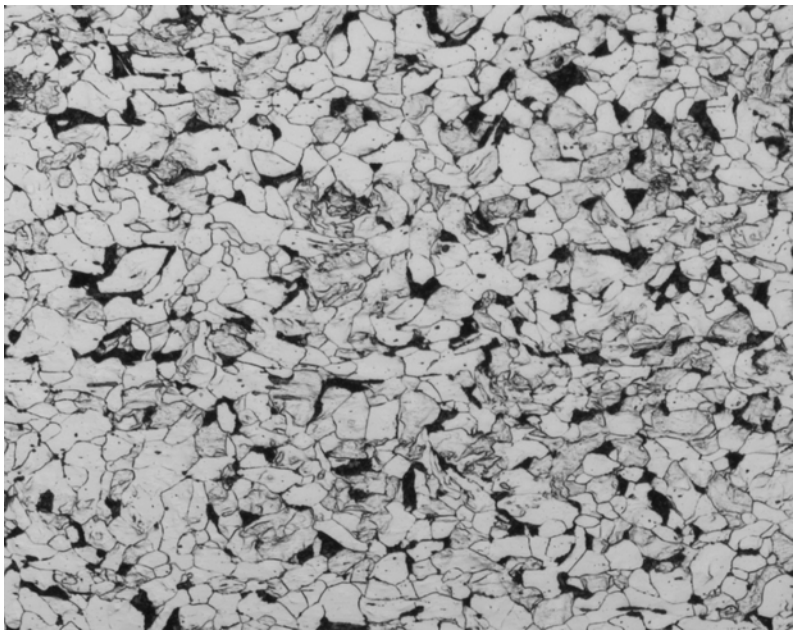

Figure 4.3 Micrograph of Steel (100x Magnification)

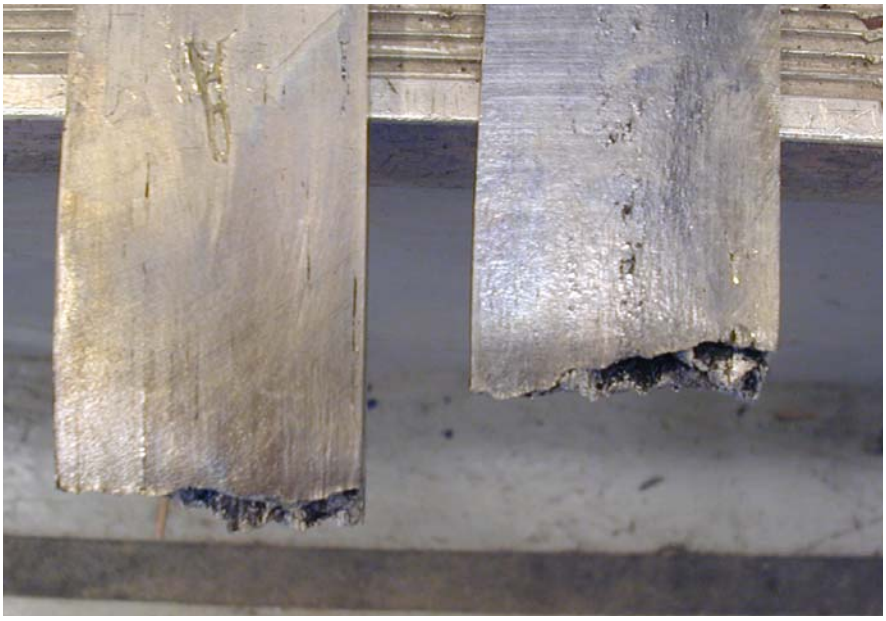

Figure 4.4 Typical Fracture Surface of Wrought Iron Tensile Coupons

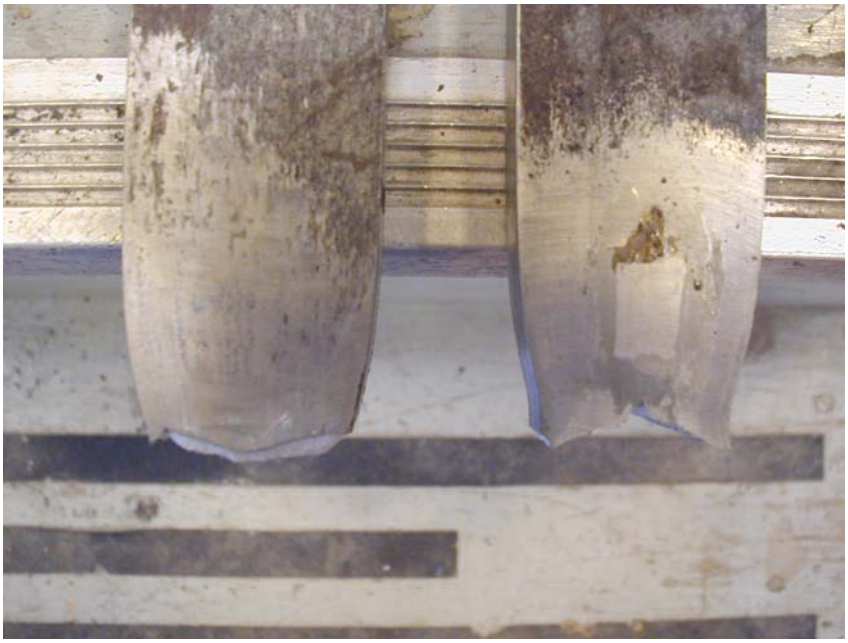

Figure 4.5 Fracture Surface of Ductile Steel

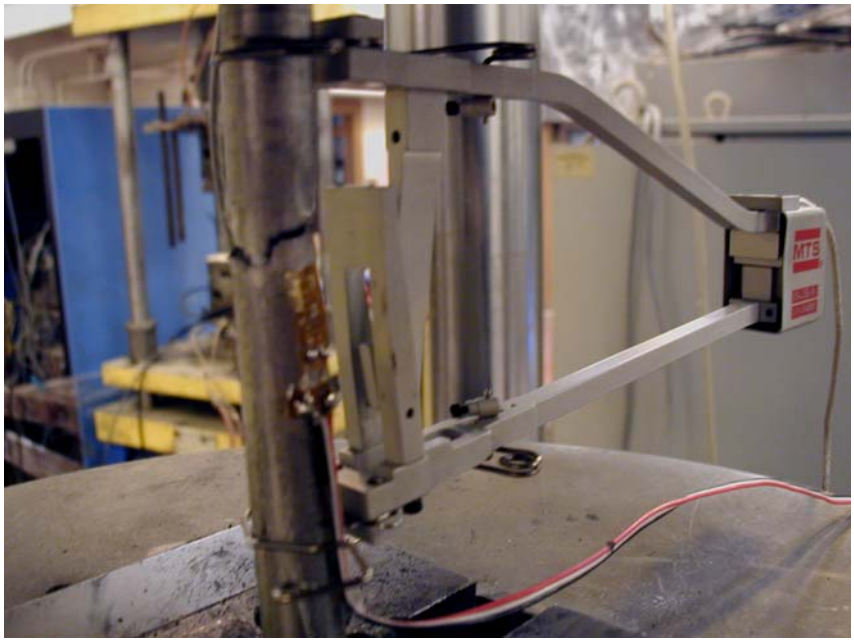

Figure 4.6 Fracture of Tensile Testing Coupon Immediately after Failing

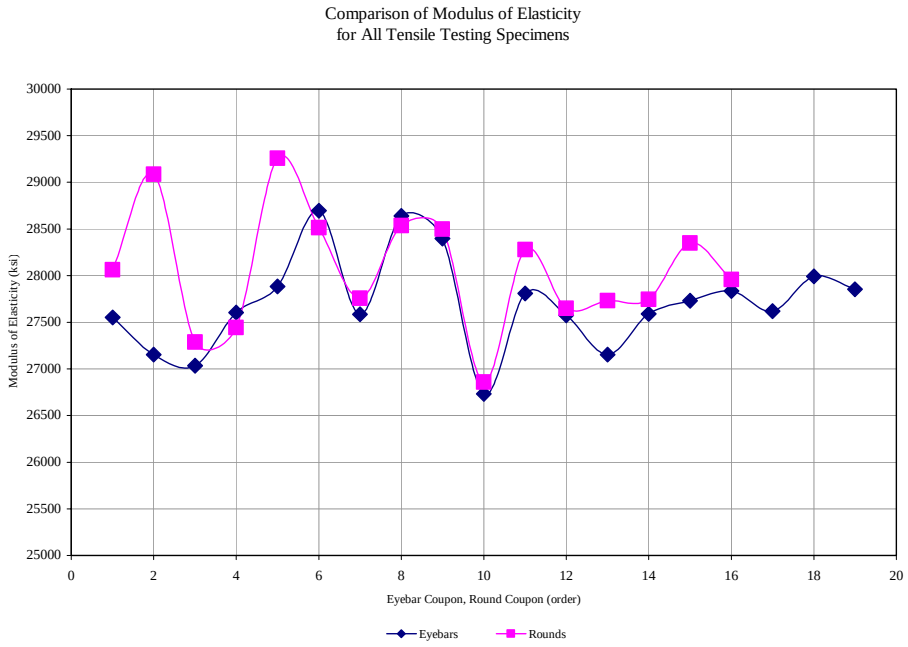

Figure 4.7 Modulus of Elasticity of Tensile Test Coupons

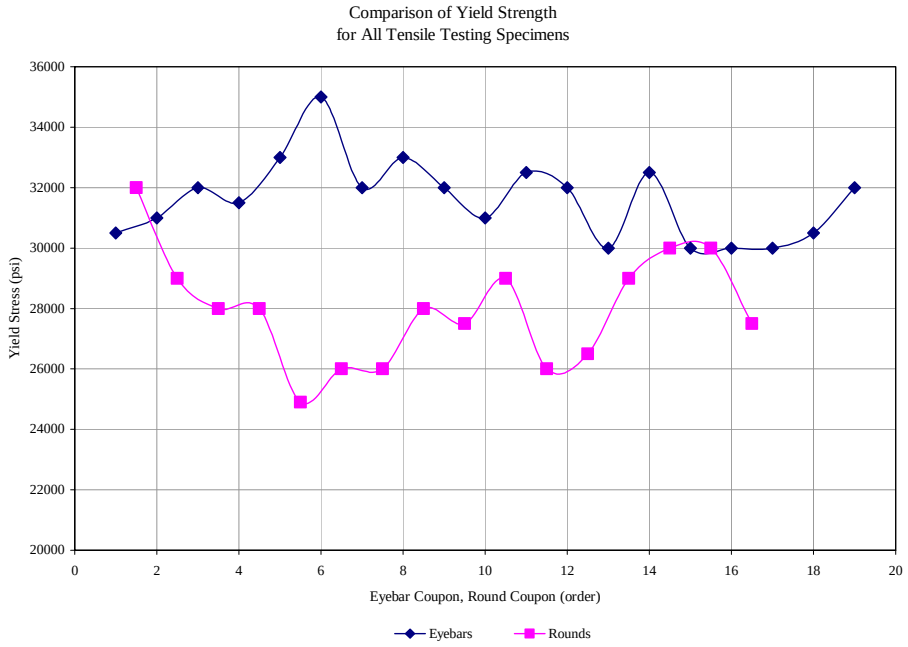

Figure 4.8 Yield Strength of Tensile Test Coupons

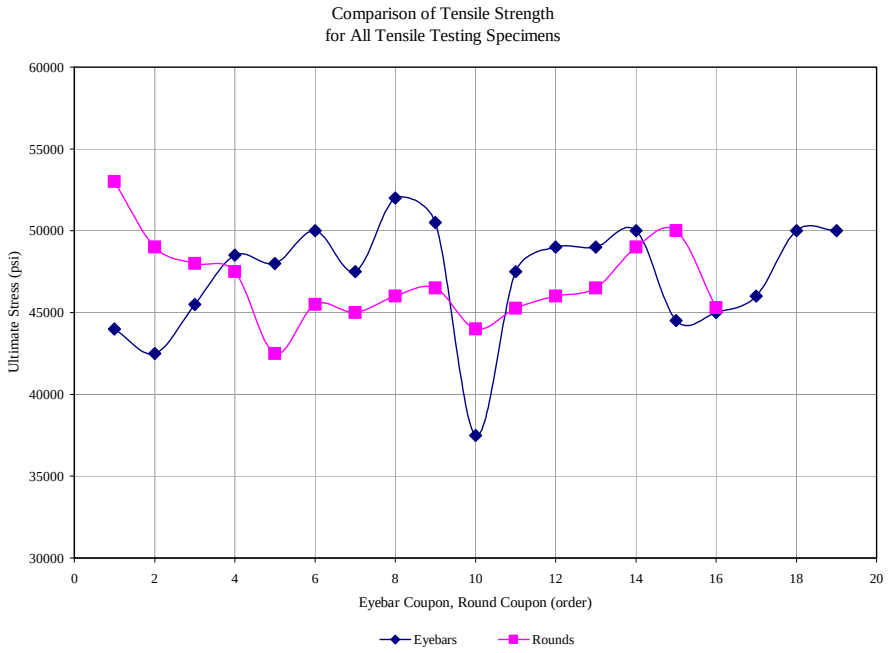

Figure 4.9 Tensile Strength of Tensile Test Coupons

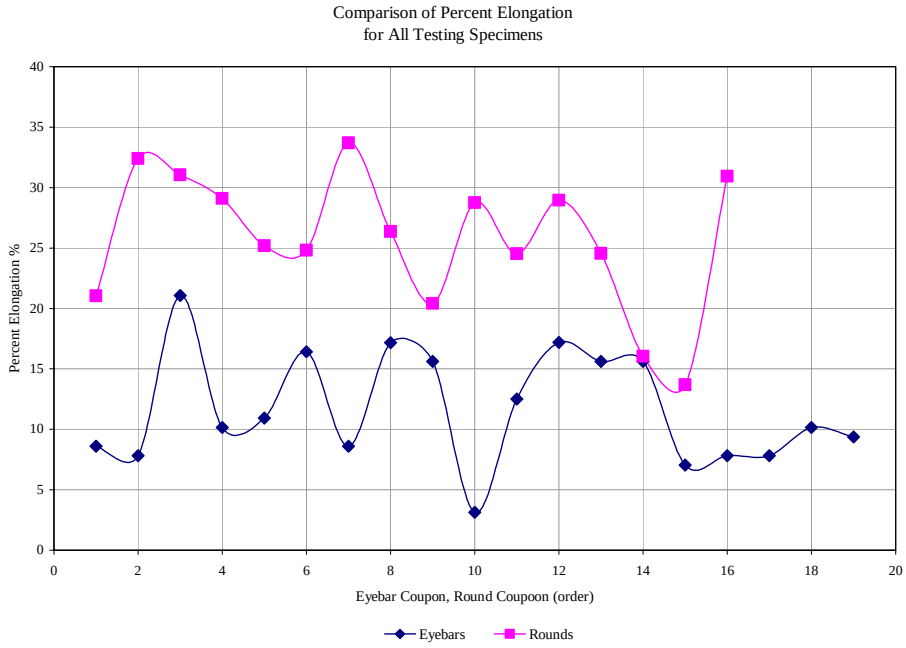

Figure 4.10 Percent Elongation of Tensile Test Coupons

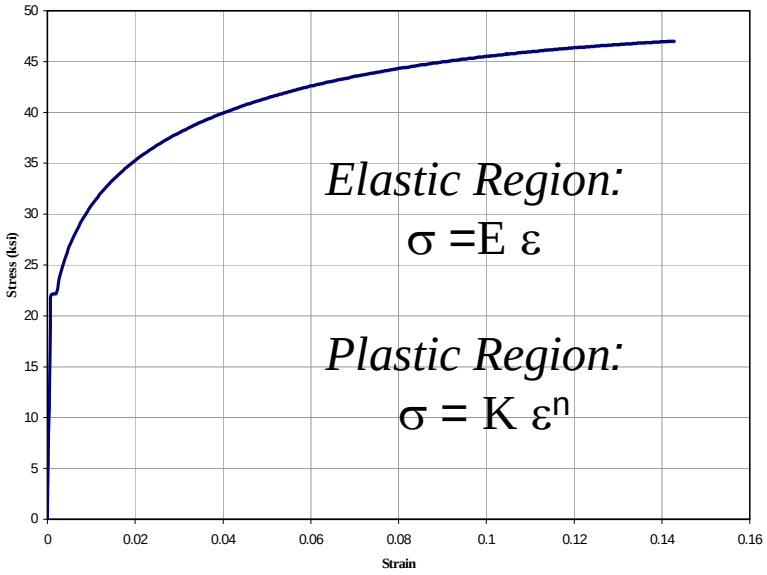

Figure 4.11 Theoretical Stress vs. Strain Curve for Wrought Iron

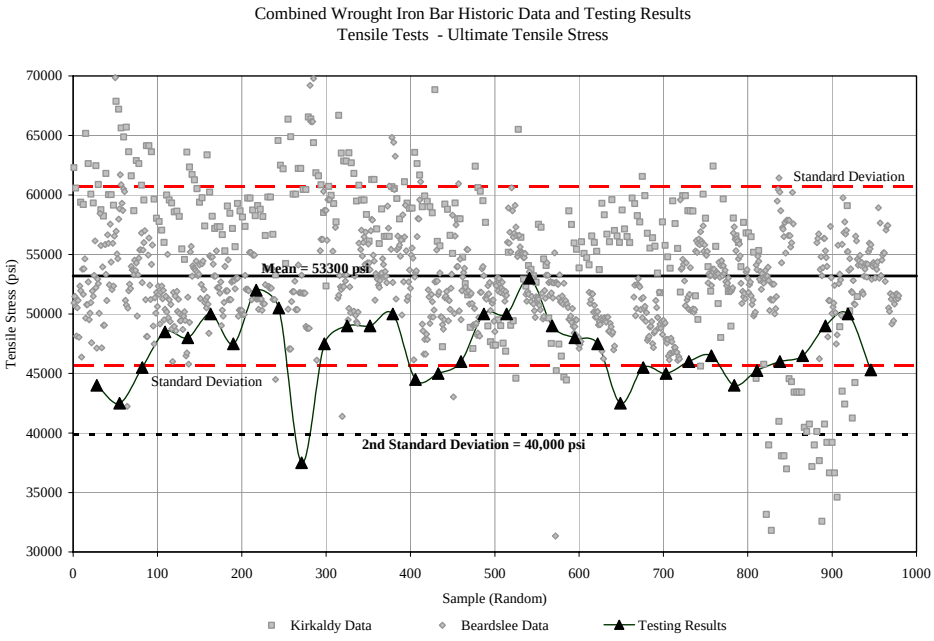

Figure 4.12 Comparison of Historical to Testing Results for Tensile Strength

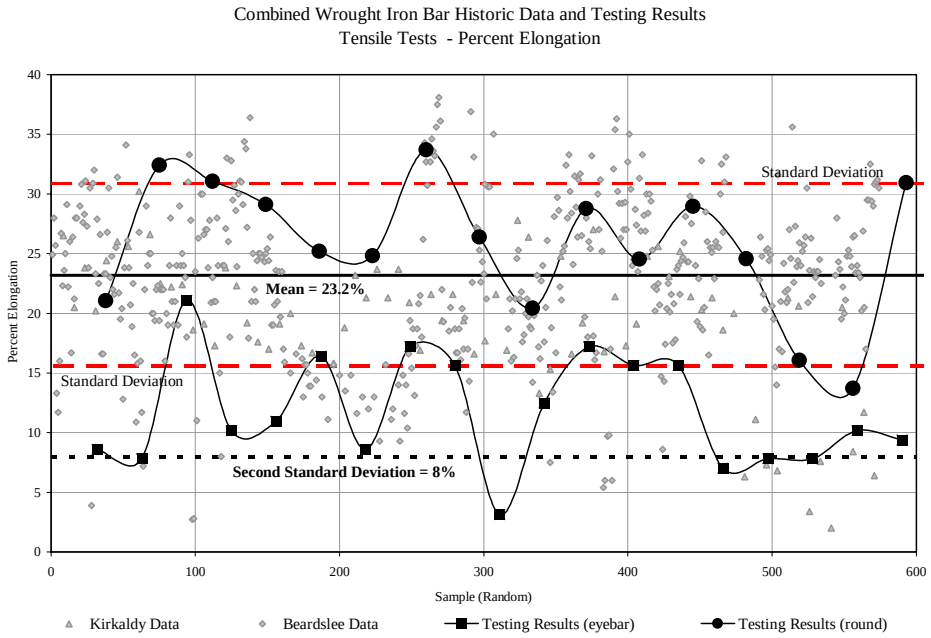

Figure 4.13 Comparison of Historical to Testing Results for Percent Elongation

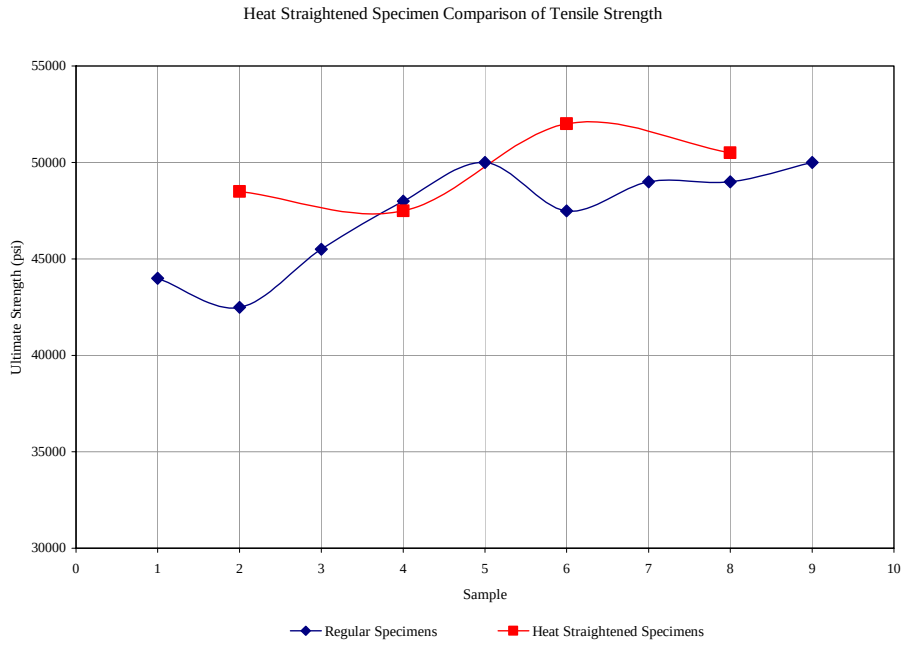

Figure 4.14 Comparison of Heated Straightened Specimens for Tensile Strength

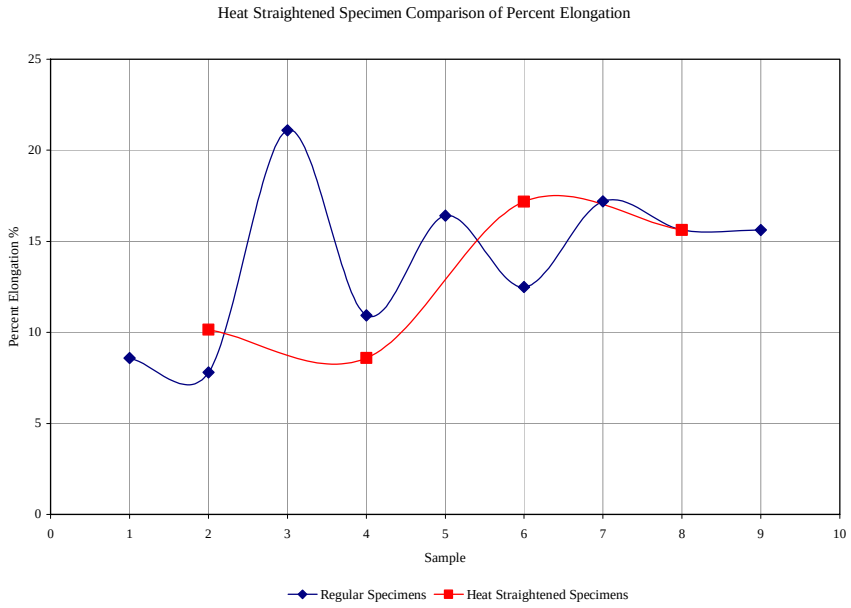

Figure 4.15 Comparison of Heated Straightened Specimens for Percent Elongation

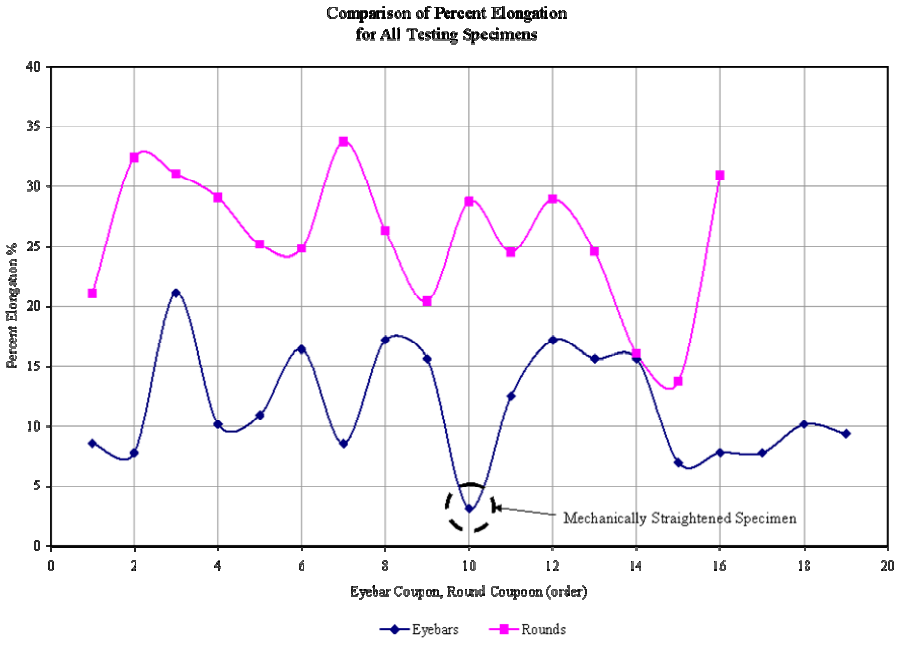

Figure 4.16 Mechanically Straightened Coupon Resulting Percent Elongation

Figure 4.17 Macrograph of Weld used in Welded Tensile Testing Coupons

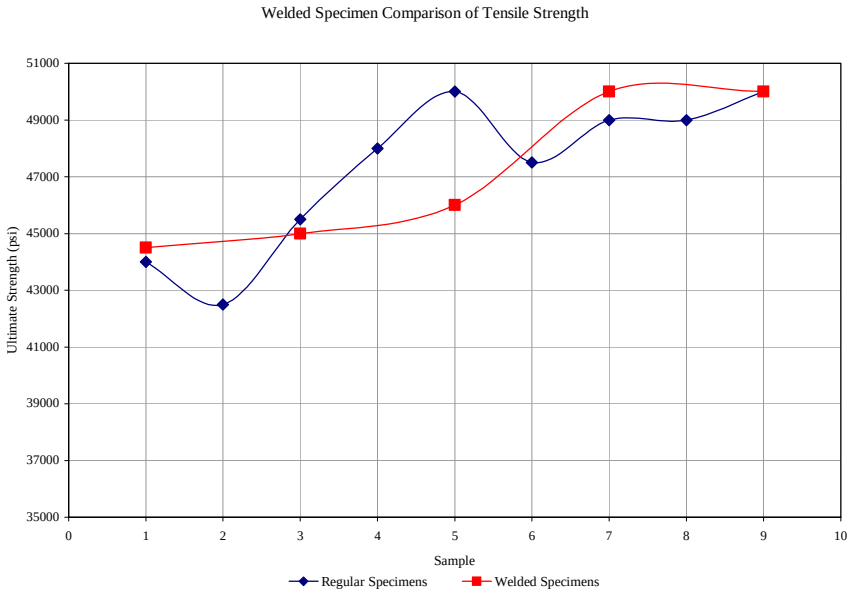

Figure 4.18 Comparison of Welded Specimens for Tensile Strength and Yield Stress

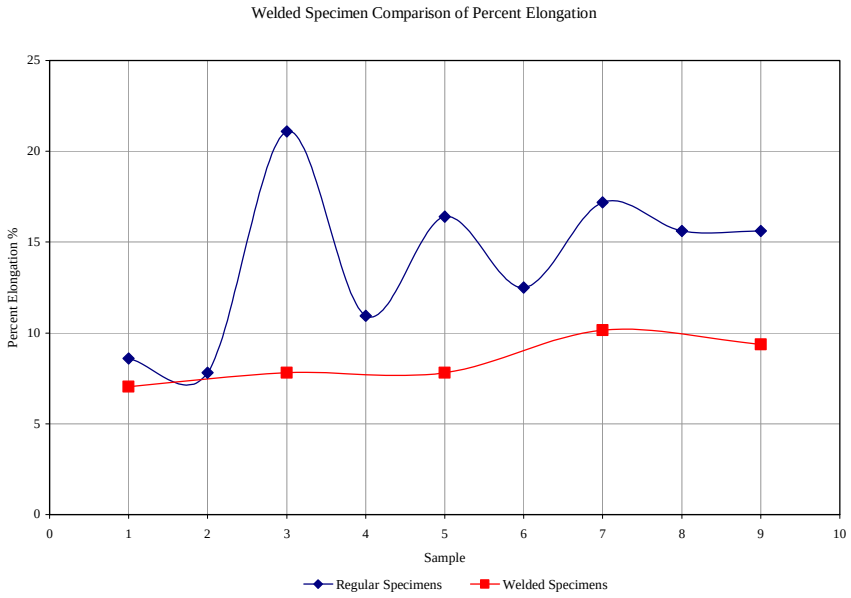

Figure 4.19 Comparison of Welded Specimens for Percent Elongation

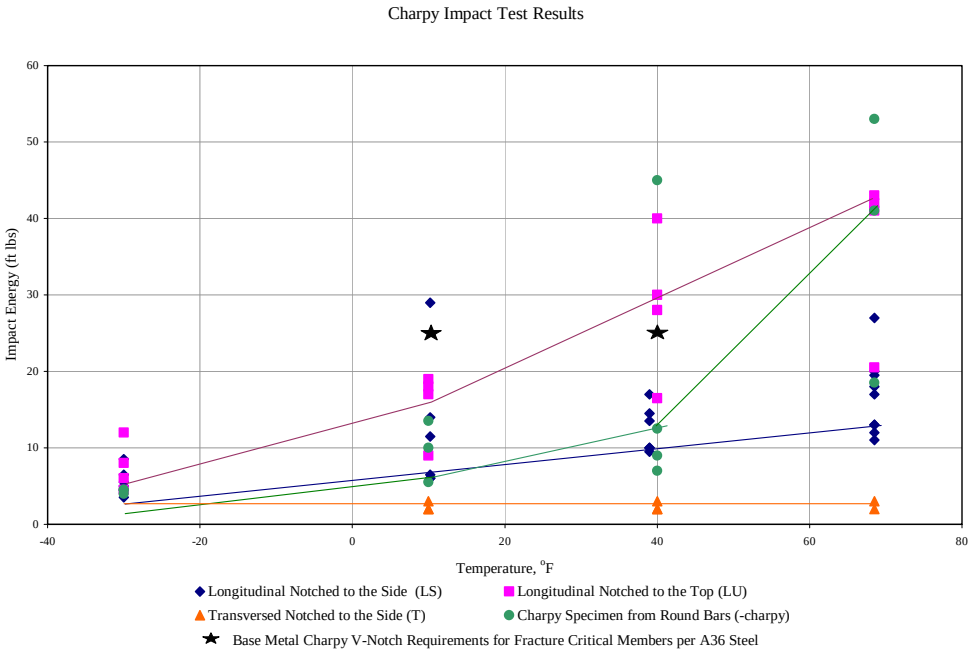

Figure 4.20 Charpy Impact Testing Results

Figure 4.21 Cleavage Fracture of Charpy Impact Specimen (LU, LS Type)

Figure 4.22 Slip Plane Fracture of Charpy Impact Specimen (T Type)

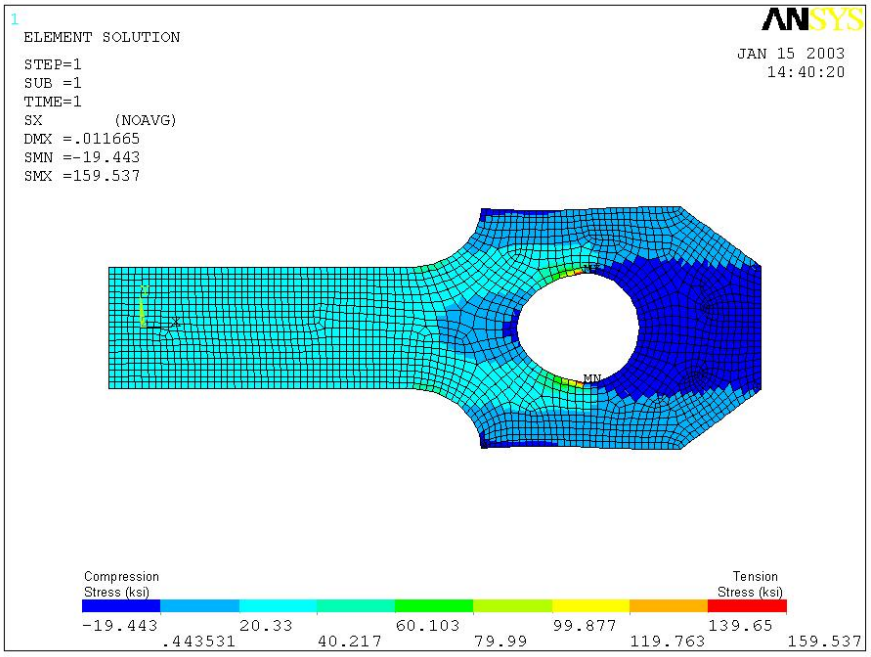

Figure 4.23 Stresses in the Eye Connection by Finite Element Analysis

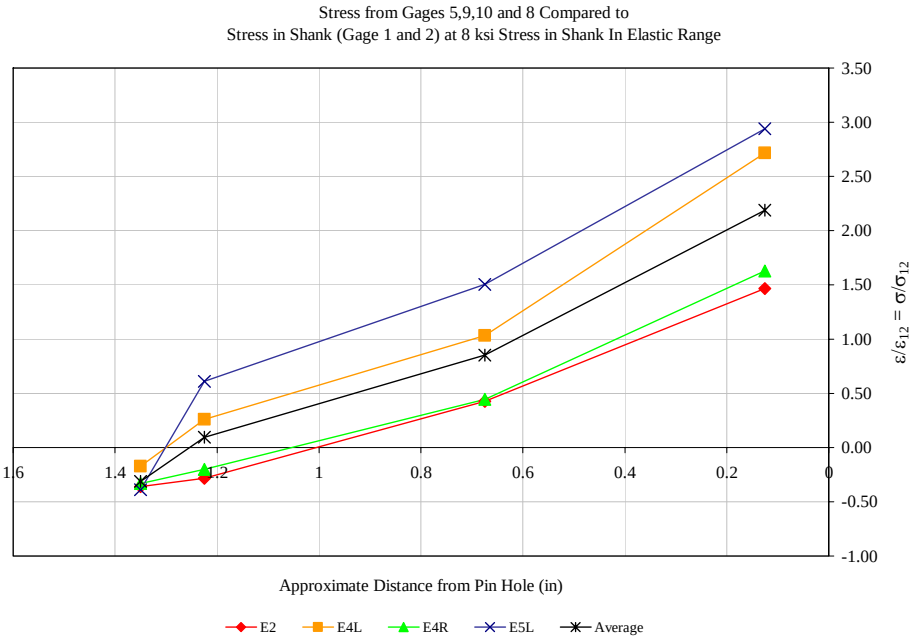

Figure 4.24 Stress Distribution Through Eyebar End Connection Detail

Figure 4.25 Elongation of Hole in Eye Connection after Testing to Failure

5. REPAIR AND REHABILITATION RECOMMENDATIONS

When investigating the condition and capacity of a historic iron truss bridge, it is often beneficial to study the behavior of the truss members in reference to each other. Unexpected movement, shaking, and deflections could reflect underlying structural problems within the truss bridge. For historic truss bridges, common problems usually consist of un-symmetric connections, severely strained and damaged pins, eyebar cracking and failure, elongated and slack members, traffic damaged and bent members, and various stages of corrosion resulting in loss of cross-section. Once trouble areas are found in the bridge, the material properties of the structural members should be determined and the damage repaired accordingly.

5.1 Determination of Material Properties of Bridge Members

Before any repairs can be completed on an iron truss bridge it is first essential to determine the materials that are present in the bridge. Many engineers initially may have trouble in determining the existing materials from visual inspection alone. Bridges that were constructed during the late nineteenth century could consist of a variety of materials commonly used at that time, such as cast iron, timber, steel or wrought iron. It is extremely important to accurately determine the materials used in these historic bridges to properly evaluate their condition.

To determine what materials were utilized in any existing historic bridge, it is useful to locate the history and manufacturer of the bridge. Often agencies that maintain the bridge will have documentation of the bridge's history and construction documents. If these are unavailable, however, it might be beneficial to search for any ornamental

signs on or near the bridge that might lead to an estimate of the age and manufacturer of the existing bridge. Figure 5.1 is an example of a typical sign that marks the year the bridge was constructed and the manufacturer.

Once the manufacturer and age of the bridge is collected, an estimate can be made of the materials utilized in the existing bridge. Typically in the Midwest, bridges that were constructed approximately before the late 1890s consist of historic wrought iron tension members with either wrought iron, cast iron, or timber compression members. Bridges constructed approximately after the late 1890's were primarily constructed using steel.

Often it is useful to fully clean a piece of metal by removing any surface corrosion and investigate its surface appearance to determine if the metal is wrought iron. This is because wrought iron has distinctive slag inclusions that are often present on the surface of the metal and visible by the naked eye. These inclusions are typically darker than the rest of the metal and are elongated in one direction. Figure 5.2 is a photograph of a test coupon that shows some of these large surface inclusions.

If during the bridge inspection some fractured tension members are found, the appearance of the fractured surface could help to identify if the metal is wrought iron or steel. Wrought iron's fractured surfaces that had failed in tension are typically fibrous and jagged in nature unlike typical smooth and angled fractured surfaces of steel. Typically there is very little necking near the fractured surface of wrought iron which is common in steel. Figures 4.4 and 4.5 illustrate the differences between the fracture surface for both wrought iron and steel.

If it is determined that the bridge being investigated is most likely historical wrought iron, the AASHTO Manual for Condition Evaluation of Bridges (1994) recommends using an operating maximum unit stress of 20,000 psi, and an inventory maximum unit stress of 14,000 psi when determining the load rating for these bridges.

The inventory maximum unit stress should be used if the structure has corrosion damage or cracking which might lead to a lower load capacity. The operating maximum unit stress should be used if the bridge has been recently rehabilitated and in good condition. AASHTO also states that, “coupon tests should also be performed to confirm material properties used in the rating.”

The unit stress values outlined in the AASHTO Manual for Condition Evaluation of Bridges were compared to the resulting strength data found during this research study. One standard deviation below the mean yield strength found from investigating the historical data is about 30,000 psi, which is also roughly equal to the average yield strength found from the experimental testing completed. When using this value for a maximum yield stress and requiring that the allowable stress to be equal to 0.6 * Fy, the allowable stress for wrought iron would be 18,000 psi. This number is comparable to the operating maximum stress provided by AASHTO.

Even if the exact year and manufacturer of an existing historic bridge are known, it is still beneficial to undertake material testing. This enables the engineer to have a better understanding of the material properties of the members in the bridge. Some material tests that are beneficial are chemical analysis testing, charpy impact testing and tensile coupon testing. From these results the chemical content and strength of the material can be determined.

In these tests, there are some defining results that help determine if the materials tested are historic wrought iron. The results from a chemical analysis of historical wrought iron, when compared with structural steel, would show a relatively low carbon content ($C<0.1\%$), while a relatively high carbon content ($C>2.0\%$) would indicate that the material is cast iron (Aston, 1941). An excess of silicon along with phosphorous and sulfur is also typically found from a chemical analysis of wrought iron. The presence of silicon is especially important in determining if the material is wrought iron, because the defining slag in wrought iron consists mainly of this element. Also, the tensile coupon

testing of historic wrought iron would show that the tensile strength is typically lower than the tensile strength found in most structural steels.

5.2 Verification and Repair of Connection Symmetry

In the beginning of a bridge examination it is important to inspect the bottom chord members for any misalignment either vertical or horizontal which may indicate failure of the joint connections or the need for adjustments of an individual truss member. In historic metal truss bridges, it is very common for the bottom chord to consist of pairs of eyebars with pin connections. Figure 5.3 is a photograph of a typical bottom chord found on many historic wrought iron truss bridges.

The pin connections consist of multiple two component eyebar members and a one component diagonal member that are connected by a large diameter pin. Figure 5.4 shows a typical eye pin connection. In the original design of the bridge, the eye pin connections are symmetric in the third dimension to ensure that force is equally distributed amongst all the members. But over time, the members can move and the connection losses symmetry due to dynamic live load effects on the bridge and the addition of past repairs. Figure 5.5 is a drawing of a typical pin connection that has become unsymmetrical due to a shift in the diagonal.

Since the capacity of a truss bridge is usually analyzed two dimensionally, it is important that the eye pin connections remain symmetric to ensure that the forces are equally distributed and the actual behavior of the bridge is two dimensional. If the connections are not symmetric, a buckling or fracture could occur in members from lateral forces in the third dimension. Moreover, past repairs to these bridges may include adding another component to a two component member to increase the capacity. This repair, however, alters the symmetric properties in the bridge and actually causes more serious problems within the bridge.

If an existing historic bridge has connections that are lacking symmetry the third component members should be removed and the original members should be moved so the connections are acting symmetrically again. To ensure that future symmetrical behavior is present in the bridge, spacers are typically added in the connection.

5.3 Damaged Pin Replacement

Once the connections are evaluated symmetrically, the capacity of the connections should also be determined. One essential part of the connection that could control the capacity are the eye pins. An analysis of the forces that are acting on the pins should be performed to determine their live load capacity. In one historical bridge rehabilitation, the analysis indicated that the pins had very little live-load capacity and governed the load rating of the bridge (Taavoni, 1994). If it is determined that the pin's live load capacity is not adequate, the existing pins should be removed and the connections should be replaced.

Difficulties typically arise upon removing the pins in the truss bridges. This is because they often are severely corroded and strained or deflected. If the pins are severely bent it may indicate that they were undergoing too much force and their removal is appropriate. The addition of heat causes thermal expansion and is often used along with force when removing the pins to help in the difficult process, as seen in Figure 5.6 and Figure 5.7. After the pins are removed, it is common to replace them with a higher strength material and place spacers to ensure symmetry in the connections. Replacing the existing pins with higher strength pins could increase the load capacity of the bridge and be an affordable alternative to bridge replacement.

In the case of the Carroll Road Bridge in Maryland, the existing pins were replaced with new higher strength pins and the members of the connections were moved

so that they would act in symmetry again. Also, the deck and certain members were replaced, and the bridge was sandblasted and repainted. The overall cost of the bridge rehabilitation was $300,000 dollars and the operating rating for H and HS trucks was 23 and 37 tons, respectively (Taavoni, 1994). This proved to be a very affordable method to rehabilitate this bridge for the state of Maryland.

5.4 Investigation of Crack Growth in Eyebars

When investigating the capacity of pin connections of an existing historic wrought iron truss bridge, it is also important to investigate the strength of the connections at the end of the eyebars of the bottom tension cord. These eyebars are typically fracture critical members and should be thoroughly checked for any sign of distress due to fatigue or corrosion.

The eyebar end connections found from the historic wrought iron trusses have a variety of different geometries. Under dynamic and cyclic conditions, the strength of the eyebar end connections vary due to geometrical differences. Therefore, the geometry of the eyebar should be analyzed to determine any points of higher stress that might induce fatigue cracking. These stress concentrations are typically found in the eyebar at the pin hole and the fillet where the eye head meets the shank.

In the testing completed for this study, an analysis of the resulting stress found in the eyebar connection from the Bell Ford Bridge under elastic loading was completed. The resulting stress distribution, of the eyebar connections showed that very high stress concentrations were located on the outside of the pin hole. This suggests that cracking might develop in this area under cyclic loading and lead to failure of the connection detail.

A study conducted at Iowa State University in 1976 on the strength of eyebar connections included some fatigue testing on damaged and undamaged eyebars. Fatigue tests were completed on twenty three undamaged eyebars and nine damaged and repaired eyebars. Of the undamaged eyebars, twenty one failed in one of the eyes of the eyebar. Of the damaged and repaired eyebars only two fractured in the presence of a repair and the rest failed in the eyes (Elleby, 1976).

The results from testing completed in this study and from the testing at Iowa State University support the need to check for fatigue cracking at the holes of the eyebars. This is especially true since these members are considered to be fracture critical and have been in service for such a long time.

Regardless of the geometry, existing eyebars tend to perform well and fail outside of the connection area under static loading conditions. Evidence of this can be seen in the testing that was completed during this research study. Four eyebar connections were statically tested in tension until they failed. All of the eyebar connections failed outside of the connection detail area.

Testing that was completed at Iowa State University in 1976 also included static testing on eyebars. In this testing, seventeen undamaged specimens and three damaged and repaired specimens were tested. Of these eyebars, none failed in the eye and all failed either in the shank of the eyebar or at an original forging (Elleby, 1976). Therefore, for the statically tested specimens, the eye connections of the eyebars are adequate but the forgings in the eyebars need to also be checked for cracking.

Charpy impact testing of historic wrought iron was also completed in the present study to determine the fracture toughness of the material. Charpy impact specimens were machined from eyebars in different orientations simulating crack growth in different direction along the eyebar. It was determined that the fracture toughness of wrought iron varies according to the direction of crack growth in the material.

The reasons for the differences in fracture toughness relates to the fibrous structure of historic wrought iron. As mentioned in chapter two, the structure of wrought iron consists of elongated strands of iron and iron silicate, also known as slag, that typically run along the length of an eyebar. The charpy impact strengths found from testing for a crack running perpendicular to the length of the eyebar, or against the grain structure of the wrought iron, was found to be between 10 ft lbs and 40 ft lbs at room temperature. The charpy impact strength for a crack running parallel to the grain of an eyebar, however, was never found to exceed 3 ft lbs for all temperatures.

Since the charpy impact strength was so low for a crack running parallel to the direction of rolling, it is essential to inspect existing eyebars to ensure no cracking is running along this direction. It is also very important to ensure that any repair does not create stress concentrations that might propagate a crack in this direction. Fortunately, cracking is not very common in this direction since it is parallel to the primary member stresses. Figure 5.8 is a diagram showing the various directions and locations where potential crack growth might occur.

The impact strength for cracks growing perpendicular to the grain structure of the wrought iron varied considerably and were mainly below the AASHTO Zone 2 minimum requirements for the charpy v-notch strength for fracture critical members of A36 steel. Hence, low fracture toughness values indicate that it is essential to have thorough inspection procedures to identify any existing fatigue cracking. This can be done by many methods such as visual inspection, dye penetrant examination, magnetic particle or ultrasonic examination which are outlined in AASHTO's Manual for Condition Evaluation of Bridges.

5.5 Evaluation and Repair of Corrosion Damage

The slag in wrought iron helps the metal to be very resistant to corrosion. While in open air, the material will develop a patina that turns into a pitted surface but typically does not progress inward to create section loss (Griggs 1999). However, the material does corrode when it is frequently covered in soil or water, which is a common occurrence at the connection joints in a historic truss bridge.

Since the connection joints in historic wrought iron bridges typically collect heavy moisture and debris, eyebars and diagonal members that frame into these connections typically experience heavy corrosion. In some cases, half of the original thickness of the end of an eyebar is lost due to heavy corrosion, as can be seen in Figure 5.9. If heavy corrosion is present in an existing bridge the corroded area should be cleaned and repaired, or the member should be replaced.

Also eyebars can develop severe corrosion at the eye connection from the collection of water. This corrosion reduces the cross section of the eyebar connection and lowers the load capacity. If considerable section loss is found at an eyebar end connection it is beneficial to either replace or repair the eyebar. One method that could be used to repair this severe corrosion is filling in the corroded area with filler weld material.

This corrosion repair was evaluated experimentally in this study. Two different corrosion patterns were modeled. The first pattern modeled was section loss from corrosion on the edge of eye connection similar to the repair seen in Figure 5.10. For this corrosion repair, material was removed from the eyebar connection (Eyebar A) in the same pattern as the corrosion to half the thickness of the eyebar, as seen in Figure 3.25. Then a filler weld was utilized to fill the removed area. A detailed description of the welding process used is described in Appendix D.

The second corrosion pattern modeled was section loss from corrosion through the entire cross section of the eyebar including the area around the pin hole (Eyebar B). As before, material was removed to half the thickness of the eyebar, as is shown in Figure 3.28. This corrosion pattern was considered to be the most severe situation that could be found on an existing bridge since it involved the effective net section of the eye. Filler weld was placed in the removed area according to the procedure outlined in Appendix D.

Both eyebar connections were tested in tension and failed in the shank of the eyebar, showing that the weld repair did not reduce the strength of the eyebar. Therefore, if it is found necessary to repair an eyebar in this manner, then a procedure similar to that outlined in Appendix D for filling in the corroded area with a filler weld should be followed.

If the eye connection of the eyebar is too corroded to repair using a filler weld, the eye could be removed and a new eye could be attached to the existing eyebar using a full penetration groove weld. This repair should be located in the shank of the eyebar member at a section at least two times the eye head diameter from the fillet region. Also the repair, should be done using a weld detail and procedure similar to the groove weld that was determined adequate from testing in this study. A detailed description of the welding procedure for the butt joint groove weld is described Appendix D.

Along with the eyebars, diagonals in existing iron truss bridges are also prone to excessive corrosion near the connection joints. When this occurs it is often advisable to either replace the diagonal member or the section of the member that has experienced the corrosion.

Typically, a moderate amount of corrosion is present on members in existing bridges. This corrosion usually consists of mild pitting and slight corrosion over the entire surface of the members. When rehabilitating an existing bridge, it is beneficial to

remove the members and sandblast them before repainting and assembling them again to minimize future corrosion, as seen in Figure 5.11.

5.6 Investigation and Repair of Elongated Eyebars and Diagonal Bracing

Another problem that commonly occurs in existing historic iron truss bridges deals with the condition of the eyebars and diagonal members. Often over time these members are elongated from heavy use and become slack or loose in the truss bridge. When these members are slack they no longer carry any load and other members are forced to carry greater loads than what they were originally designed for. This can create a dangerous and unsafe situation in the bridge.

Shortening the loose or slack members in a metal truss bridge is a reasonable method to fixing this problem. Some bridges already have turnbuckles that were designed to correct the problem of elongating bridge members. A photograph of a turnbuckle can be seen in Figure 5.12. To shorten the member the turnbuckle is turned and the two ends of the members are brought closer together. It is important not to turn the turnbuckle too much and induce an unnecessary amount of strain in the member. Moreover, the turn-buckles themselves are often corroded and not easily maneuverable. Hence, it may be beneficial to add heat when trying rotate the turn-buckle and examine the threaded region for section loss and cracking.

In one of the Norfolk and Western Railway Bridges in Missouri, a method to shorten wrought iron eyebars without turnbuckles consisted of removing a piece of the eyebar and then welding the eyebar back together again with a pair of steel splice plates. Fatigue tests were completed on the splice plate repairs and determined that the repairs were adequate even though cracking occurred at the toe of the splice plate welds (Keating, 1984).

Keating (1984) stated that the splice plate detail was an adequate repair since the fatigue lives for these connections were comparable to the steel components. This was because the crack growth was "arrested by the wrought iron stringers." The crack would begin propagating through the thickness of the wrought iron eyebar and then turn and propagate along the length of the eyebar (in the direction of rolling). The stress being applied to the eyebar with the splice plate was then parallel to the crack growth, making crack propagation minimal and the fatigue life of the wrought iron higher. Even though the fatigue life of the splice plate repair was very long, the pattern of the crack growth creates the need to check for any type of block shear failure that might occur.

The splice plate repair may be an adequate repair, but for aesthetic reasons, a better method to shorten a loose eyebar is two remove a section from the eyebar and then directly weld the two pieces together using the welding procedure tested in this study. Tensile coupons that included a full-penetration butt welded joints were evaluated. It was determined that weld detail and process utilized in preparing the tensile testing coupons provided sufficient overall performance. The welded wrought iron tensile strength was not affected, but the ductility was slightly lower.

It is recommended that a similar procedure and detail be utilized when shortening a wrought iron eyebar. The welding procedure utilized in this study is outlined in detail in Appendix D. It is also recommended that, if possible, a welding procedure specification (WPS) be developed and a sample of the repaired material be tested to ensure proper performance when using the WPS.

It is important to recognize the lack of ductility that may exist in a shortened member. Although, elastic shortening of a member will not typically reduce the ductility of a member, additional shortening that induces plastic strain will reduce the ductility. This is due to the amount of overall plastic strain that is lost during the life of the member when it is elongated. This phenomenon was prevalent during testing that was completed during this study when comparing the wrought iron that had experienced visual damage

to wrought iron that had not. The wrought iron that experienced significant damage exhibited a much lower percent elongation and, therefore, was much less ductile.

5.7 Investigation and Repair of Damaged and Bent Members

Many existing historic iron truss bridges have been damaged by vehicular traffic or severe storms. In these bridges, there are typically a number of members that have been bent or twisted to the point where the member either fails or its strength is compromised. In extreme cases, the bridge may collapse due to severe damage. For example, Figure 5.13 shows a number of members from the Bell Ford Bridge after it had collapsed. As seen in the photograph, the members are severely misshaped and damaged.

In the testing that was completed for this study, some of the damaged Bell Ford Bridge members were machined into tensile testing coupons and then tested to determine their strength. Of the damaged members, some had been heat straightened and one had been mechanically straightened. The results from the heat straightened samples were superior to the results of the mechanically straightened specimen. The heat straightened samples were more ductile and had adequate tensile strength, while the mechanically straightened specimen was less ductile and failed at a lower tensile stress.

The mechanically straightened tensile coupon had poor percent elongation results and a lower ductility because repeated straightening of the specimen without heat depleted the amount of plastic strain that was available in the material. When using heat to straighten a wrought iron member, the plastic strain in the material is not affected. Therefore, it is recommended that when straightening any damaged wrought iron bridge member, heat should be added.

Figure 5.14 illustrates the method that was used to heat straighten the eyebars from the Bell Ford Bridge. In this method, the wrought iron is first heated slowly in a

charcoal fire until it is red hot in appearance. When the metal is dark cherry red in color it is typically between 1160 and 1270 ^{o}F. After sufficient heating the member is then straightened by bending and/or pounding the surface to work the metal into the desired position. The process may require repeated cycles of heating and pounding to work the metal in the (fluid) red-hot condition. This method is usually performed by a blacksmith and is similar to the original process that was used to form the wrought iron bridge members. To heat the pieces in this manner, the members to be straightened must be removed from the bridge.

Figure 5.1 Typical Bridge Sign Found on Existing Historic Iron Bridges (Historic American Buildings Survey/Historic American Engineering Record)

Figure 5.2 Typical Surface Appearance of Wrought Iron in Many Existing Bridges

Figure 5.3 Picture of Bottom Chord of Laughery Creek Bridge, Spanning Laughery Creek, Aurora vicinity, Dearborn County, IN (Historic American Buildings Survey/Historic American Engineering Record)

Figure 5.4 Typical Eye Pin Connection (Walnut Street Bridge, Spanning Susquehanna River at Walnut Street, Dauphin County, PA - Historic American Buildings Survey/Historic American Engineering Record)

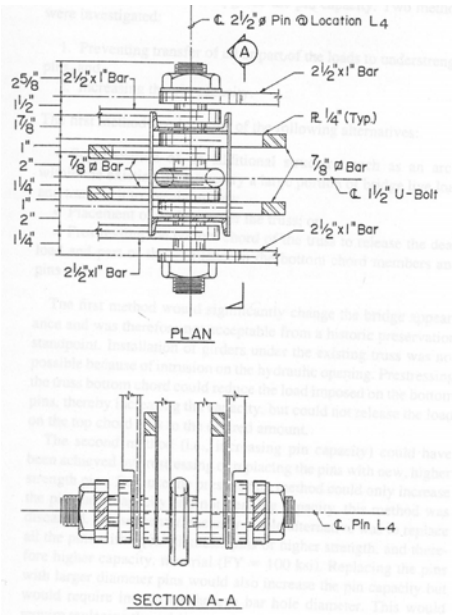

Figure 5.5 Sketch of Typical Resulting Unsymmetrical Condition of a Pin Connection (Taavoni, 1994).

Figure 5.6 Using Heat to Help Remove a Pin During a Rehabilitation of a Bridge In Plainfield, IN.

Figure 5.7 Using Force After Using Heat to Disassemble A Pin Connection During a Rehabilitation of a Wrought Iron Bridge In Plainfield, IN.

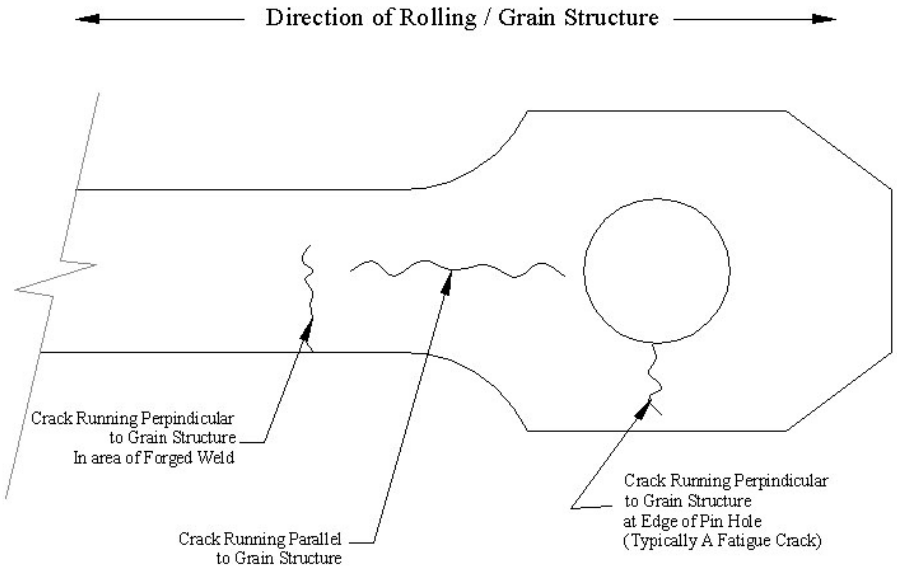

Figure 5.8 Diagram of Potential Crack Growth in Eyebar

Figure 5.9 Heavy Corrosion in an Eyebar End Connection

Figure 5.10 Filler Weld Completed in the Field to Repair Corroded Eyebar Connection

Figure 5.11 Reassembling a Pin Connection After Members Have Been Sand Blasted and Repainted During A Rehabilitation of a Bridge in Plainfield, IN

Figure 5.12 Typical Turnbuckle found in and Existing Wrought Iron Bridge (Penn. Railroad, Selinsgrove Bridge, Spanning Susquehanna River, Snyder County, PA - Historic American Buildings Survey/Historic American Engineering Record)

Figure 5.13 Bent and Damaged Members from the Bell Ford Bridge

Figure 5.14 Heating and Straightening Damaged Members of the Bell Ford Bridge

6. SUMMARY, CONCLUSIONS AND IMPLEMENTATION

The objective of the research project was to determine the material and mechanical properties of common wrought iron bridge members and develop some suggested recommendations and repair techniques. To determine the properties of the historic wrought iron, a literary search was completed along with extensive materials testing. The results from the literary search and materials testing were evaluated and compared to develop a basic understanding of the material properties and behavior of historic wrought iron. After determining these properties, different repair procedures were also experimentally evaluated. Based upon information gathered through the experimental testing, material properties, and literary search, a number of inspection and repair recommendations were developed for implementation of the research.

6.1 Summary

6.1.1 Summary of Literature Search

An in-depth literature search was completed to gather pertinent information regarding the repair and rehabilitation of historic wrought iron bridges. A few articles were found describing the rehabilitation of wrought iron bridges, but none of the articles outlined any specific repair procedures for wrought iron. Along with articles about specific bridge rehabilitations, much information about wrought iron material properties and the manufacturing processes that were utilized to make the existing historic wrought

iron bridges was also found. From this information a better understanding of the material and structural properties of wrought iron was developed.

Information and data were also collected from historical sources containing results from tensile testing of wrought iron used for construction purposes during the nineteenth century. These sources included works from authors such as Kiraldy, Humber, and Beardslee. From these data it was found that the average tensile strength, yield strength, and percent elongation are 54,000 psi, 33,300 psi, 23.2%, respectively. These data were also compared to results found from experimental testing completed in this study.

Along with the literary search a survey was also prepared and distributed to State Department of Transportations, State Local Technical Assistance Programs, Indiana County Engineers, and various engineering consultants to collect information on existing repair and inspection procedures used for historic iron bridges. The results from this survey did not lead to any existing wrought iron bridge member repair procedures, but it did lead to a better understanding of the need for more knowledge concerning the behavior of historic wrought iron.

6.1.2 Summary of Testing Results

The material testing completed in this research consisted of: micrographs, chemical analysis, hardness testing, tensile coupon testing, charpy impact testing, tensile testing of eyebar end connections, and some limited fatigue testing.

Specimens utilized in the testing for this study were machined from members of two different bridges, the Bell Ford Bridge in Jackson County, Indiana and the Adams Mill Covered Bridge in Carroll County, Indiana. The specimens from the Bell Ford Bridge were machined from eyebars that made up the bottom tension chord and were

rectangular in shape. These eyebars had been visually damaged in the collapse of the bridge. The specimens from the Adams Mill Covered bridge were machined from round diagonal tension members that had been replaced with steel diagonals in the bridge.

From the micrographs taken of the historic wrought iron, it was determined that the microstructure consists mainly of ferrite particles along with numerous deposits of impurities. A majority of these impurities are categorized as slag, or iron oxide that is dispersed in elongated deposits throughout the metal leading to a fibrous structure in the metal.

A chemical analysis of the wrought iron revealed a carbon content lower than most mild carbon steels. However, the wrought iron had relatively high excess quantities of silicon, phosphorous and sulfur. The excess amount of silicon found in the chemical analysis is what comprises the slag that is dispersed throughout the metal. The excess silicon and could be an important indicator to determine if the metal is historic wrought iron.

The Rockwell B hardness test was performed on wrought iron samples from the Bell Ford Bridge. The average of all the resulting hardness values was 70 with a standard deviation of 6.5. It was difficult to determine a correct correlating tensile strength from this hardness value due to the lack of previous hardness testing data performed on wrought iron relating hardness to tensile strength. If the metal was a nonaustenitic steel, the correlating tensile strength would be 61 ksi, which is higher than the tensile strength determined for the wrought iron. Therefore, the hardness of the wrought iron may be less than a typical structural steel.

The tensile strength, yield strength, modulus of elasticity, and percent elongation for wrought iron were determined from tensile coupon testing that was completed during this study. These values were determined for each tensile testing coupon test and averaged together. The average tensile strength, yield strength, modulus of elasticity and

percent elongation found from testing was 47,000 psi, 30,000 psi, 27,900 ksi, and 18.1 percent, respectively. The strain hardening coefficient and exponent were also determined for each tensile coupon test. These values were then averaged together and a theoretical stress-strain curve was developed for wrought iron.

The average percent elongation for the specimens from the Bell Ford Bridge was 11.7% which was much lower than the average percent elongation for the specimens from the Adams Mill Covered Bridge (25.7%). This might be due to the damage that the Bell Ford material had endured in the collapse of the bridge. The specimens have been plastically strained and, therefore, lost some ductility, which effectively lowered the amount of available plastic strain in the wrought iron.

To evaluate the adequacy of some common repairs, tensile coupons were prepared that utilized heat straightening, mechanically straightening, and welding. The heat straightened specimens were machined from areas of damaged eyebars from the Bell Ford Bridge that had been straightened by repeatedly heating the metal until it was a red hot color and then beating it into a desired shape. Little variation in the tensile strength, yield strength, and percent elongation compared to the non-repaired specimens was observed.

Along with the heat straightened specimens, a single mechanically straightened specimen was tested. This specimen was machined from an 18” section of an eyebar from the Bell Ford Bridge that was still bent from the collapse of the bridge. This section was mechanically straightened using a three point force method and then a tensile test coupon was machined from it. The mechanically straightened specimen had a much lower tensile strength (37,500 psi) and percent elongation (3.1%) compared to the other test specimens.

Welded tensile test coupons were also investigated during this study. These specimens consisted of two wrought iron pieces from eyebars of the Bell Ford Bridge that

were joined together with a full penetration double V butt joint groove weld utilizing E6010 or E7018 SMAW weld metal. The welded test specimens had comparable tensile strength and yield strength results to the non-repaired specimens, but the percent elongation results from the welded specimens was slightly lower than the other specimens.

Charpy impact testing was also completed on material from the Bell Ford Bridge and Adams Mill Bridge. Charpy impact specimens were machined from the eyebars of the Bell Ford Bridge in three different orientations. These orientations were Longitudinal Notched to the Side (LS), Longitudinal Notched to the Top (LU), and Transverse Notched (T). A fourth type of Charpy impact specimen was machined from the round tensile rods of the Adams Mill Bridge. The Charpy impact strength of all the specimens, except for the longitudinal notched to the top, were lower than the base metal Charpy V-notch requirements for fracture critical members of ASTM A36 steel in a Zone 2 environment. The transverse specimens did not have an impact strength greater than 3 ft lbs at any temperature.

The ends of the eyebars from the Bell Ford Bridge were also investigated to obtain a better understanding of the stress distribution in the connection. To accomplish this, a finite element analysis of the eye connection was completed along with tensile testing utilizing strain gages. Both of these methods verified that high stress concentrations existed directly adjacent to the pin hole, with the second highest stress concentration being though the shank of the eye connection. When testing to full failure, all the connections failed in the shank.

A filler weld repair for severe section loss from corrosion in an eyebar connection was also investigated in this study. Two eyebar end connections were modeled with two different types of section loss and then repaired using a filler weld procedure. Both the repaired eyebar end connections were then tested in tension until failure, where they both fractured in the shaft of the eyebar.

6.2 Conclusions

Based upon information gathered through the literary search and the experimental testing program, a number of conclusions about wrought iron material properties and suitable repair procedures were obtained.

1. Wrought iron mainly consists of ferrite particles with numerous deposits of impurities due to the manufacturing process. In this process iron ore is heated until it is in a pasty condition and then squeezed and rolled into shapes used for construction purposes. Since the iron ore is never heated to a fluid condition, many impurities become imbedded throughout the metal. These impurities, which are mostly categorized as slag, or iron oxide, are dispersed in elongated deposits throughout the iron leading to a fibrous structure in the metal. This leads to lower strength than most common steels.

2. The average tensile strength from materials testing completed in this study was 47,000 psi, while the tensile strength found from historical sources was 54,000 psi. The lower second standard deviation for the tensile strength of wrought iron from historical sources was 40,000 psi. This means that 97.7% of the historical wrought iron specimens have tensile strengths greater than this value and it may be a conservative estimate for the tensile strength of wrought iron in existing bridges.

3. The percent elongation data from the tensile coupons machined from the damaged eyebars from the Bell Ford Bridge were much lower than the percent elongation of the testing coupons machined from the replaced diagonal tension rods from the Adams Mill Bridge. This may be due to the amount of plastic strain that was induced during the collapse of the bridge. This overload condition may have depleted the amount of plastic strain available and, therefore effectively reduced the ductility and the resulting percent elongations.

4. The Charpy impact energy of the wrought iron was found to be lower than most common structural steels. This was especially true for the transverse specimens that had maximum impact energy of 3 ft lbs for a wide range of temperatures.

5. There was little difference in the tensile strength, yield strength, and percent elongation of the heat straightened tensile coupon specimens compared to the non-repaired specimens.

6. The mechanically straightened specimen had a lower percent elongation and tensile strength than the non-straightened specimens. This was because when straightening the bar, the cold metal is forced past the yield stress until permanent deformations and residual stresses are induced. These permanent deformations remove some of the ductility available in the material, thus making it less ductile.

7. The welded tensile coupons had tensile strength and yield strength values comparable to the non repaired coupons. Also, none of the welded coupons fractured in the vicinity of the weld. A macrograph of selected test welds showed that full penetration of the weld was acquired using the welding procedure developed herein. Therefore, it is concluded that development of a suitable weld procedure can be used to successfully implement the repair of wrought iron tension members in an existing bridge structure.

8. All of the eyebar end connections failed in the shank of the eyebar during the full connection test in tension. Large stress concentrations were found to exist at the edge of the pin hole. These stress concentrations could lead to fatigue cracking if an eyebar is loaded and unloaded frequently. Therefore, the eyebar connections should be inspected for any severe cracking in this area and then repaired adequately.

9. A method to repair section loss due to corrosion at an eyebar end connection was examined using two different eyebar end connection specimens. Both failures occurred in the shank of the eyebar, indicating that the filler weld repair procedures proved to be an adequate method to repair section loss from corrosion in an eyebar end connection.

6.3 Implementation of Inspection and Repair Recommendations

Upon completion of this research study, recommendations were developed to aid in the implementation of inspection and rehabilitation procedures for existing historic bridges consisting of wrought iron members. For most wrought iron applications these will involve tension members in truss bridges.

1. When inspecting an old, existing bridge it is important to know the type of material for the bridge members. For bridges consisting of wrought iron members, it is helpful to determine the year and manufacturer of the bridge. A visual inspection of the surface of the material after it has been thoroughly cleaned aids in determining if the material is wrought iron. If possible, it is also recommended to perform a chemical analysis, tensile test, and charpy impact test for the material to determine its specific material properties.

2. It is important to investigate the condition of the connections in an existing historic wrought iron truss bridge. Most bridge connections are designed to act symmetrically, but after time dynamic loading and previous repairs can cause members to move and the connection to have unsymmetrical loading. When this occurs, forces are not equally distributed through the connection, resulting in some members with an unsafe amount of load placed on them while others become loose and slack. If it is decided to rehabilitate a bridge and the

connections are unsymmetrical, it would be beneficial to move the members and add spacers to the joint to hold them in place, and thereby ensure that force is equally distributed through each member in the future.

3. When inspecting a bridge it is important to check the condition of the pins and determine their load capacity. If the pins are severely corroded, deformed, and/or control the load capacity of the bridge, it is recommended that they be replaced with a stronger material.

4. Upon inspecting an existing historic wrought iron truss bridge, it is not uncommon to find severe corrosion near the joints of the bridge. The eyebars and diagonals should be checked thoroughly for section loss from corrosion. If severe section loss has occurred the engineer should consider either replacement or repair of the member. Repair of a corroded member could involve one of two procedures. One option is to grind the corroded areas to clean metal and then use a filler weld repair procedure similar to the one developed in this research project. The second option involves removing the corroded section entirely and welding on a new steel section using a full penetration groove weld.

5. Slack or elongated members are also prevalent in existing wrought iron truss bridges. It is important to shorten these members to ensure that load is being distributed evenly to all the members in the bridge, as the designer intended. This should be done by removing the needed amount of material from the center of a wrought iron member and then joining the pieces together using either a bolted splice plate or a full penetration groove weld. Exceptions to the member shortening recommendation would involve situations where shortening the member would deform the structure in a manner that changes the load path, or for certain members such as zero-force members for which there may be no need to perform any retrofit at all.

6. Vehicle collisions often result in the deformation, and even fracture, of the members in an existing wrought iron bridge. When repairing a bent wrought iron tension member, is it essential to utilize heat to minimize the reduction in ductility and strength of the member. The member should be heated to a “cherry red hot” color and then straightened with judicious hammering while in that color/temperature state. Fractured members should probably be replaced altogether, due to a likely loss in ductility related to the fracture of the member. Reuse of fractured members by removal of damaged regions and then splicing with new material is not recommended.

LIST OF REFERENCES

AASHTO (1998). Standard Specifications for Highway Bridges (LRFD), 2-nd ed., American Association of State Highway and Transportation Officials, Washington D.C.

AASHTO (1994). Manual for Condition Evaluation of Bridges, 2-nd ed., American Association of State Highway and Transportation Officials, Washington D.C.

Aitchison, Leslie, (1960). *A History of Metals*, 2 vols. London, Macdonald & Evans Ltd.

ASM (1967). *Ductility*, American Society for Metals, Metals Park OH.

ASTM (1916). *A.S.T.M. Standards*, American Society for Testing Materials, Pennsylvania, PA.

ASTM A 370 (1997). *Standard Test Methods and Definitions for Mechanical Testing of Steel Products*, American Society of Testing Materials, West Conshohocken PA.

ASTM E23 (2001). *Standard Test Methods for Notched Bar Impact Testing of Metallic Materials*, American Society of Testing Materials, West Conshohocken PA.

Aston, James (1941), *Wrought Iron, Its Manufacture, Characteristics, and Applications*; Pittsburgh, PA, A.M. Byers Company.

Baker, B. (1870). *On the Strengths of Beams, Columns, and Arches*;, E. & F.N. Spon, London.

Barlow, Peter (1845). *A Treatise on the Strength of Timber, Cast Iron, Malleable Iron and Other Materials*;, J. Weale, London.

Beardslee, Commander L.A., U.S.N., (1879), "Experiments on the Strength of Wrought-Iron and of Chain Cables," *Report of the Committees of the United States Board Appointed to Test Iron, Steel and Other Metals, on Chain Cables, Malleable Iron, and Wrought Iron*, Government Printing Office, Washington D.C.

Boyer, Howard E. (1987). *Hardness Testing*, ASM International, Metals Park, OH.

Bruhwiler, E., Smith, F.C., Hirt, M.A., (1990). "Fatigue and Fracture of Riveted Bridge Members," *Journal of Structural Engineering*, ASCE, Vol.: 116 Issue: 1, pp. 198-214.

Cullimore, M.S.G. (1967). "Fatigue Strength of Wrought Iron after Weathering In Service," *The Structural Engineer*, Vol. 45, No. 5, pp. 193-199.

Cywinski, Z. (1985). "Simplified Evaluation of Wrought Iron Bridges," *Stahlbau*, Vol. 4, pp. 103-106.

Dennis, W.H. (1964). *A Hundred Years of Metallurgy*, Aldine Publishing Company, Chicago, IL.

Elban, Wayne, L., Borst, Mark A., Roubachewsky, Natalie M., Kemp, Emory L., Tice, Patrica C. (1998). "Metallurgical Assessment of Historic Wrought Iron: U.S. Custom House, Wheeling, West Virginia," *Association for Preservation Technology*, Vol. 29. pp.27-34.

Elleby, Hotten A., Sanders, Wallace W. Jr., Klaider, F. Wayne, Reeves, M. Douglas, (1976). "Service Load and Fatigue Tests on Truss Bridges," *Journal of Structural Engineering*, ASCE, Vol.: 102 No.St.:12, pp. 2285-2300.

Fairbairn, William (1869). *Iron, its History, Properties and Processes of Manufacture*, Adam and Charles Black, Edinburgh.

Fairbairn, William (1870). *On the Application of Cast and Wrought Iron to Building Purposes*, Longmans, Green, London.

Fu, Chung C., Harwood, Ken (2000). "Practice of Restoring Damaged Historical Truss Bridge," *Practice Periodical on Structural Design and Construction*, ASCE, Vol. 5, No. 3. pp. 122-125.

Green, Perry S., Connor, Robert J., Higgins, Christopher (1999). "Rehabilitation of a Nineteenth Century Cast and Wrought Iron Bridge," *1999 New Orleans Structures Congress* , ASCE, pp. 259-262.

Griggs, Francis E. Jr., (1998). "1864 Moseley Wrought-Iron Arch Bridge: Its Rehabilitation," *Practice Periodical on Structural Design and Construction*, Vol.: 2 Issue: 2, pp. 61-72.

Griggs, Francis E. Jr., (2002). "Squire Whipple – Father of Iron Bridges," *Journal of Bridge Engineering*, May/June, pp. 146-155.

Fisher, Douglas, *The Epic of Steel*, New York, Harper & Row, Publishers, 1963.

Hodgkinson, Eaton (1840). *Experimental Researches on the Strength of Pillars of Cast Iron and other Materials*, R.and J.E. Taylor, London.

Humber, William (1870). *A Complete Treatise on Cast and Wrought Iron Bridge Construction;*, Lockwood, London.

Hutchinson, E.M. (1879). *Girder-Making and the Practice of Bridge Building in Wrought Iron;*, E. & F.N. Spon, London.

Johnson, J.B., Withey, M.O., Aston, James, (1939). *Johnson's Materials of Construction Rewritten and Revised*, John Wiley & Sons, Inc. New York.

Keating, Peter B., Fisher, John W., Yen, Ben T., Frank, William J. (1984). "Fatigue Behavior of Welded Wrought-Iron Bridge Hangers," *Transportation Research Record*, Vol: 2 No. 950, pp. 113-120.

Kirkaldy, David (1862). *Results of an Experimental Inquiry into the Comparative Tensile Strength and other Properties of Various Kinds of Wrought Iron and Steel*, Bell & Bain, Glasgow.

Linnert, George E., (1994). *Welding Metallurgy, Carbon and Alloy Steels*, American Welding Society, Miami, FL.

Lyman, Taylor, (1948). *Metals Handbook*, American Society for Metals, Cleveland, OH.
Gordon, Robert B. (1988). "Strength and Structure of Wrought Iron," *Archeomaterials* Vol.:2, No.: 2 pp.109-137.

McEvily, Arthur J. (2002). *Metal Failures, Mechanisms, Analysis, Prevention*, John Wiley & Sons, Inc. New York.

Mills, Adelbert P. (1915). *Materials of Construction, Their Manufacture Properties and Uses*, 1st Ed. John Wiley & Sons, Inc. New York.

Mills, Adelbert P., Hayward, Harrison W. (1931). *Materials of Construction, Their Manufacture Properties and Uses*, 4th ed. John Wiley & Sons, Inc. New York.

Mills, Adelbert P., Hayward, Harrison W., Rader, Lloyd F. (1939). *Materials of Construction, Their Manufacture Properties and Uses*, 6th ed. John Wiley & Sons, Inc. New York.

Messler, Robert W. Jr., (1999). *Principles of Welding, Processes, Physics, Chemistry, and Metallurgy*, John Wiley & Sons, Inc. New York.

Morison, Elting E., (1966). *Men, Machines and Modern Times*, Massachusetts Institute of Technology, MA.

Prucz, Zolan, Bruestle, Kenneth E. (1992). "Evaluation of the Burlington Northern Railroad Bridge No. 3.80 at Plattsmouth Nebraska for Increased Coal Traffic," *9th International Bridge Conference*, IBC, Pittsburg, PA.

Rostoker, W. and Dvorak, James, (1990). "Wrought Irons: Distinguishing Between Processes," *Archeomaterials* Vol.: 4, No.: 2 pp. 153-166.

Sauveur, Albert (1938). *The Metallography and Heat Treatment of Iron and Steel*, McGraw-Hill, New York, NY.

Stoughton, Bradley (1934). *The Metallurgy of Iron and Steel*, McGraw-Hill, New York, NY.

Taavoni, Shahin, (1994). "Upgrading and Recycling of Pin-Connected Truss Bridge by Pin Replacement," *Transportation Research Record*, No. 1465, pp. 16-21.

Thorne, Robert (2000). "Structural Iron and Steel, 1850-1900," *Studies in the History of Civil Engineering*, Ashgate Publishing Limited, Burlington, Vermont.

Tiemann, Hugh P. (1919). *Iron and Steel, A Pocket Encyclopedia*, McGraw-Hill, New York, NY.

Tredgold, Thomas (1846). *Practical Essay on the Strength of Cast Iron and Other Metals*;, J Weale, London.

United States Steel Corp. (1957). The *Making, Shaping and Treating of Steel*, 7th ed. United States Steel Corportation, Pittsburg, PA.

Watkinson, F., Boniszewski, T., (1964). "Selection of Weld Metal for Welding of Wrought Iron," *Welding and Metal Fabrication* Vol.:34 No.: 2, pp. 54-57.

Warren, Kenneth, (1973). *The American Steel Industry 1850-1970*, Oxford, Clarendon Press.

Appendix A. Data Collected From Historical Studies

One of the most comprehensive sets of data acquired on the strength of wrought iron was completed by David Kirkaldy while he worked at Robert Napier's Vulcan Foundry Works in Glasgow. During this time period, the company was using wrought iron and steel to construct boilers and pressure vessels and was interested in ensuring the materials used were strong enough and well understood. Between 1858 and 1861, Kirkaldy completed a series of tensile load tests of common metals used during this time. He published *Results of an Experimental Inquiry into the Comparative Tensile Strength and other properties of various kinds of Wrought-Iron and Steel* in 1862.

Table A.1 lists the tensile test results of wrought iron bars that Kirkaldy had reported. In this table the diameter of the bar, tensile strength (psi), and percent elongation of the bars were recorded from Kirkaldy's publication. The percent elongation reported by Kirkaldy was typically the average of four tensile tests, and therefore the percent elongation data from every test performed was not available. Also the manufacturers of each iron bar was not recorded due to the fact that majority of the manufacturers were from Europe and would not be found in many wrought iron truss bridges throughout the United States.

Along with testing wrought iron bar material, Kirkaldy also tested wrought iron plate and angle iron material that was commonly used for construction purposes. Tables A.2 and A.3 include the results from this plate and angle iron testing that were recorded from Kirkaldy's publication. These tables include the thickness and tensile strength of the plate and angle iron material tested.

Commander L. A. Beardslee U.S.N. was the chairman in charge of a committee that was appointed in1875 by President U. S. Grant of the United States to complete a thorough testing program with the purpose to determine the material properties of wrought iron. The majority of the material tested in his study was round bar material that

could be forged into chain link or tension rods in bridges. The committee completed more than two thousand tests on wrought iron bar material from nineteen different manufacturers in the United States. Half of these tests were standard tensile tests where the bar specimens were pulled monolithically and resulted in a determination of the tensile strength and other material properties.

Table A.4 lists a summary of the results of 959 tensile tests that Beardslee performed on different wrought iron bars from different manufacturers that were not revealed but labeled with a corresponding letter. In this testing he reported the diameter (size) of the bar tested in inches, the name of the iron (manufacturer), the fracture strength (lbs), the tensile limit (psi), and the elastic limit (psi) were reported. The elastic limit correlates to a modern day yield strength, but is not as accurate. Beardslee simply recorded the load where the first noticeable stretch occurred while testing each specimen. Some of these values were not available for every test due to this inexact method. Percent Elongation was not determined in this set of testing performed by Beardslee.

Table A.5 lists the detailed testing results that were completed by Beardslee and the rest of the committee appointed by U.S. Grant on other iron bars. This table includes the diameter, original length, percent elongation (per original length), elastic limit (psi), and tensile strength (psi). The manufacturer of each bar tested was not recorded from the original due to the fact that they were unknown and the large amount of data that had to be collected. The elastic limit and tensile limit were found in the same manner as described in Table A.4. The percent elongation was found by dividing the fractured length by the original length.

Tables A.6 and A.7 consist of wrought iron tensile strength data that was reported by Fairbairn (1869) and Humber (1870) respectively. These sources are general handbooks that discuss basic concepts of building with wrought iron. In these sources the manufacturer and type of iron that could purchased during the late 19th century were listed along with the tensile strength found from testing their material.

Table A.1 Wrought Iron Bar Tensile Strength Reported by Kirkaldy

Index	Diameter (in)	Tensile Strength (psi)	Average Percent Elongation (%)
101	1.03	62,298	24.9
102	1.02	60,565	
103	1.03	59,390	
104	1.03	59,202	
105	1.00	65,166	26.5
106	1.00	62,635	
107	1.00	60,069	
108	1.00	59,320	
109	0.69	62,451	20.5
110	0.69	60,876	
111	0.69	58,756	
112	0.69	58,228	
113	0.78	61,805	23.8
114	0.78	60,020	
115	0.78	60,020	
116	0.78	59,135	
117	0.77	67,876	20.2
118	0.78	67,198	
119	0.80	65,622	
120	0.77	64,871	
121	1.00	65,701	24.4
122	1.00	63,634	
123	1.00	61,602	
124	1.00	58,678	
125	1.00	62,885	26
126	1.00	62,635	
127	1.00	60,817	
128	1.00	59,570	
129	1.00	64,133	25.6
130	1.00	64,133	
131	1.00	63,634	
132	1.00	59,642	
133	1.00	58,036	30.2
134	1.00	57,757	
135	1.00	57,039	
136	1.00	56,004	
137	1.00	59,998	26.6
138	1.00	59,570	
139	1.00	59,320	
140	1.00	58,571	
141	0.75	58,632	22.5
142	0.75	58,190	
143	0.75	55,463	
144	0.75	54,575	
145	0.89	63,604	22.2
146	0.89	62,344	
147	0.89	61,714	
148	0.89	61,263	
149	0.81	60,528	22.4
150	0.81	59,387	
151	0.81	59,767	
152	0.81	57,387	
153	0.70	63,373	18.6
154	0.70	60,244	
155	0.70	58,207	
156	0.70	57,188	
157	0.77	57,328	19.1
158	0.77	57,328	
159	0.77	56,667	
160	0.77	55,297	
161	0.76	59,070	17.3
162	0.76	58,452	
163	0.76	57,190	
164	0.76	55,653	
165	1.15	59,276	23.8
166	1.16	58,658	
167	1.15	58,135	
168	1.15	57,362	
169	1.02	59,726	22.3
170	1.02	59,726	
171	1.02	58,732	
172	1.02	58,252	
173	0.90	59,104	19.2
174	0.90	58,796	
175	0.90	58,180	
176	0.90	56,595	
177	0.77	59,820	17.6
178	0.77	59,820	
179	0.77	56,694	
180	0.77	53,266	
181	1.13	64,575	17
182	1.12	62,495	
183	1.13	62,201	
184	1.13	54,245	
185	1.01	66,363	19.1
186	1.01	64,895	
187	1.00	60,069	
188	1.00	60,069	
189	0.90	62,229	20
190	0.90	62,229	
191	0.89	60,453	
192	0.89	60,453	
193	0.77	66,553	17.3
194	0.77	66,373	
195	0.77	64,390	
196	0.77	61,864	
197	1.15	61,594	16.7
198	1.15	60,840	
199	1.15	58,521	

Table A.1 (continued) Wrought Iron Bar Tensile Strength Reported by Kirkaldy

Index	Diameter (in)	Tensile Strength (psi)	Average Percent Elongation (%)
200	1.15	52,348	
201	1.04	60,722	16.4
202	1.02	59,965	
203	1.04	59,272	
204	1.02	57,738	
205	0.90	66,683	15.8
206	0.90	63,505	
207	0.90	62,845	
208	0.90	62,845	
209	0.77	63,547	18.8
210	0.77	62,705	
211	0.77	61,804	
212	0.77	59,493	
213	1.00	60,817	23.2
214	1.00	59,569	
215	1.00	59,569	
216	0.98	58,351	
217	0.99	56,121	21.3
218	0.92	61,296	
219	0.92	61,296	
220	0.92	57,134	
221	0.92	55,913	23.7
222	0.87	58,823	
223	0.87	56,515	
224	0.87	56,515	
225	0.87	56,515	21.3
226	0.78	60,695	
227	0.77	60,541	
228	0.77	59,700	
229	0.72	57,976	23.7
230	0.79	56,316	
231	0.76	61,106	
232	0.76	59,316	
233	0.76	58,884	20.9
234	0.75	58,886	
235	0.75	63,577	
236	0.75	62,626	
237	0.75	61,678	16.9
238	0.75	59,013	
239	0.75	59,900	
240	0.75	59,457	
241	0.75	59,013	21.6
242	0.75	58,506	
243	0.81	68,848	
244	0.81	56,104	
245	0.81	55,726	19.4
246	0.81	47,248	
247	0.70	59,226	
248	0.70	58,789	
249	0.70	56,606	21.6

Index	Diameter (in)	Tensile Strength (psi)	Average Percent Elongation (%)
250	0.70	55,078	
251	0.75	59,330	
252	0.75	58,000	
253	0.75	58,000	19.4
254	0.75	54,766	
255	0.75	52,547	
256	0.75	51,596	
257	0.75	48,870	16.6
258	0.75	47,095	
259	0.67	62,411	
260	0.71	60,621	
261	0.70	60,317	17.7
262	0.74	59,512	
263	0.74	57,690	
264	0.90	48,987	
265	0.90	47,664	21.6
266	0.90	47,384	
267	0.90	47,384	
268	0.91	49,505	
269	0.93	49,022	16.9
270	0.92	47,534	
271	0.90	46,869	
272	0.89	55,190	
273	0.91	49,049	27.8
274	0.89	49,418	
275	0.88	44,600	
276	0.91	65,516	
277	0.95	56,447	26.4
278	0.92	52,923	
279	0.92	52,334	
280	0.76	54,070	
281	0.75	53,739	13.3
282	0.76	53,205	
283	0.77	52,665	
284	0.76	57,526	
285	0.75	57,290	15.3
286	0.75	54,626	
287	0.76	54,070	
288	0.88	49,671	
289	0.87	47,519	24.8
290	0.87	49,167	
291	0.86	45,234	
292	1.00	47,459	
293	1.00	46,450	16.6
294	1.00	44,703	
295	1.00	44,453	
296	.75*1	58,661	
297	.75*1	57,520	19.2
298	.75*1	55,960	
299	.75*1	55,437	

Table A.1 (continued) Wrought Iron Bar Tensile Strength Reported by Kirkaldy

Index	Diameter (in)	Tensile Strength (psi)	Average Percent Elongation (%)
300	.75*1	53,866	
701	1.25	56,067	27
702	1.25	55,081	
703	1.25	54,731	
704	1.25	54,123	
705	1.00	56,539	16.8
706	1.00	56,005	
707	1.00	55,256	
708	1.00	53,723	
709	1.25	59,302	21.4
710	1.25	58,321	
711	1.25	56,701	
712	1.25	56,067	
713	1.00	59,605	17.3
714	1.00	57,003	
715	1.00	56,539	
716	1.00	56,005	
717	0.99	58,740	19.1
718	0.99	57,141	
719	0.99	56,500	
720	0.99	56,000	
721	1.02	59,726	24.8
722	1.03	59,270	
723	1.02	58,252	
724	1.02	57,738	
725	0.63	61,558	25.6
726	0.63	59,929	
727	0.63	56,784	
728	0.63	55,526	
729	1.25	56,404	23.1
730	1.25	55,697	
731	1.25	53,439	
732	1.25	51,776	
733	1.02	57,738	25.2
734	1.02	55,761	
735	1.02	54,791	
736	1.02	53,844	
737	1.03	59,506	21.4
738	1.03	57,590	
739	1.00	55,505	
740	1.03	51,846	
741	0.63	59,929	20.3
742	0.63	59,929	
743	0.63	58,671	
744	0.63	58,671	
745	1.25	58,640	21.3
746	1.25	51,521	
747	1.25	49,536	
748	1.25	45,611	
749	1.00	60,069	18.6

Index	Diameter (in)	Tensile Strength (psi)	Average Percent Elongation (%)
750	1.00	58,036	
751	1.00	53,972	
752	1.00	51,905	
753	1.03	62,429	20
754	1.03	55,675	
755	1.03	50,870	
756	1.03	48,014	
757	1.02	59,657	6.3
758	1.02	52,906	
759	1.02	51,879	
760	1.02	48,966	
761	1.00	58,049	11.1
762	1.00	56,539	
763	1.00	56,005	
764	1.00	53,972	
765	1.12	57,692	7.3
766	1.12	56,811	
767	1.10	56,805	
768	1.10	56,481	
769	1.12	55,191	6.8
770	1.09	44,584	
771	0.92	55,323	
772	0.93	52,847	
773	0.92	45,765	21.3
774	0.96	33,150	
775	1.22	39,000	
776	1.20	31,812	
777	1.21	27,173	20.6
778	1.20	20,521	
779	.7*1.02	40,977	
780	.7*1.03	38,075	
781	.7*1.04	38,075	3.4
782	.7*1.05	36,979	
783	1.00	44,561	
784	1.00	44,311	
785	1.00	43,420	0.6
786	1.00	43,420	
787	1.00	43,420	
788	1.00	43,420	
789	1.01	40,467	2
790	1.02	40,124	
791	1.00	40,745	
792	1.02	37,177	
793	1.01	39,000	20.5
794	1.02	40,124	
795	1.00	37,680	
796	1.00	32,582	
797	1.00	40,745	8.4
798	1.00	39,213	
799	1.00	36,646	

Table A.2 Wrought Iron Plate Tensile Strength Data Reported By Kirkaldy

Thickness (in)	Tensile Strength (psi)
0.312	57,881
0.312	54,153
0.312	50,548
0.312	49,986
0.312	47,426
0.312	55,368
0.312	52,669
0.312	48,682
0.395	48,429
0.4	47,426
0.325	53,488
0.4	52,770
0.375	51,991
0.375	51,485
0.412	50,136
0.4	48,014
0.4	46,008
0.325	44,972
0.375	43,074
0.375	59,443
0.355	57,602
0.375	55,437
0.245	51,541
0.25	50,136
0.23	49,054
0.25	45,152
0.245	41,541
0.25	61,184
0.245	58,645
0.25	55,631
0.25	60,756
0.75	60,396
0.75	52,804
0.75	50,625
0.75	50,396
0.75	49,612
0.75	62,544
0.75	58,686
0.75	56,347
0.78	56,172

Thickness (in)	Tensile Strength (psi)
0.775	56,546
0.78	56,546
0.75	54,082
0.87	52,955
0.78	54,403
0.775	51,718
0.48	47,613
0.5	47,613
0.5	46,664
0.48	46,511
0.5	46,062
0.5	58,534
0.35	55,070
0.412	53,889
0.388	55,414
0.35	48,705
0.392	47,532
0.47	60,985
0.415	60,374
0.37	55,925
0.48	55,188
0.37	54,819
0.4	54,687
0.388	55,697
0.5	54,021
0.39	51,922
0.39	49,462
0.512	48,997
0.4	47,410
0.4	60,697
0.5	55,131
0.5	51,295
0.51	51,025
0.51	50,012
0.51	47,238
0.316	54,406
0.304	54,301
0.505	48,853
0.5	45,621
0.505	45,621

Thickness (in)	Tensile Strength (psi)
0.505	42,066
0.5	41,002
0.3	49,441
0.31	49,194
0.312	48,513
0.312	46,943
0.312	46,394
0.312	43,347
0.312	42,581
0.312	51,284
0.4	44,696
0.41	44,195
0.4	43,992
0.41	43,295
0.4	43,012
0.41	43,875
0.4	42,487
0.4	38,007
0.4	56,317
0.66	55,510
0.375	55,176
0.375	54,907
0.4	53,166
0.58	48,016
0.4	52,959
0.375	50,659
0.4	48,761
0.375	48,000
0.66	46,947
0.62	45,761
0.188	53,371
0.637	50,989
0.312	49,395
0.637	47,730
0.715	47,680
0.39	37,474
0.18	49,842
0.312	49,395
0.73	45,310
0.62	44,766

Table A.2 (continued) Wrought Iron Plate Tensile Strength Data Reported By Kirkaldy

Thickness (in)	Tensile Strength (psi)
0.637	44,366
0.39	32,450
0.425	49,838
0.425	49,439
0.675	48,835
0.625	48,766
0.425	45,422
0.238	43,290
0.25	44,512
0.33	42,072
0.245	40,482
0.365	40,055
0.245	39,644
0.38	37,331
0.525	49,677
0.36	37,330
0.245	49,677
0.38	46,806
0.505	46,373
0.365	43,834
0.365	38,570
0.345	38,398
0.65	43,069
0.64	42,783
0.5	39,761
0.55	38,395
0.45	36,798
0.55	36,460
0.645	48,544
0.455	48,487
0.655	48,354
0.55	47,926
0.55	47,481
0.65	46,885
0.65	44,798
0.5	44,417
0.5	43,723
0.45	42,670
0.65	38,605
0.45	45,379

Thickness (in)	Tensile Strength (psi)
0.5	45,379
0.65	45,148
0.5	42,876
0.8	40,794
0.625	39,982
0.265	39,975
0.7552	39,646
0.875	39,073
0.485	38,506
0.55	37,878
0.48	57,804
0.265	56,835
0.625	56,464
0.625	55,838
0.625	55,377
0.75	54,868
0.775	54,410
0.562	53,427
0.885	53,317
0.55	53,196
0.88	52,819
0.785	52,432
0.89	52,229
0.48	51,895
0.265	51,803
0.485	51,240
0.65	50,618
0.75	46,528
0.5	49,083
0.625	45,786
357	44,317
0.55	42,490
0.645	42,460
0.65	42,056
0.65	42,053
0.65	41,287
0.625	41,164
0.625	39,664
0.685	39,297
0.385	39,202

Thickness (in)	Tensile Strength (psi)
0.39	39,170
0.385	37,237
0.63	53,553
0.587	51,581
0.637	51,172
0.65	47,069
0.42	52,679
0.55	52,466
0.625	53,801
0.55	47,453
0.35	55,758
0.887	54,416
0.47	53,799
0.75	53,328
0.637	53,058
0.47	52,441
0.567	52,074
0.47	51,609
0.56	51,509
0.45	50,943
0.755	50,650
0.337	50,160
0.437	48,450
0.45	48,163
0.437	47,759
0.45	47,686
0.587	47,372
0.887	47,239
0.45	46,835
0.567	45,429
0.595	43,720
0.45	43,360
0.437	41,902
0.637	41,130
0.55	53,353
0.55	51,606
0.437	50,352
0.637	50,280
0.4733	50,043
0.47	49,900

Table A.2 (continued) Wrought Iron Plate Tensile Strength Data Reported By Kirkaldy

Thickness (in)	Tensile Strength (psi)
0.45	49,811
0.42	47,372
0.43	47,314
0.45	46,823
0.575	46,302
0.59	46,206
0.45	46,117
0.57	46,089
0.42	45,993
0.437	45,538
0.45	44,660
0.345	44,266
0.47	44,266
0.4	44,131
0.695	43,919
0.44	43,803
0.345	42,100
0.395	40,873
0.47	57,769
0.455	56,631
0.4	56,406
0.915	54,061
0.93	53,683
0.9	51,675
0.65	52,173
0.65	50,948
0.637	49,850
0.75	50,362
0.637	49,775
0.75	47,034
0.637	46,044
0.65	45,775
0.65	45,612
0.637	45,111
0.75	44,255
0.75	41,997
0.355	40,807
0.373	56,233
0.44	55,332
0.445	53,925

Thickness (in)	Tensile Strength (psi)
0.373	48,656
0.373	47,684
0.445	47,255
0.373	43,675
0.44	42,980
0.355	42,288
0.425	38,905
0.428	56,080
0.4	55,954
0.415	52,507
0.4	46,745
0.41	44,425
0.415	52,021
0.415	48,948
0.415	48,610
0.41	44,338
0.4	41,866
0.41	40,192
0.63	52,035
0.587	50,189
0.637	50,053
0.65	49,841
0.42	49,565
0.55	44,184
0.625	47,609
0.55	45,908
0.435	45,026
0.887	43,601
0.47	42,690
0.75	47,903
0.637	47,113
0.47	46,846
0.567	46,789
0.47	35,007
0.565	57,659
0.755	57,653
0.637	55,822
0.42	53,014
0.567	52,761
0.595	50,953
0.45	52,303
0.437	52,303
0.637	49,387
0.47	49,000
0.47	47,274
0.47	46,127

Table A.3 Wrought Iron Angle Tensile Strength Data Reported by Kirkaldy

Thickness (in)	Tensile Strength (psi)
0.63	60,455
0.587	54,712
0.637	54,575
0.65	54,066
0.42	56,538
0.55	55,301
0.625	54,858
0.55	54,444
0.435	51,985
0.887	44,797
0.47	39,534
0.75	56,649
0.637	55,443
0.47	53,112
0.567	51,917
0.47	51,470
0.56	48,141
0.45	54,962
0.755	54,103
0.637	51,125
0.437	43,037
0.45	43,817
0.437	43,370
0.45	40,449
0.587	37,909
0.887	58,353
0.45	56,936
0.637	56,860
0.42	56,275
0.755	54,546
0.637	53,594
0.56	57,119
0.435	56,695
0.637	54,967
0.625	54,967
0.45	59,336
0.567	57,932
0.595	53,527
0.45	51,284
0.437	57,123
0.637	56,472
0.55	52,595
0.559	47,012
0.437	52,491
0.637	52,306
0.47	51,511
0.47	50,892

Thickness (in)	Tensile Strength (psi)
0.47	57,917
0.42	56,492
0.45	54,061
0.437	52,333
0.42	52,363
0.57	51,780
0.44	52,807
0.425	51,551
0.59	50,044
0.59	56,534
0.45	54,250
0.42	53,394
0.43	52,333
0.45	51,491
0.575	46,457
0.59	56,109
0.45	53,884
0.57	53,314
0.42	53,314
0.437	52,334
0.45	52,334
0.47	63,715
0.75	62,888
0.637	59,667
0.45	58,772

Table A.4 Summary of Wrought Iron Bar Tensile Strength, Elastic Limit (Yield Strength) Data of 959 Specimens Reported by Beardslee

Size of Bar	Name of Iron	Number of Tests	Strength (lbs)	Tensile Strength (psi)	Elastic Limit (psi)
0.25	F	1	2,920	59,885	
0.38	F	4	5,886	54,090	40,980
0.50	C	6	12,331	62,700	
0.50	C	7	11,699	59,000	
0.50	C	8	11,388	57,700	
0.50	C	11	10,881	55,400	
0.50	F	1	10,359	52,275	39,126
0.63	F	11	16,977	55,450	
0.63	F	4	15,928	52,050	
0.63	F	11	17,644	57,660	
0.75	F	4	22,746	51,546	35,933
0.88	F	4	30,850	50,630	33,931
1.00	K	13	48,456	61,727	
1.00	D	1	47,975	61,115	33,486
1.00	O	1	45,030	57,363	37,415
1.00	Fx1	5	43,778	55,768	34,729
1.00	P	2	45,378	57,807	39,230
1.00	A	3	42,932	54,690	34,881
1.00	Fx2	3	44,580	56,790	36,885
1.00	Fx3	2	42,323	53,915	36,336
1.00	F	2	40,758	51,921	31,300
1.00	D	8	41,527	52,900	
1.00	F	5	41,463	52,819	32,267
1.00	F	4	40,349	51,400	34,600
1.13	K	3	60,066	60,458	37,344
1.13	D	1	59,196	59,582	33,597
1.13	C	2	57,097	57,470	31,990
1.13	Fx1	5	56,068	56,434	34,682
1.13	P	2	57,125	57,498	41,311
1.13	N	2	55,779	56,143	32,267
1.13	Fx2	3	55,564	55,927	37,250
1.13	E	1	52,753	53,097	33,549
1.13	Fx3	2	54,290	54,644	34,695
1.13	D	2	54,332	54,687	28,166
1.13	A	3	53,550	53,900	26,787
1.13	F	3	53,501	53,850	33,457
1.13	O	1	52,691	53,035	32,410
1.13	F	2	49,824	50,149	35,493
1.13	F	5	51,928	52,267	32,019
1.25	K	2	59,075	59,461	36,501
1.25	P	2	56,507	56,876	36,868
1.25	C	1	57,522	57,897	32,469

Table A.4 (continued) Summary of Wrought Iron Bar Tensile Strength, Elastic Limit (Yield Strength) Data of 959 Specimens Reported by Beardslee

1.25	D	2	57,601	57,977	31,996
1.25	P	2	55,420	55,782	35,596
1.25	Px	2	55,969	56,334	33,921
1.25	N	2	56,112	56,478	33,251
1.25	Fx1	6	54,895	55,253	34,784
1.25	D	1	55,190	55,550	28,166
1.25	E	1	53,544	53,893	32,712
1.25	Fx2	3	54,775	55,132	38,603
1.25	Fx3	2	52,902	53,247	32,520
1.25	A	3	53,548	53,897	27,643
1.25	M	20	53,403	53,752	
1.25	M	20	53,739	54,090	
1.25	F	2	52,627	52,970	32,075
1.25	F	2	52,387	52,729	39,608
1.25	M	20	52,678	53,022	
1.25	F	5	52,279	52,620	33,220
1.25	O	1	49,716	50,040	30,730
1.31	P	94	73,724	54,518	35,898
1.38	M	48	87,454	58,926	37,548
1.38	M	35	85,559	57,649	38,578
1.38	D	1	86,111	58,021	32,152
1.67	K	2	121,653	55,790	31,034
1.67	C	1	119,819	54,949	31,030
1.67	M	28	118,563	54,373	35,820
1.67	N	2	118,354	54,277	33,622
1.67	Fx1	5	115,500	52,968	33,275
1.67	Fx3	2	114,987	52,733	34,606
1.67	E	1	113,943	52,254	25,930
1.67	A	3	116,784	53,557	33,650
1.67	P	1	114,601	52,556	30,802
1.67	F	5	114,560	52,537	34,469
1.67	F	2	114,128	52,339	39,103
1.67	M	4	115,604	53,016	35,379
1.67	Fx2	3	112,270	51,487	35,911
1.67	F	2	111,854	51,296	31,992
1.67	O	1	110,323	50,594	34,940
1.44	P	1	86,532	53,345	
1.44	E	1	87,504	53,944	32,543
1.44	G	1	86,359	53,238	32,534
1.44	B	4	84,816	52,287	32,411
1.44	C	1	83,955	51,756	32,655
1.44	J	1	81,755	50,400	
1.50	M	12	100,768	57,052	38,417
1.50	K	2	101,236	57,317	33,412
1.50	D	1	99,802	56,505	32,496
1.50	M	25	97,967	55,466	34,780
1.50	M	26	97,375	55,131	33,771
1.50	P	2	95,658	54,159	33,140

Table A.4 (continued) Summary of Wrought Iron Bar Tensile Strength, Elastic Limit (Yield Strength) Data of 959 Specimens Reported by Beardslee

1.50	M	17	96,331	54,540	
1.50	C	4	97,857	55,404	34,770
1.50	E	1	97,877	55,415	32,869
1.50	M	20	96,819	54,816	34,716
1.50	Px	2	96,003	54,354	34,617
1.50	M	27	95,545	54,095	35,544
1.50	E	1	96,338	54,544	33,027
1.50	P	1	96,911	54,868	29,636
1.50	M	20	94,516	53,512	
1.50	M	23	93,507	52,941	
1.50	Fx3	2	93,292	52,819	34,840
1.50	Fx1	5	94,478	53,491	34,307
1.50	M	4	94,592	53,555	34,901
1.50	N	2	93,081	52,700	34,690
1.50	C	1	92,661	52,462	35,880
1.50	H	1	92,119	52,155	29,992
1.50	D	1	91,640	51,884	27,708
1.50	A	2	91,834	51,994	28,794
1.50	F	2	89,936	50,919	32,054
1.50	O	1	90,884	51,456	32,312
1.50	F	5	90,928	51,481	34,591
1.50	Fx2	3	90,162	51,047	34,917
1.50	J	1	90,162	51,047	
1.50	M	1	87,062	49,292	32,597
1.63	N	2	116,795	56,344	35,889
1.63	K	4	118,428	57,132	35,026
1.63	M	10	118,988	57,402	35,701
1.63	P	2	115,323	55,634	33,522
1.63	C	4	116,552	56,227	33,207
1.63	Px	2	113,364	54,689	33,427
1.63	A	2	112,628	54,334	32,163
1.63	D	1	111,304	53,695	30,087
1.63	Fx3	2	110,566	53,339	33,540
1.63	T	5	110,976	53,537	34,335
1.63	D	1	111,136	53,614	30,664
1.63	J	1	109,341	52,748	
1.63	E	1	109,190	52,675	33,745
1.63	Fx2	3	110,771	53,438	35,870
1.63	H	1	108,441	52,314	29,364
1.63	E	1	107,678	51,946	27,695
1.63	O	1	108,622	52,401	34,012
1.63	F	2	108,128	52,163	33,907
1.63	G	1	106,142	51,205	33,318
1.63	F	2	104,741	50,529	35,390
1.63	F	5	105,655	50,970	33,625
1.63	C	1	101,634	49,030	31,099
1.69	K	1	126,513	56,595	38,310

Table A.4 (continued) Summary of Wrought Iron Bar Tensile Strength, Elastic Limit (Yield Strength) Data of 959 Specimens Reported by Beardslee

1.69	B	1	121,117	54,181	
1.69	J	1	120,967	54,114	
1.69	B	3	118,242	52,895	33,145
1.69	E	1	116,510	52,120	35,549
1.69	G	1	129,182	57,789	34,160
1.69	C	1	111,370	49,821	33,184
1.75	K	1	139,133	57,874	
1.75	P	2	130,329	54,212	33,908
1.75	C	5	130,805	54,410	31,354
1.75	P	2	127,040	52,844	33,842
1.75	F	5	129,449	53,846	36,573
1.75	J	1	129,339	53,800	27,856
1.75	M	2	132,267	55,018	34,283
1.75	D	1	128,550	53,472	31,802
1.75	K	1	128,050	53,264	
1.75	D	1	126,692	52,699	27,817
1.75	F	2	127,786	53,154	35,323
1.75	E	1	124,064	51,606	26,541
1.75	A	2	123,831	51,509	29,404
1.75	F	1	121,862	50,690	32,229
1.75	G	1	121,153	50,395	36,254
1.75	C	1	120,953	50,312	30,852
1.75	F	2	121,518	50,547	35,954
1.75	F	3	125,766	52,314	35,320
1.75	E	1	119,761	49,816	31,214
1.75	F	5	119,573	49,738	28,907
1.75	O	1	120,513	50,129	32,271
1.81	K	1	145,903	56,577	
1.81	B	4	138,368	53,655	
1.81	C	1	131,441	50,969	30,814
1.81	G	1	129,742	50,310	33,565
1.81	E	1	129,734	50,307	29,767
1.81	J	1	126,242	48,953	
1.88	K	2	148,484	53,803	31,031
1.88	C	1	150,261	54,447	32,334
1.88	D	1	146,544	53,100	32,074
1.88	M	1	149,038	54,004	33,610
1.88	F	5	145,923	52,875	35,641
1.88	F	2	147,264	53,361	35,032
1.88	P	2	144,901	52,505	32,312
1.88	E	2	140,417	50,880	27,100
1.88	D	1	142,015	51,459	27,816
1.88	P	2	142,851	51,762	32,261
1.88	,	2	138,990	50,363	
1.88	A	2	139,600	50,584	28,713
1.88	F	2	140,856	51,039	33,067
1.88	F	3	141,187	51,159	33,970
1.88	F	2	137,282	49,744	35,615
1.88	F	3	136,208	49,355	32,855
1.88	F	2	134,318	48,670	23,250
1.88	O	1	131,028	47,478	30,842
1.94	M	2	151,684	51,474	

Table A.5 Detailed Investigation of the Strength of Wrought Iron Bars Part II, Reported by Beardslee

(includes Elastic Limit, Tensile Strength, and Percent Elongation per original length)

Test Number	Diameter (in)	Length (in)	Percent Elongation (per original length)	Elastic Limit (psi)	Tensile Limit (psi)
1	0.874	3.5	24.9	31172	50925
2	0.875	3.5	28	31598	51470
3	0.875	3.5	25.7	31598	50640
4	0.872	3.5	13.3	39080	48141
5	0.875	3.5	11.7	34256	50527
6	0.976	3.5	16	34092	51139
7	0.976	3.9	26.7	27466	48048
8	0.976	3.9	22.3	35204	52339
9	0.976	3.9	23.6	32578	51958
1	0.976	3.92	25	28338	46378
11	0.976	3.92	29.1	34521	53762
12	0.976	3.88	22.2	32181	51657
13	0.976	0.9	26	31977	53796
14	0.976	3.9	16.7	37423	54631
15	0.976	3.9	26.4	29404	49652
16	0.976	3.92	21.2	33519	50788
17	0.976	3.92	28	32649	50788
18	0.976	3.92	28	34621	52693
19	0.976	3.87		2864	49519
2	0.964	3.9	29	30141	50075
21	0.964	3.9	3.8	33646	50958
22	0.976	3.92	27.6	23559	47580
23	0.976	3.92	28.3	27402	51924
24	0.565	3.92	31.1	26467	51490
25	0.564	2.27	27.3	35500	53250
26	0.56	2.26	23.8	33623	56145
27	0.564	2.26	3.5	33008	52213
28	0.564	2.23	3.9	26821	47138
29	0.564	2.23	3.9	37270	52922
3	0.564	2.28	32	34327	52542
31	0.565	2.27	23.3	33075	50059
32	0.565	2.26	27.9	3893	58436
33	0.565	2.27	22.5	35400	55743
34	0.565	2.23	26.6	29916	47168
35	0.564	2.23	16.6	41484	53949

Table A.5 (continued) Detailed Investigation of the Strength of Wrought Iron Bars Part II, Reported by Beardslee

Test Number	Diameter (in)	Length (in)	Percent Elongation (per original length)	Elastic Limit (psi)	Tensile Limit (psi)
36	0.565	2.23	16.6	38431	49039
37	0.565	2.27	23.3	30115	49062
38	0.565	2.27	23.3	40128	55843
39	0.565	2.27	26.8	37295	53330
40	0.565	2.26	30.5	30514	51136
41	0.565	2.26	23	39090	56641
42	0.565	2.26	24.8	39609	55943
43	0.564	2.27	22	34928	52442
44	0.564	2.27	21.6	39832	57546
45	0.564	2.27	25.5	38130	54363
46	0.565	2.26	31.4	30514	52054
47	0.565	2.26	21.7	39888	55943
48	0.565	2.26	19.5	37216	52353
49	0.564	2.26	20.4	25551	56545
50	0.564	2.26	12.8	47896	69856
51	0.564	2.26	23.8	32064	56945
52	0.564	2.26	34.1	35028	55044
53	0.564	2.26	26.1	36869	54644
54	0.564	2.26	23.8	39970	57968
55	0.517	1.98	20.7	NA	58837
56	0.518	1.98	18.9	NA	61700
57	0.517	1.98	22.5	NA	60862
58	0.402	1.57	16.5	NA	59300
59	0.402	1.56	10.9	NA	58700
60	0.402	1.5	15.8	NA	60500
61	0.402	1.58	26.8	NA	60285
62	0.875	3.5	16	34259	51139
63	0.875	3.5	11.7	34092	50751
64	0.789	3.87	7.2	32009	42237
65	0.782	3.87	22	33989	50490
66	2.02	6	29	34199	51960
67	2.06	9	24	26403	52500
68	1.95	6	25	22059	52138
69	1.95	10	25	29000	54000
70	1.99	13.25	20	27781	53710
71	2.02	10	20	30600	53670
72	2.03	8.5	19.4	34939	53290
73	2.03	8.5	22	35217	54525
74	2.02	8.5	22.3	35295	53664
75	2.02	8.5	19.4	35444	54290

Table A.5 (continued) Detailed Investigation of the Strength of Wrought Iron Bars Part II, Reported by Beardslee

Test Number	Diameter (in)	Length (in)	Percent Elongation (per original length)	Elastic Limit (psi)	Tensile Limit (psi)
76	1.84	12.3	22	31049	49823
77	1.83	13	22	30110	53292
78	1.61	7.37	22	29233	54695
79	1.6	9.65	16	28165	55375
80	1.61	7.4	20	27853	55402
81	1.6	7.33	19	29139	56807
82	1.62	9.44	24	33071	52634
83	1.6	9.44	28	34848	55375
84	1.63	20	21	28850	56000
85	1.63	20	19	29500	57000
86	1.61	9	21	29000	51200
87	1.5	10	24	28000	48100
88	1.23	5	19	25000	48100
89	1.14	4	29	24480	54960
90	1.12	4	24	24900	56387
91	1.81	10	25	33000	52420
92	1.851	7.38	24	28434	51217
93	1.51	7.4	23	32764	54167
94	1.02	4	18	35000	55800
95	0.99	4.06	31	26027	48992
96	0.92	3.9	33.3	25617	47483
97	0.987	3.93	27.8	34374	51365
98	0.974	3.89	2.72	32210	50066
99	0.974	3.89	2.8	30197	51805
100	0.565	2.26	23.5	33805	50618
101	0.565	2.26	11	36896	52333
102	0.565	2.28	26.3	34623	51655
103	0.565	2.28		33306	49162
104	0.56	2.28	30	34943	51854
105	0.565	2.28	30	35600	52353
106	0.566	2.29	26.6	39546	51271
107	0.567	2.29	27	39306	51980
108	0.567	2.22	27	31683	49505
109	0.567	2.3	23.8	32871	50396
110	0.567	2.25	27.8	36831	51485
111	0.562	2.25	20.9	38291	50181
112	2	7	23	31786	55014
113	2	8	21	27507	49662
114	2	8	21	17627	51193
115	2	9	28	28118	49360

Table A.5 (continued) Detailed Investigation of the Strength of Wrought Iron Bars Part II, Reported by Beardslee

Test Number	Diameter (in)	Length (in)	Percent Elongation (per original length)	Elastic Limit (psi)	Tensile Limit (psi)
116	2	11	24	28729	50796
117	2	11	15	27507	48748
118	2	11	8	30869	45998
119	2	11	24	29353	51805
120	978	11	24	NA	48962
121	0.978	3.91	27.1	28620	51502
122	0.998	3.91	33	27954	48587
123	0.999	4	26	31958	51901
124	1	4	18	33177	50217
125	1	4	32.8	32597	51225
126	1	4	29.5	30812	50064
127	1	4	30.7	26738	49424
128	1	4.01	28.6	46738	49436
129	1	4.02	23.9	30557	49898
130	1	3.99	30	29603	48701
131	1	3.99	31.1	30049	49816
132	1	3.99	31	29539	50191
133	1	3.99	29.1	31691	49465
134	1	3.99	34.4	25464	46486
135	1	3.99	33.8	25460	46728
136	0.975	3.9	27.2	3352	51405
137	0.975	3.9	17.9	25448	45779
138	0.975	3.9	36.4	26204	49289
139	1	6	21	35124	55218
140	1	6	25	34071	55683
141	1	5.5	22	35448	53170
142	1.125	7	21	25789	54050
143	1.125	7	24.4	26249	53860
144	1.125	5.5	25	28324	53790
145	1.25	7	25	25036	53670
146	1.25	7	24.7	26118	54451
147	1.25	5.5	29	31295	53515
148	1.375	7	24.3	33215	53210
149	1.375	7	25	33867	53340
150	1.375	7	25.4	33800	54122
151	1.5	7	24.4	28794	51286
152	1.5	7	26.4	28800	52482
154	1.625	11	19	32605	54218
155	1.625	9	19	31722	54451
156	1.75	11	20.7	29718	52058

Table A.5 (continued) Detailed Investigation of the Strength of Wrought Iron Bars Part II, Reported by Beardslee

Test Number	Diameter (in)	Length (in)	Percent Elongation (per original length)	Elastic Limit (psi)	Tensile Limit (psi)
157	1.75	9	23.6	29210	50960
158	1.875	12	21	29741	51200
159	1.875	12	23.5	27765	50508
160	2	12	19.7	30709	51402
161	2	12	23.5	30225	50828
162	2.125	12	17	30459	48382
163	1.4375	27	15.9	NA	54892
164	1.4375	27	NA	NA	54773
165	1.4375	27	NA	NA	54773
166	1.4375	27	NA	NA	54773
167	1.6875	27	15	NA	54181
168	1.6875	27	NA	NA	53183
169	1.6875	27	NA	NA	53183
170	1.6875	27	NA	NA	53183
171	1.8125	27	16.6	NA	55294
172	1.8125	27	NA	NA	52217
173	1.8125	27	NA	NA	52217
174	1.8125	27	NA	NA	52217
175	1.4375	27	16.2	32655	51756
176	1.5	27	13	35880	52700
177	1.625	27	15.7	31099	49030
178	1.6875	27	15.7	30852	50312
179	1.75	27	15	33184	49821
180	1.8125	27	13.9	30814	50969
181	1.4375	27	13.9	32542	53994
182	1.4375	27	NA	NA	51936
183	1.4375	27	NA	NA	51936
184	1.4375	27	NA	NA	51936
185	1.5	27	14.4	33027	54544
186	1.5	27	NA	NA	51200
187	1.5	27	NA	NA	51200
188	1.5	27	NA	NA	51200
189	1.675	27	13	33745	52675
190	1.675	27	NA	NA	52800
191	1.675	27	NA	NA	52800
192	1.675	27	NA	NA	52800
193	1.6875	27	11.1	33549	52120
194	1.6875	27	NA	NA	53000
195	1.6875	27	NA	NA	53000
196	1.6875	27	NA	NA	53000

Table A.5 (continued) Detailed Investigation of the Strength of Wrought Iron Bars Part II, Reported by Beardslee

Test Number	Diameter (in)	Length (in)	Percent Elongation (per original length)	Elastic Limit (psi)	Tensile Limit (psi)
237	1.75	27	11.1	27856	53800
238	1.75	27	NA	NA	51217
239	1.75	27	NA	NA	51217
240	1.75	27	NA	NA	51217
241	1.5	27	NA	NA	44500
256	1.4375	27	12	NA	50400
257	1.4375	27	NA	NA	47067
258	1.4375	27	NA	NA	47067
259	1.4375	27	NA	NA	47067
260	1.5	27	14	NA	51047
261	1.5	27	NA	NA	51867
262	1.5	27	NA	NA	51867
263	1.5	27	NA	NA	51867
264	1.625	27	9.3	NA	52748
265	1.625	27	NA	NA	50367
266	1.625	27	NA	NA	50367
267	1.625	27	NA	NA	50367
268	1.6875	27	14.8	NA	54114
269	1.6875	27	NA	NA	51783
270	1.6875	27	NA	NA	51783
271	1.6875	27	NA	NA	51783
272	1.75	27	11.6	NA	53264
273	1.75	27	NA	NA	51750
274	1.75	27	NA	NA	51750
275	1.75	27	NA	NA	51750
276	1.75	27	NA	NA	51750
277	1.8125	27	14	NA	48953
278	1.8125	27	NA	NA	48800
279	1.8125	27	NA	NA	48800
280	1.8125	27	NA	NA	48800
281	1.8125	27	NA	NA	48800
282	1.4375	NA	NA	32162	69205
283	1.4375	NA	NA	NA	66167
284	1.4375	NA	NA	NA	66167
285	1.4375	NA	NA	NA	66167
286	1.5	NA	NA	28579	69779
287	1.5	NA	NA	NA	75167
288	1.5	NA	NA	NA	75167
289	1.5	NA	NA	NA	75167
290	1.625	NA	NA	44792	46116

Table A.5 (continued) Detailed Investigation of the Strength of Wrought Iron Bars Part II, Reported by Beardslee

Test Number	Diameter (in)	Length (in)	Percent Elongation (per original length)	Elastic Limit (psi)	Tensile Limit (psi)
350	1.8125	1.3	38.1	NA	49200
352	1.8125	1.3	36.1	NA	50162
353	1.5	17	22	29881	55956
354	1.5	15.5	19.3	NA	53726
355	1.5	NA	NA	35857	55419
356	1.5	NA	NA	57487	57045
357	1.5	NA	NA	35857	54872
358	1.625	19.5	18.5	33309	56010
359	1.625	19.5	20.5	32402	56473
360	1.625	NA	NA	319.9	54158
361	1.625	NA	NA	35180	56878
362	1.75	20	18.7	31531	53883
363	1.75	12	16.7	32329	54285
364	1.75	12	16.7	31930	55873
365	1.75	10	18.7	31057	54290
366	1.75	20	16.1	29935	53723
367	1.125	11	20.4	30000	56992
368	1.125	11	17	33802	57948
369	1.25	14	19.6	32469	57897
370	1.375	18	11.7	31034	54940
371	1.625	21	17	32334	54447
372	2	21	14.3	29335	51153
373	1.125	5.07	36.9	NA	53387
374	1.125	4.65	22.6	NA	53073
375	1.125	4.15	33.1	NA	52899
376	1.125	4.18	26.5	NA	52436
377	1.125	3.67	27.2	NA	52228
378	1.125	4.15	27.1	NA	52805
379	1.125	3.45	25.3	NA	53354
380	1	3.8	22.63	NA	53454
381	1	3.7	24.3	NA	54644
382	1	3.4	23.3	NA	54159
383	1	3.97	30.8	NA	53120
384	1	4	21.2	NA	53582
385	1	4.07	30.6	NA	53171
386	1	4.07	30.6	NA	52640
387	0.5	2.72	53	NA	59066
388	0.5	2.87	53	NA	57216
389	0.5	2.9	35	NA	60739
390	0.5	2.9	57	NA	76032

Table A.5 (continued) Detailed Investigation of the Strength of Wrought Iron Bars Part II, Reported by Beardslee

Test Number	Diameter (in)	Length (in)	Percent Elongation (per original length)	Elastic Limit (psi)	Tensile Limit (psi)
391	0.5	2.92	45	NA	55428
392	0.5	2		NA	64837
393	0.5	2.15	52	NA	52649
394	0.5	2.15	55	NA	64431
395	0.5	2.15	57	NA	60461
396	0.5	2.15	45	NA	63246
397	0.5	2.15	47	NA	51257
398	0.5	2.15	50	NA	55400
399	0.5	2.1	18.7	NA	56540
400	0.5	2	21.2	NA	55555
401	0.5	2.65	16	NA	55791
402	0.5	2.47	20.2	NA	54849
403	0.5	2.45	16.3	NA	56216
404	0.5	2.45	21.2	NA	49920
405	0.5	1.99	24.6	NA	58333
406	0.5	2.25	25.3	NA	52705
407	0.5	2	21.2	NA	56467
408	0.5	1.98	21.8	NA	59132
409	0.5	1.85	17.6	NA	55311
410	2	22	18.2	28567	51146
411	1.625	22	20	27816	51459
412	1.75	20	21.2	27817	52699
413	1.625	19	19.7	30087	53695
414	1.5	18	18.9	27708	52155
415	1.423	16	18.7	31676	54949
416	1.25	14	14.2	28166	55550
417	1.125	10	19.8	29476	54687
418	2	9	NA	NA	46151
419	1.625	9.25	23.2	32074	53100
420	1.75	9	17.2	31892	53472
421	1.625	9	16.2	30664	53614
422	1.5	8.5	22.7	32496	56505
423	1.425	7.55	24	62152	58021
424	1.25	7	17.6	31996	57979
425	1.125	6.5	20.5	33597	59582
426	1	6	26.1	33486	61115
428	2	10.75	7.5	33068	49146
429	2	3.2	18.8	32071	48585
430	2	3.2	13.4	30066	46624
431	1.825	3.2	28.1	29866	47850

Table A.5 (continued) Detailed Investigation of the Strength of Wrought Iron Bars Part II, Reported by Beardslee

Test Number	Diameter (in)	Length (in)	Percent Elongation (per original length)	Elastic Limit (psi)	Tensile Limit (psi)
432	1.825	3.18	16.7	33464	46624
433	1.75	3.2	29.7	30060	48300
434	1.75	3.18	28.6	32071	47850
435	1.625	2.25	22.2	38862	52030
436	1.625	2.27	21.1	34823	51435
437	1.5	2.28	25.2	33322	49209
438	1.5	2.28	25.63	31910	49758
439	1.25	2.25	32.4	36821	51635
440	1.25	2.25	28	36845	51034
441	1.125	2.25	33.3	32022	49734
442	1.125	2.25	30.2	30020	50334
443	1	4.4	28.4	36129	52701
444	1	4.43	24.1	35495	52715
445	1	4.03	31.5	37330	55377
446	1	3.9	28.9	32544	52769
447	1	3.75	26.4	33830	51625
448	1	3.65	31.2	33838	51848
449	1	3.63	31.7	34913	53453
450	2	6	26.5	24050	49768
451	2	6	41.3	23574	49735
452	1.9375	10	19.7	27087	49095
453	1.9375	8	28	27010	48726
454	1.825	11	18	33183	49512
455	1.825	7.5	26	29934	51367
456	1.8125	10	25.4	27700	51499
457	1.8125	5	33.2	32990	51895
458	1.75	11	18.1	29748	51233
459	1.75	7	16.1	30222	49419
460	1.625	10	16.7	27268	51127
461	1.625	5.5	30	32279	50385
462	1.5	6	27	32472	52156
463	1.5	5	31.2	33681	53347
464	1.375	6.5	25.2	33422	58296
465	1.25	5.75	1.4	34188	43040
466	1.125	7.25	0.7	37088	50045
467	1	6	56.7	36960	56541
468	1.375	6.5	9.7	35026	57486
469	1.25	5.5	9.8	33740	53952
470	1.125	7	17	33495	54000
471	1	5.75	6	37694	60947

Table A.5 (continued) Detailed Investigation of the Strength of Wrought Iron Bars Part II, Reported by Beardslee

Test Number	Diameter (in)	Length (in)	Percent Elongation (per original length)	Elastic Limit (psi)	Tensile Limit (psi)
472	1.375	2.98	32.1	26526	50267
473	1	2.45	35.4	30799	54608
474	1.375	3.02	36.3	26526	49515
475	1	2.55	30.2	30431	51949
476	1.15	5	29.2	33549	53097
477	1.09	6	26.3	28086	53497
478	1.26	4	29.2	22712	53836
479	1.17	6	27	23306	52254
480	1.39	6	29.3	25930	51843
481	1.35	6	27	30181	55415
482	1.5	4	32.7	32869	55409
483	1.44	6	35	29591	51940
484	1.63	5	30.4	27695	50844
485	1.54	6	24	27110	51606
486	1.75	8	24.5	26541	51740
487	1.64	8	28.7	27722	50880
488	1.89	9	27.4	27156	49044
489	1.87	10	23.5	25445	49088
490	0.976	3.9	31.3	27667	50458
491	0.976	3.9	26.9	28071	49054
492	0.976	3.9	33.3	27147	49225
493	0.976	3.9	28.2	27077	48199
494	0.976	3.9	26.9	25395	48399
495	0.976	3.9	30	25997	49709
496	0.976	3.9	28.4	26732	48152
497	0.976	3.9	30	26231	51818
498	2.03	6	29.4	27318	51818
499	1.12	13.5	25.3	32640	53800
500	1.12	13.5	22.2	34180	53978
501	1.25	15.5	20.2	32469	53211
502	1.25	15.5	22	31687	21730
503	1.38	16.5	22.5	32346	51347
504	1.38	16.5	20.7	31639	51245
505	1.5	17.5	14.7	31511	51612
506	1.5	17.5	8.6	32597	52375
507	1.62	19	14.3	33766	51698
508	1.62	19	17.4	34048	52629
509	1.75	18	20.4	32329	50291
510	1.75	18	22.5	32130	51089
511	1.88	20	20.1	32508	50902

Table A.5 (continued) Detailed Investigation of the Strength of Wrought Iron Bars Part II, Reported by Beardslee

Test Number	Diameter (in)	Length (in)	Percent Elongation (per original length)	Elastic Limit (psi)	Tensile Limit (psi)
512	1.87	20	21.6	33625	51176
513	1.99	20	17.5	27779	49385
514	1.99	20	20.8	27490	48522
515	1.015	3.8	17.8	NA	52539
516	1.014	4	23.7	NA	52370
517	1.017	4	24	NA	53025
518	0.897	3.52	21.6	NA	51946
519	0.896	3.47	24.4	NA	52975
520	0.895	3.57	24.7	NA	52575
521	1.018	3.95	25.9	NA	51800
522	1.017	3.72	28.1	NA	52175
523	1.018	3.9	24.3	NA	52660
524	1.016	3.9	24.3	NA	51987
525	0.872	3.6	29.8	NA	51657
526	0.897	3.54	27.5	NA	51076
527	0.892	0.57	29.1	NA	51888
528	0.892	0.57	29.1	NA	51564
529	0.632	2.46	24	NA	56022
530	0.643	2.48	19.3	NA	58900
531	0.64	2.48	22.9	NA	55950
532	0.641	2.48	18.9	NA	56864
533	0.646	2.5	32.8	NA	55210
534	0.643	2.47	18.6	NA	60594
535	0.526	2	20.5	NA	58670
536	0.525	2	28.5	NA	56460
537	0.526	2	26	NA	56775
538	0.526	2	16.5	NA	59130
539	0.526	2	25.5	NA	57295
540	0.632	2.55	25.1	NA	56585
541	0.642	2.47	25.5	NA	54825
542	0.637	2.5	22.9	NA	55140
543	0.631	2.5	26	NA	56610
544	0.636	2.5	25.6	NA	55630
545	0.637	2.47	25.5	NA	55090
546	0.525	2.1	30	NA	55195
547	0.525	2.05	32.5	NA	55085
548	0.525	2.05	26.8	NA	54733
549	0.525	2.06	31	NA	54735
550	0.525	2.05	33.1	NA	55080
551	0.572	3.6	30	25164	51658

Table A.5 (continued) Detailed Investigation of the Strength of Wrought Iron Bars Part II, Reported by Beardslee

Test Number	Diameter (in)	Length (in)	Percent Elongation (per original length)	Elastic Limit (psi)	Tensile Limit (psi)
552	0.897	3.54	27.7	33389	51073
553	0.892	3.58	29.36	34245	51887
554	0.892	3.58	28.5	35205	51667
555	0.564	2.25	0.7	36725	53530
556	0.564	2.25	1.1	37625	53036
557	0.564	2.19	32.4	32022	51036
558	0.566	2.26	30	33684	51470
559	0.564	2.25	31.1	37625	53036
560	0.564	2.27	30	34075	50840
561	0.565	2.27	30.4	34501	50275
562	0.567	2.26	26.5	35645	49705
563	0.565	2.2	31.4	33205	51454
564	0.565	2.27	31.7	35890	51154
565	0.566	2.18	34.4	34739	51371
566	0.564	2.23	30.9	34023	51235
567	0.804	3.19	31.3	35454	50717
568	0.79	3.19	28.8	34683	50342
569	0.799	3.13	30.9	35899	20171
570	0.803	3.13	32.9	35543	51734
571	0.798	3.14	30.2	31991	49586
572	0.8	3.06	33	27852	49786
573	0.99	5	22.8	31826	51963
574	0.99	5	26.4	32216	51312
575	0.99	5	24.8	32475	53260
576	0.99	5	21.6	32475	54299
577	0.99	6	20.3	32346	53260
578	1.1	7	25.3	31579	52631
579	1.1	7	25.4	31368	51579
580	1.1	6.75	24.4	32831	52720
581	1.1	6.75	24.9	32421	51773
582	1.1	7.5	20.6	31894	52631
583	1.23	7	19.5	31986	51346
584	1.23	7	15.5	33670	52609
585	1.23	7	14	34511	55134
586	1.23	5.5	31.6	32823	31346
587	1.24	6	17	33123	52666
588	1.38	8	21	35427	52550
589	1.38	8	16.8	36764	52489
590	1.38	8.25	24.2	33763	51347
591	1.38	7	21.8	32092	53286

Table A.5 (continued) Detailed Investigation of the Strength of Wrought Iron Bars Part II, Reported by Beardslee

Test Number	Diameter (in)	Length (in)	Percent Elongation (per original length)	Elastic Limit (psi)	Tensile Limit (psi)
592	1.38	7	20.9	34298	51013
593	1.5	9	22	35993	50993
594	1.5	9	27	35936	51499
595	1.5	7.5	24.6	33105	50820
596	1.5	9	35.6	33331	52572
597	1.625	6	22.6	34978	21590
598	1.625	6	27.3	36499	51109
599	1.625	9.75	23.9	32635	50782
600	1.625	9	24.4	32779	50830
601	1.625	10	25.9	33236	50538
602	1.73	8	24	29987	49553
603	1.73	8	25.2	29561	49553
604	1.74	7	25.7	29859	49831
605	1.74	7.2	26.4	24852	49287
606	1.74	10	30.5	30278	50464
607	1.86	11	20.9	23408	48943
608	1.86	11	23.6	23187	48398
609	1.87	10	26.3	33711	48948
610	1.87	9	21.4	33861	49517
611	1.86	9	23.5	31593	49499
612	2	12	23	27021	47581
613	2	12	23.5	27371	48058
614	2	12	23.5	27307	47099
615	2	10	24.5	30844	47428
616	2	10	22.5	31417	47682
617	0.95	5	28	32798	52810
618	0.99	6.75	23.7	33762	51675
619	1.13	5.5	22.2	33300	51949
620	1.3	7	21.1	30212	50403
621	1.4	7.5	25.3	32675	50709
622	1.55	9	23.9	31400	49605
623	1.61	7.2	26.5	34482	50201
624	1.71	8.6	24	33972	49682
625	1.87	8.65	23.9	31166	48170
626	0.502	2.5	25.2	41940	51823
627	0.504	2.58	NA	37844	50877
628	0.503	2.35	30.1	36739	51205
629	0.503	2.25	30.8	37493	51708
630	0.503	2.32	NA	33866	51675
631	0.5	2.55	NA	32742	50165

Table A.5 (continued) Detailed Investigation of the Strength of Wrought Iron Bars Part II, Reported by Beardslee

Test Number	Diameter (in)	Length (in)	Percent Elongation (per original length)	Elastic Limit (psi)	Tensile Limit (psi)
632	0.5	2.5	28	33725	50728
633	0.552	2.72	28.6	36982	49726
634	0.554	2.77	29.6	32054	50197
635	0.601	2.97	31.6	37102	49087
636	0.601	2.99	20	38646	49351
637	0.654	3.25	31.1	28575	49118
638	0.653	3.21	29.8	38818	49641
639	0.653	3.2	29.6	38444	46865
640	0.725	3.63	28.1	34934	49539
641	0.728	3.62	31.2	38437	46250
642	0.726	3.55		31718	49676
643	0.8	4	30.2	37996	49437
644	0.801	3.97	29.7	39687	49314
645	0.805	4.04	30.4	35790	49710
646	0.8	4.1	30.5	33819	49736
647	0.875	4.3	29.5	NA	48559
648	0.875	4.3	29.5	26110	48560
649	0.875	3.85	32.5	25364	49225
650	0.874	4.37	29.4	320505	48922
651	1.01	5	29	32676	48308
652	1.19	5.88	30.8	35790	48473
653	1	4.93	31	35790	46982
654	1	4.89	31.2	29284	47301
657	0.5	2.46	26	32340	50178
658	0.5	2.4	29.1	32300	50178
659	0.5	2.41	28.2	31991	50165
660	0.552	2.73	31.1	37401	49935
661	0.55	2.73	29.6	26826	49877
662	0.53	2.72	31.3	31224	49962
663	0.55	2.68	25.5	32302	50825
664	0.601	2.93	32.4	41067	49175
665	0.603	3	32.1	NA	49024
666	0.602	2.99	32.1	38386	48853
667	0.654	3.26	27.6	37806	49267
668	0.653	3.22	28.4	32323	49865
669	0.653	3.25	28.2	29859	50015
670	0.725	3.62	29	36350	50143
671	0.726	3.6	26.9	32466	49676
672	0.727	3.6	28.5	31588	49867
673	0.801	4.01	30.2	37497	49266

Table A.5 (continued) Detailed Investigation of the Strength of Wrought Iron Bars Part II, Reported by Beardslee

Test Number	Diameter (in)	Length (in)	Percent Elongation (per original length)	Elastic Limit (psi)	Tensile Limit (psi)
674	0.8	4.05	29.9	34615	49438
675	0.876	4.36	28.2	39741	48531
676	0.875	4.31	29.4	36587	48809
677	0.802	4.01	27.5	29693	48597
678	1.004	4.96	31.2	34408	46862
679	1.01	5	29.2	38192	51422
680	1.01	5	27	39940	52420
681	1.13	8	24.5	35493	49850
682	1.13	8	23.7	35493	50448
683	1.25	9	13.6	39608	52485
684	1.25	9	21.7	39608	52974
685	1.38	10	20.8	39037	52406
686	1.38	10	17.5	39170	52272
687	1.5	13	23.9	34522	50367
688	1.5	13	25	35653	51273
689	1.62	13	23	34934	49684
690	1.61	13	25.5	35854	51375
691	1.74	13	27	35996	50464
692	1.74	13	25.5	35912	50630
693	1.87	13	19.1	36416	49380
694	1.87	13	25.5	34818	50109
695	2.01	13	NA	35297	47777
696	2.01	13	NA	36432	47967
697	2.24	37.5	20	31059	48112
698	2.24	37.5	20.4	31415	48898
699	2.09	11	26.7	32002	48965
700	2.1	12	27	31931	49364
701	2.5	37.5	20.5	30456	47507
702	2.5	37.5	20.6	29060	47181
703	2.34	14	17.9	28644	48407
704	2.38	14	16	29220	48550
705	0.504	2.57	22.5	38596	51128
706	0.502	2.43	22.8	0.7771	50530
707	0.552	2.67	22.8	40534	49709
708	0.601	2.96	17.8	NA	48819
709	0.65	3.18	23.9	36467	51838
710	0.727	3.64	23.7	34208	49144
711	0.802	3.97	23.9	38992	48792
712	0.877	4.19	24.1	37042	49370
713	1.055	4.99	NA	31892	48280

Table A.5 (continued) Detailed Investigation of the Strength of Wrought Iron Bars Part II, Reported by Beardslee

Test Number	Diameter (in)	Length (in)	Percent Elongation (per original length)	Elastic Limit (psi)	Tensile Limit (psi)
714	1	4.99	NA	32854	49465
715	1.005	4.82	NA	31679	49155
716	0.997	4.84	24.2	31958	49250
717	0.986	4.88	22.5	28810	47865
718	1.002	4.84	23.8	30406	47558
719	0.995	4.84	24.9	30607	47871
720	1	4.87	23.2	26228	46473
721	1.002	4.86	23.4	27584	46146
722	1.003	4.9	23.5	25186	46702
723	0.979	4.78	31.8	27656	47954
724	0.982	4.67	31.9	27297	47663
725	1.001	4.9	35	24208	46755
726	0.999	4.99	30.8	24687	46823
727	0.999	4.97	31.2	24496	47205
729	1.002	4.97	29.3	25555	47178
730	0.999	5	27.5	24368	46823
731	1	4.9	30	24255	46791
732	1.002	4.9	30.6	23018	4653
733	1.002	4.9	31.2	23082	46417
734	1.002	4.9	28.9	23779	46227
735	0.192	0.98	12	NA	59585
736	0.377	2.44	20.6	37858	53763
737	0.387	1.47	19	44157	53865
738	0.374	1.82	20	38626	54595
739	0.269	1.17	25.3	39750	54180
740	0.374	1.55	27.9	39126	52775
741	0.628	2.86	19.7	34146	50694
742	0.624	2.84	13.5	35971	54284
743	0.624	3.35	16.4	32537	51177
744	0.49	2.14	22	35525	51431
745	0.755	3.54	22.9+	35068	50386
746	0.774	3.48	17.4	36291	51647
747	0.783	3.44	11	37279	53893
748	0.48	1.87	26	35094	50276
749	0.882	3.99	21.1	30810	50327
750	0.889	4.54	18	33833	50427
751	0.889	4.16	17.4	34963	51393
752	0.553	2.44	26.6	36115	50374
753	1.01	6.1	22.1	34323	55292
754	1.01	6.1	26.2	34947	56165

Table A.5 (continued) Detailed Investigation of the Strength of Wrought Iron Bars Part II, Reported by Beardslee

Test Number	Diameter (in)	Length (in)	Percent Elongation (per original length)	Elastic Limit (psi)	Tensile Limit (psi)
755	1.01	6	18.3	34448	55167
756	1.02	5.25	23.8	33656	55929
757	1.02	5.25	21.5	34022	56296
758	1.14	8	22.5	34867	55827
759	1.14	8	21.6	34280	56905
760	1.14	8	21.7	35259	56121
761	1.14	6.75	17	34867	55925
762	1.14	6.75	21.2	34140	57394
763	1.26	6.5	21.1	34883	55253
764	1.26	6.5	20.7	35284	55814
765	1.26	6.5	21.5	34643	55012
766	1.25	6.5	23.8	34392	54931
767	1.25	6.5	26.1	34718	55256
768	1.39	7.25	31	33091	52603
769	1.39	7.25	32.4	33487	53394
770	1.39	7.25	30.6	33882	53194
771	1.39	8	22.5	32827	53243
772	1.39	8	23.5	33091	52406
773	1.5	9	22.2	34069	53763
774	1.5	10	25	34295	53537
775	1.5	10	23.5	34522	53763
776	1.5	8	23.7	34748	53140
777	1.5	8	24.4	33899	53254
778	1.62	7	20.6	34109	53517
779	1.62	7	23.6	33964	53372
780	1.62	7	20.3	34449	53372
781	1.62	5.5	14.4	34546	54342
782	1.62	5.5	11	34109	53081
783	1.75	7.5	21.6	36590	54054
784	1.75	8	21.9	36424	54470
785	1.75	8.5	26.5	36340	53222
786	1.75	6.5	18.1	36590	54054
787	1.75	6.5	19.2	36923	53430
788	1.88	9	15.1	35663	53674
789	1.88	9	11.7	35414	52705
790	1.88	9	8.4	35414	52377
791	1.88	8	25	35983	52596
792	1.88	8	24.4	35734	53025
793	2	9	23.5	34691	51877
794	2	9	24.4	34595	52069

Table A.5 (continued) Detailed Investigation of the Strength of Wrought Iron Bars Part II, Reported by Beardslee

Test Number	Diameter (in)	Length (in)	Percent Elongation (per original length)	Elastic Limit (psi)	Tensile Limit (psi)
835	1.63	7	23.9	52994	52994
836	1.63	7	22.3	53665	53665
837	1.74	10	22.7	53112	53112
838	1.74	10	24.2	53196	53196
839	1.87	10	21.5	53918	53918
840	1.87	10	25.2	52804	52805
841	2	10.5	26.5	50286	50286
842	NA	10.5	23.4	515241	51241
843	NA	NA	NA	NA	51171
844	0.5	2.5	NA	51171	52511
845	0.501	2.5	NA	52511	51171
846	1.73	75	NA	32709	52511
847	1.73	20	NA	34240	50021
848	1.73	10	NA	34028	50446
849	1.25	13.5	19.4	36700	59493
850	1.25	13.5	20.3	36700	60458
851	1.25	13.5	19.4	38631	61424
852	1.25	16	18	37551	60244
853	1.25	16	16	35452	58676
854	1.375	15.75	21.4	31034	54303
855	1.375	15.75	23.8	31034	57277
856	1.5	19	17.7	32597	58132
857	1.5	19	21.7	34227	56502
858	1.625	19	20.7		57674
859	1.625	19	15.1	34717	55132
860	1.625	18	20.6	35180	57862
861	1.625	18	19.2	35180	57862
862	1.71	9	10	38310	56595
863	1.75	9	17.6	33124	57874
864	1.83	11.56	21.8	32486	56577
865	1.875	19.5	18.4	30944	55630
866	1.875	18	22	31118	55977
867	2.03	18	13.3	31441	60213
868	2.04	19	17.8	30839	57567
869	0.997	3.95	21.5	NA	62444
870	0.998	3.95	21	NA	61900
871	0.999	3.95	21.5	NA	62465
872	0.9	3.56	23.3	NA	59439
873	0.9	3.56	20.8	NA	61930
874	0.9	3.56	21.6	NA	60240

Table A.5 (continued) Detailed Investigation of the Strength of Wrought Iron Bars Part II, Reported by Beardslee

Test Number	Diameter (in)	Length (in)	Percent Elongation (per original length)	Elastic Limit (psi)	Tensile Limit (psi)
875	0.995	3.97	22.2	NA	62100
876	0.992	3.92	23.2	NA	62360
877	0.996	3.89	22.1	NA	61609
878	0.993	3.94	23.7	NA	61711
879	0.898	3.55	23.9	NA	61067
880	0.893	3.5	18.3	NA	62747
881	0.9	3.55	26.5	NA	61656
882	1.02	4.4	28.4	NA	52695
883	1.01	4.45	20.2	NA	52806
884	1.02	4.42	24.3	NA	52710
885	1.01	4.02	31.6	NA	55390
886	0.969	3.89	29	NA	52712
887	0.97	3.75	26.6	NA	51623
888	0.966	3.65	30.8	NA	51848
889	0.97	3.62	31.7	NA	53450
890	1.005	4.14	18.1	38029	61333
891	0.986	4.36	19.2	39289	62341
892	1	4.24	19.3	38356	61752
893	0.797	3.58	22.6	35078	61887
894	0.797	3.71	22.9	35579	62088
895	0.797	3.65	19.4	36080	62438
896	1.13	7	18.3	31963	55994
897	1.13	7	25.1	32567	56343
898	1.25	7	20.6	33414	56723
899	1.25	7	23.6	33088	46234
900	1.38	8	26.5	33823	53743
901	1.38	8	22.5	33422	54812
902	1.49	9	21.4	34977	53211
903	1.49	9	25.5	34403	53899
904	1.64	8.7	20.6	35984	56344
905	1.64	8.7	24.9	35795	56344
906	1.73	9	21	35368	55295
907	1.73	9	21.4	34198	54742
908	1.87	9	22.2	33357	54004
909	1.87	9	18.7	33867	48070
910	2.01	9	11.2	32461	52127
911	2.01	9	6.3	NA	51370
912	1.01	5	16.2	37415	57363
913	1.1	6	23	32410	53035
914	1.25	8	23.7	30073	50040

Table A.5 (continued) Detailed Investigation of the Strength of Wrought Iron Bars Part II, Reported by Beardslee

Test Number	Diameter (in)	Length (in)	Percent Elongation (per original length)	Elastic Limit (psi)	Tensile Limit (psi)
915	1.35	9	27.5	34940	50594
916	1.51	10	27.3	32312	50919
917	1.62	8	22.1	34012	52401
918	1.72	10	23.8	32271	50120
919	1.86	10	24	30842	47478
920	2	11	25.6	31413	48249
921	1.27	6.7	31.5	35596	55782
922	1.38	7	29.6	30802	52550
923	1.46	NA	NA	NA	53345
924	1.52	8	28	29630	52865
925	2.02	10	24	29959	49872
926	0.99	4.25	0.9	38971	55858
927	0.99	4.25	18.8	39489	59755
928	1.12	6	20	41006	56840
929	1.12	6	17.7	41615	57739
930	1.28	7	25.4	37218	56721
931	1.28	7	23.9	36519	57031
932	1.4	8	25.6	33788	55230
933	1.4	8	23.7	37737	55230
934	1.52	10	22.2	33057	53664
935	1.52	10	24	33233	54655
936	1.64	8	1	33522	53799
937	1.77	9	24.7	33238	51889
938	1.77	9	22	33726	51801
939	1.88	10	23.8	32420	52806
940	1.88	10	25.6	32204	50866
941	2.01	11	23	31673	50803
942	2.01	11	29.1	32083	56535
943	1.26	7.5	29.3	34482	56134
944	1.26	7.5	21	33360	54606
945	1.51	7.5	22.3	34617	54103
946	1.51	9	23	NA	54455
947	1.64	7	26.4	33143	54924
948	1.64	7	25.4	33712	54089
949	1.76	9	22.8	33703	54336
950	1.76	9	24.7	34112	51860
951	1.87	10	28.4	32046	51665
952	1.87	10	27.1	32477	53172

Table A.6 Tensile Strength Data Reported by Fairbairn

	Description of Material Tested (Manufacturer and Grade)	Mean Breaking Weight tons/in^2	Tensile Strength (psi)
Plate:	Yorkshire Plates	25,770	51,540
	Yorkshire Plates	22,760	45,520
	Derbyshire Plates	21,680	43,360
	Shropshire Plates	22,826	45,652
	Staffordshire Plates	19,563	39,126
Bar:	Lowmoor Iron	28,661	57,322
	Lancashire Iron	21,815	43,630
	Charcoal bar-iron	28,402	56,804
	Best-best Staffordshire Charcoal Plate	20,095	40,190
	Best-best Staffordshire Charcoal Plate	22,297	44,594
	Best Staffordshire	26,706	53,412
	Common Staffordshire	26,706	53,412
	Lowmoor rivet Iron	26,801	53,602
	Staffordshire Rivet Iron	26,563	53,126
	Staffordshire Rivet Iron	26,646	53,292
	Staffordshire Rivet Iron	37,956	75,912
	Staffordshire Bridge Iron	21,249	42,498
	Yorkshire Bridge Iron	22,290	44,580

Table A.7 Tensile Strength Data Reported by Humber

Manufacturer	Tensile Strength (psi)
Low Moor Iron Works	60,364
Low Moor Iron Works	61,798
Low Moor Iron Works	60,078
Low Moor Iron Works	60,245
Low Moor Iron Works	66,392
Bowling Iron Works	62,404
Bowling Iron Works	61,477
Farnley Iron Works	62,886
Bradley, Charcoal	57,216
Bradley, B.B. Scrap	59,370
Bradley, S.C.	56,715
Thorneycroft and Co.	62,231
Lord Ward	59,287
Govan. Ex. B. Best	59,753
Govan. Ex. B. Best	56,655
Govan. Ex. B. Best	57,591
Govan. Ex. B. Best	58,358
Govan. Ex. B. Best	59,109
Govan. Ex. B. Best	58,169
Govan. B. Best	57,400
Govan. B. Best	60,879
Govan. B. Best	52,849
Govan. B. Best	51,341
Govan. B. Best	54,795
Govan. B. Best	58,326
Govan. B. Best	59,424
Govan. B. Best	63,956
Glasgow. B. Best	61,877
Glasgow. B. Best	58,885
Glasgow. Rivet	58,940
Glasgow. B. Best	57,092
Coatbridge. G. Best Rivet	59,045
Blockairn. B. Best Rivet	59,548
St. Rollox. B. Best Rivet	61,723
R. Sollock, E. Best	59,219
Ulverstone Rivet	56,981
Mersey Co. Best	57,425
Per Eckman & Co. R. F.	53,775
Per Eckman & Co. R. F.	60,110
Prince Demidoff, C.C.N.	47,855
Prince Demidoff, C.C.N.	48,232
Prince Demidoff, C.C.N.	49,564

Manufacturer	Tensile Strength (psi)
Prince Demidoff, C.C.N.	56,802
Prince Demidoff, C.C.N.	53,420
Prince Demidoff, C.C.N.	55,878
Prince Demidoff, C.C.N.	47,582
Prince Demidoff, C.C.N.	44,758
Low Moor Iron Works	52,000
Low Moor Iron Works	50,515
Bowling Iron Works	52,235
Bowling Iron Works	46,441
Farnley Iron Works	56,005
Farnley Iron Works	46,224
Farnley Iron Works	58,487
Farnley Iron Works	54,198
Farnley Iron Works	58,437
Farnley Iron Works	55,033
Consett Iron Works	51,245
Consett Iron Works	46,712
Bradley. S. S.	55,831
Bradley. S. S.	50,550
Bradley. L.F., S. S.	56,996
Bradley. L.F., S. S.	51,251
Bradley. S. S.	55,708
Bradley. S. S.	49,425
Wells B. Best	47,410
Wells B. Best	46,630
Wells. K. B. M.	46,404
Wells. K. B. M.	44,764
Mossend. B. Best	43,433
Mossend. B. Best	41,456
Glasgow. Boiler	53,849
Glasgow. Boiler	48,848
Glasgow. Ship	47,773
Glasgow. Ship	44,355
Glasgow. Ship	45,598
Glasgow. Ship	39,544
Govan. Best	43,942
Govan. Best	39,544
Glasgow	55,937
Dundyvan	55,285
Mossend	45,439
Thorneycroft	52,789
Consett	50,807
Dowlais	41,386

Appendix B. Survey Results

To determine if there were any existing inspection, maintenance and repair procedures throughout the country, a survey was created and distributed to the Department of Transportation and Local Technical Assistant Program offices in all fifty states. A similar survey was also distributed to all ninety-two county highway departments in Indiana, as well as a few bridge engineering consultants.

From all the surveys that were distributed, a total of 59 responses were received. The survey responses are broken down as follows: 35 were received from state DOT's, 2 were received from other state's LTAPs, 19 were received from local county highway departments in Indiana, and 3 were received from various bridge engineering consultants.

A copy of the survey that was created and distributed during this study is shown in the following pages. Also included is an itemized summary of the results from this survey.

Table B.1 Example Historic Wrought Iron Bridge Maintenance Survey

Purdue University Historic Wrought Iron Bridge Maintenance Survey

The purpose of this survey is to compile methods used in the maintenance and repair of historic wrought iron bridges. Any information that is provided will be constructive and helpful in developing guidelines that will be used in Indiana to retrofit and repair these structures. Please take a few minutes to complete this survey and return it at your earliest convenience.

1. In your state, are there any existing historic wrought iron bridges? **yes** **no**
2. If yes, then approximately how many bridges are in your state/county? **0-10** **11-20** **21-40** **41+**
3. Does your organization maintain any of the historic bridges? **yes** **no**
4. Do you know of any historic wrought iron bridges on a city street, or park? **yes** **no**
5. If yes, then please state where
6. If your organization does maintain wrought iron bridges, then are formal maintenance and repair procedures available? **yes** **no**
7. If yes, then can these be provided? **yes** **no**
8. Is heat straightening of wrought iron bridges permitted? **yes** **no**
9. Is welding of wrought iron bridges permitted? **yes** **no**
10. Are there procedures available for riveting or bolting wrought iron? **yes** **no**
11. What inspection procedures are most commonly used when dealing with the historic wrought iron bridges?
12. What procedures are used when a wrought iron bridge needs to be rated for load capacity?
13. If you can think of any other important information that is relevant, then please provide it.

Thank you very much for your time in completing this survey. If you would like a copy of the results of this survey then please note it here and provide a return address. **yes** **no**

Please Return to: Amy M. Piskorowski
School of Civil Engineering
1284 Civil Engineering Building
West Lafayette, IN 47904-1284

If you have any questions you can contact Ms. Piskorowski at: piskoroa@purdue.edu

Table B.2 Results From Wrought Iron Bridge Survey from State DOTs and Counties

Department of Transportation	In your state, are there any existing historic wrought iron bridges?	If yes, then approximately how many bridges are in your state/county?	Does your organization maintain any of the historic bridges?	Do you know of any historic wrought iron bridges on a city street, or park?
State 1	Yes	0-10	Yes	Yes
State 2	Yes	0-10	No	No
State 3	Yes	101	Yes	Yes
State 4	Yes	0-10	No	No
State 5	Yes	0-10	No	Yes
State 6	Yes	0-10	Yes	Yes
State 7	No		No	No
State 8	No		No	No
State 9	No		No	No
State 10	Yes	0-10	No	No
State 11	No		No	No
State 12	No		No	No
State 13	Yes	11-20	No	Yes
State 14	No		No	No
State 15	No		No	No
State 16	Yes	0-10	No	Yes
State 17	Yes	11-20	Yes	No
State 18	No		No	No
State 19	No		No	No
State 20	No		No	No
State 21	No		No	No
State 22	No		No	No
State 23	No		No	No
State 24	Yes	21-40	No	No
State 25	No		No	No
State 26	No		No	No
State 27	No		No	No
State 28	Yes	21-40	Yes	No
State 29	No		Yes	Yes
State 30	Yes	0-10	No	Yes
State 31	Yes	41+	Yes	Yes
State 32	No		No	No
State 33	No		No	No
State 34	No		No	No
State 35	Yes	0-10	No	No

Department of Transportation	If your organization does maintain wrought iron bridges, then are formal maintenance and repair procedures available?	Is heat straightening of wrought iron bridges permitted?	Is welding of wrought iron bridges permitted?	Are there procedures available for riveting or bolting wrought iron?
State 1	No	No	No	No
State 2	No	No	No	No
State 3	No	No	No	No
State 4	No	No	No	No
State 5	No	Yes	Yes	No
State 6	No	No	No	No
State 7	No	Yes	Yes	No
State 8	No	No	No	No
State 9	No	No	No	No
State 10	No	No	No	No
State 11	No	No	No	No
State 12	No	No	No	No
State 13	No	No	No	No
State 14	No	No	No	No
State 15	No	No	No	No
State 16	No	Yes	No	No
State 17	No	No	No	No
State 18	No	No	No	No
State 19	No	No	No	No
State 20	No	No	No	No
State 21	No	No	No	No
State 22	No	No	No	No
State 23	No	No	No	No
State 24	No	No	No	No
State 25	No	No	No	No
State 26	No	No	No	No
State 27	No	No	No	No
State 28	No	No	No	No
State 29	No	No	No	No
State 30	No	No	No	No
State 31	No	Yes	No	No
State 32	No	Yes	No	No
State 33	No	No	No	No
State 34	No	No	No	No
State 35	No	No	No	No

County	In your county, are there any existing historic wrought iron bridges?	If yes, then approximately how many bridges are in your state/county?	Does your organization maintain any of the historic bridges?	Do you know of any historic wrought iron bridges on a city street, or park?
County 1	Yes	0-10	Yes	No
County 2	Yes	11-20	Yes	No
County 3	Yes	0-10	No	Yes
County 4	No		No	No
County 5	No		No	No
County 6	No		No	No
County 7	Yes	0-10	Yes	No
County 8	Yes	0-10	Yes	No
County 9	Yes	0-10	Yes	No
County 10	No		No	No
County 11	Yes	0-10	Yes	Yes
County 12	Yes	0-10	Yes	No
County 13	Yes	11-20	Yes	No
County 14	Yes	0-10	Yes	No
County 15	Yes	0-10	Yes	No
County 16	Yes	0-10	Yes	No
County 17	No		No	No
County 18	No		No	No
County 19	Yes	0-10	Yes	Yes

County	If your organization does maintain wrought iron bridges, then are formal maintenance and repair procedures available?	Is heat straightening of wrought iron bridges permitted?	Is welding of wrought iron bridges permitted?	Are there procedures available for riveting or bolting wrought iron?
County 1	No	No	No	No
County 2	No	No	No	No
County 3	No	No	No	No
County 4	No	No	No	No
County 5	No	No	No	No
County 6	No	No	No	No
County 7	No	No	Yes	No
County 8	No	Yes	Yes	No
County 9	No	No	No	No
County 10	No	No	No	No
County 11	No	No	Yes	No
County 12	No	No	No	No
County 13	No	Yes	Yes	Yes
County 14	No	Yes	Yes	No
County 15	No	No	No	No
County 16	No	No	No	No
County 17	No	No	No	No
County 18	No	No	No	No
County 19	No	No	Yes	No

Comments:

What inspection procedures are most commonly used when dealing with the historic wrought iron bridges?

State 1: Visual

State 2: Visual acceptability

State 3: Same inspection procedures as for other bridges.

State 4: Same as for any bridge - Use of NBIS standards for determining the condition of the bridge.

State 5: No special procedures. Generally we are unsure if the bridge is wrought iron until testing is completed. Not performed unless a rehab project.

State 6: Per NBIS / DOT Standard, Visual non-destructive methods, careful look for cracks, Inspect yearly if fracture is critical.

State 12: Federal NBI requirements

State 16: Generally we do not determine if early metal bridges are wrought iron or steel.

State 17: Heat straightening and welding procedures are still undecided.

State 24: Normal visual inspection. Pins in trusses are checked for cracks via ultrasonic testing.

State 25: Visual Hands-on Inspection.

State 26: If had bridges would probably use visual hands on inspection.

State 28: Normal NBIS Inspections

State 29: Visual Inspection of wrought iron members and the others.

State 31: Visual NBIS inspections. If cracks are suspected we use dye-penetrant and UT.

State 32: Visual Inspection would be used.

State 33: Routine Inspection

County 1: Standard NBIS Procedures

County 2: Contract inspections per state program

County 7: Engineering Firm Inspects Bridges

County 8: Routine inspection on 1-2 year cycle

County 9: The highway dept. relies on consultants

County 11: The bi-annual bridge inspection

County 12: Most cover on fracture critical inspections - 2 year freq.

County 13: Refer to Book by James L. Cooper 'Restoring Historic Metal Truss Bridges'

County 15: Standard NBIS procedures

County 16: County bridge inspection (by awarded engineering firm)

County 17: We participate in the state mandatory bridge inspection every two year an engineering firm is hired that inspects all our bridges. Once a steel truss is decided to rehabilitated, an engineering firm is hired to develop plans and specs for that bridge.

What procedures are used when a wrought iron bridge needs to be rated for load capacity?

State 1: Follow AASHTO Manual for Condition Evaluation of Bridges

State 3: Rating Rules as prescribed by AASHTO

State 4: We would need to determine the capacity of wrought iron. Then use procedures outlined in AASHTO Manual for Condition Evaluation of Bridges. FHWA requires that Load Factor Design method for find rate.

State 5: Coupons have been cut from the bridge to determine mechanical properties.

State 6: Classic Structural Analysis and AASHTO Specs.

State 7: Cased upon AASHTO allowable stresses for wrought iron.

State 13: Same as structural Steel before year 1905.

State 17: Rate using allowable maximum unit stress per AASHTO Manual for Condition Evaluation of Bridges Section 6.6.2.2

State 18: Use LARs load analysis Rating system with 26,000 psi yield Strength

State 25: Normal rating procedures with use of allowable stresses for wrought iron as specified in AASHTO Manual for Condition Evaluation.

State 26: AASHTO Bridge Specs.

State 30: Follow AASHTO Specs.

State 31: The allowable stresses for the wrought iron members are reduced in accordance with AASHTO guidelines.

State 32: We would use stresses for wrought iron from AASHTO "Manual for condition evaluation of bridges"

State 33: Assume wrought iron equivalent to A36 Steel

County 1: Usually have weak deck and stringers which controls the rating.

County 2: Consultant in charge of inspection is responsible.

County 7: Engineering firm Inspects and determines what load rating needs to be on certain bridges

County 8: Normal rating procedure - slightly higher values used for steel strength

County 9: Hire a consultant.

County 12: Done by consultant, contact United

County 13: Hire a Consultant

County 15: Done by consultants

County 19: An engineering firm is hired to develop plans and specs for any bridge that is needed to be rehabilitated for service.

If you can think of any other important information that is relevant, then please provide it.

State 1: We have not done much intricate work with wrought iron.

State 2: We have some bridges with wrought iron tension members, but never weld a structural member, always replace with steel. Suggests contacting municipalities.

State 4: There is no money available to preserve historic bridges. If any bridge is deemed historic, the owner (state, county or city) is not allowed to remove the bridge, but they are not required to maintain it either. They usually won't due to lack of funds. The agency waits for the bridges to deteriorate (collapse) and then can replace it. That is why there are no procedures to repair wrought iron.

State 6: The information above describes bridges that have wrought iron tension members.

State 7: A form is attached to survey, that I believe is mentioning that 7 out of 10 districts in our state provide data in the survey.

State 13: Included in original document is a list of bridges on the National Register for Kansas. They are from 1861-1939 and consist of High Truss and Low Truss Structures. - Also another contact is included.

State 18: Excellent reference: "Wrought iron - Its Manufacture Characteristics and Applications" Second Ed. A.M. Byers Company, Pittsburg PA, 1947 - James Aston and Edward B. Story.

State 22: No welding for old steel structures, so No welding for wrought iron too.

State 27: Ask the European Countries that have more of them. England has one.

State 30: Most of the wrought iron is in structures that have tension members that are eyebars. These eyebars had to have been forged so therefore are wrought iron.

State 31: If a more accurate allowable stress value is required, either for load rating or for designing a rehabilitation project, coupon samples of the iron are taken to establish these values for the specific bridge.

State 35: The bridges are not maintained by DOT and the local agencies maintain them.

County 1: Have not had to do major repairs on the bridges -so don't know if heat straightening, welding or riveting is permitted.

County 5: The county maintains 5 covered bridges.

County 7: Maintenance procedures, if any, are prepared by contractor.

County 8: Both remaining bridges on federal - aid for repair (2002) and relocation (113) bridge (120) was relocated in 2001.

County 12: Have not done any heat straightening or welding on the bridges.

County 14: A bridge that was in this county was rehabilitated in 1996 through a state project.

County 19: We probably will not rehabilitate any more steel trusses in our county.

Appendix C. Supplementary Photographs of Experimental Testing

The following pages consist of supplementary photographs taken during experimental testing completed in this study. This testing consisted of micrographs, chemical analysis, hardness tests, tensile coupon tests, fatigue tests, charpy impact tests, and eyebar connection tests of wrought iron machined from members of two existing historical bridges in Indiana.

BF-E1 - Original Heated Areas, Test Specimen Locations

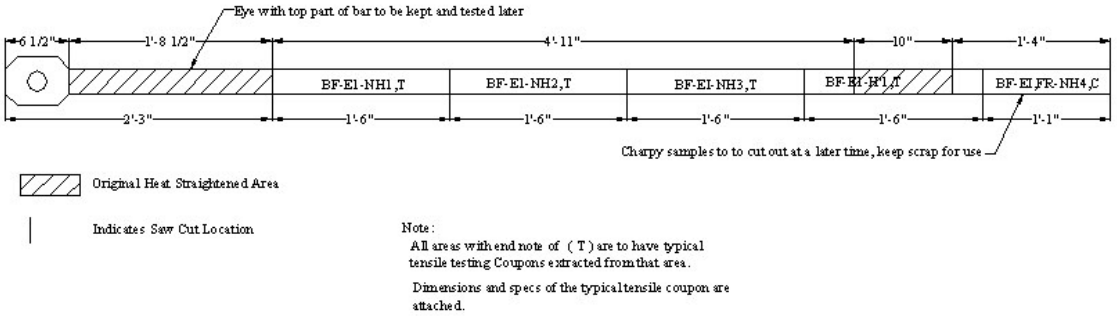

BF-E2 - Original Heated Areas, Test Specimen Locations

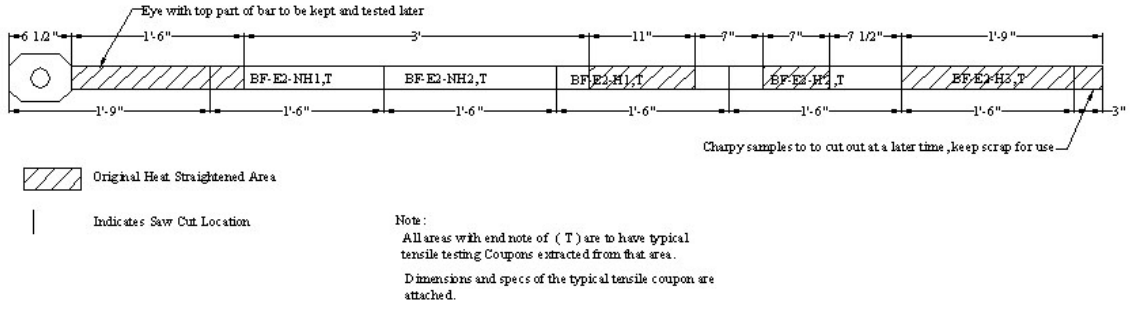

BF-E3 - Original Heated Areas, Test Specimen Locations

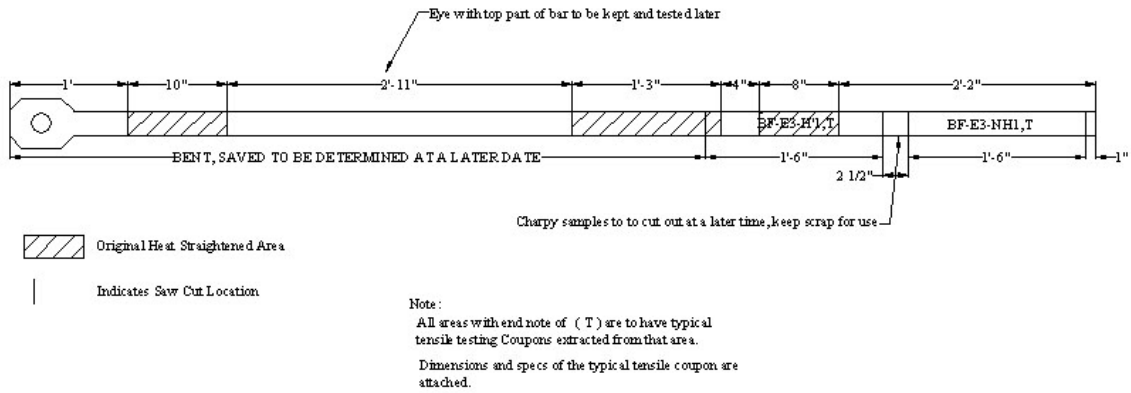

Figure C.1 Diagrams Showing Location for Extraction of Specimen Machined from Eyebars

BF-E4 - Original Dimensions, Test Specimen Locations

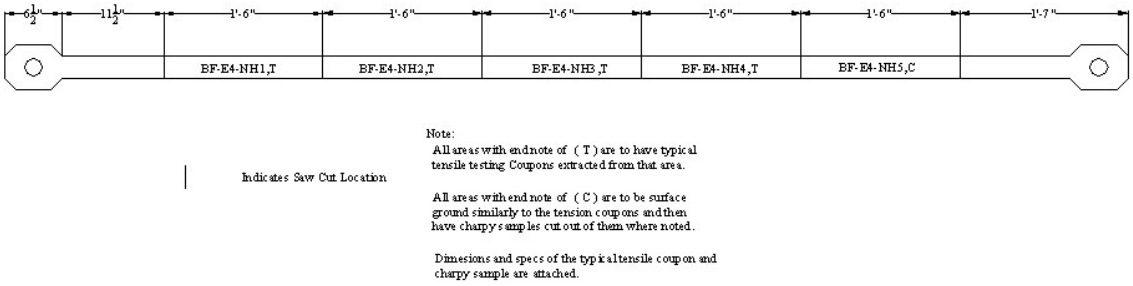

BF-E5 - Original Dimensions, Test Specimen Locations

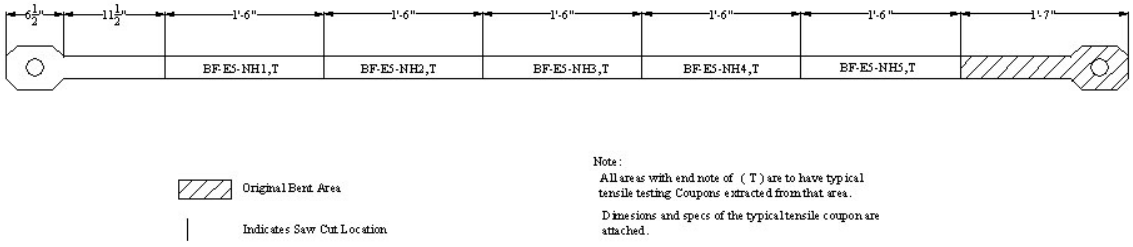

Figure C.1 (cont.) Diagrams Showing Location for Extraction of Specimen Machined from Eyebars

Figure C.2 Indentations from Hardness Testing on Wrought Iron Samples from the Bell Ford Bridge.

Figure C.3 Heating of Eyebar from Bell Ford Bridge Prior to Straightening

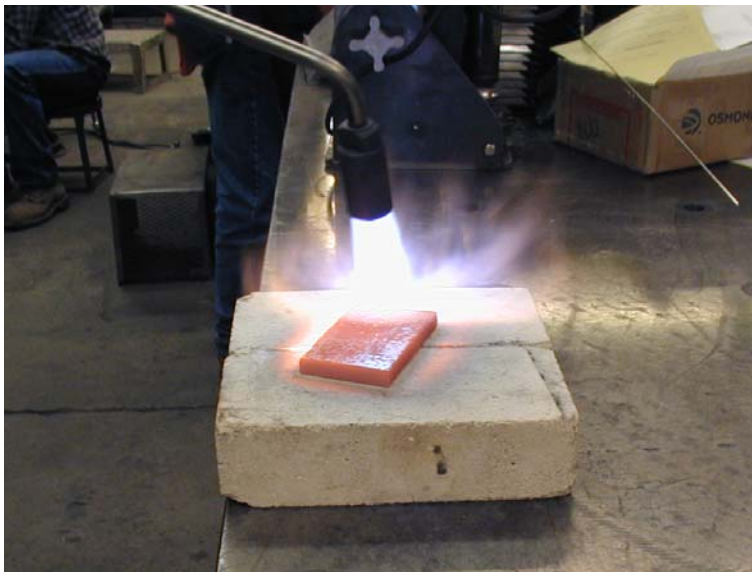

Figure C.4 Wrought Iron Plate from the Bell Ford bridge being Heated to the “Red Hot” State.

Figure C.5 Pyrometer Used to Determine Temperature of “Red Hot” Wrought Iron.

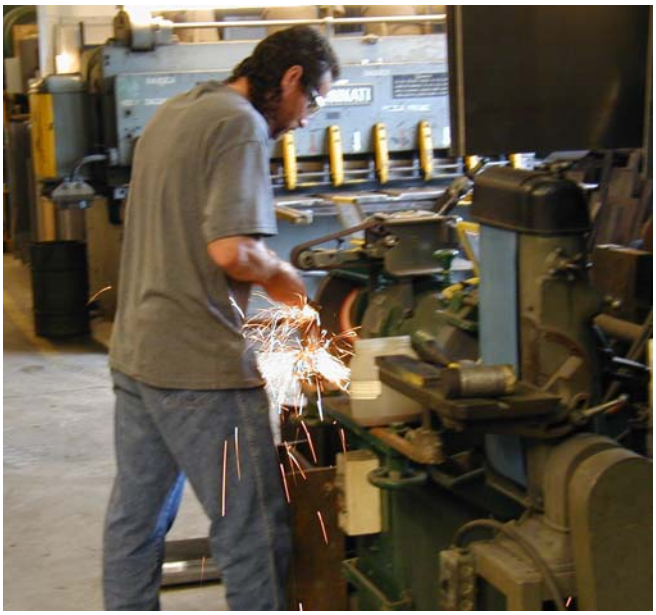

Figure C.6 Rotary Grinder used to form Double V Butt Joint in Welded Specimens

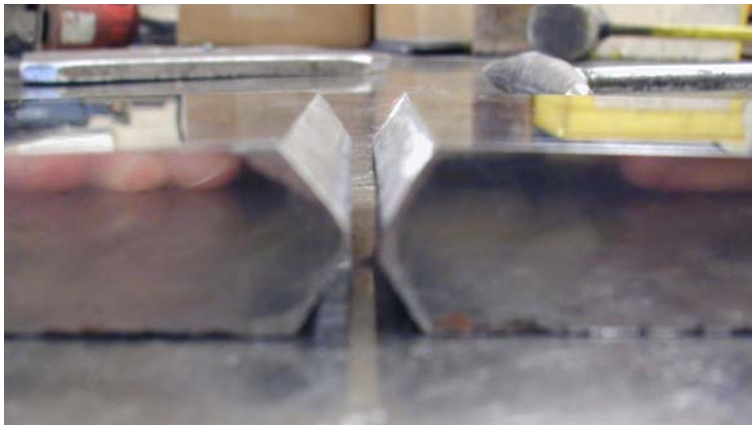

Figure C.7 Double V Butt Joint used in Welded Specimens

Figure C.8 Weld Joint Utilized in Testing After Initial Root Pass

Figure C.9 Back-grinding of Initial Root Pass before Second Weld Pass is Placed

Figure C.10 Finished Weld of Testing Specimen before Surface Grinding

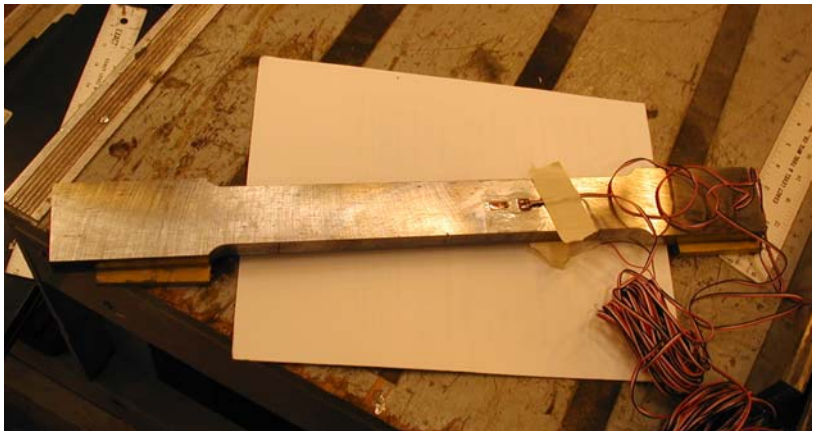

Figure C. 11 Welded Tensile Coupon Test Specimen before Testing

Figure C.12 Tensile Coupon Test Specimen from Adams Mill bridge before Testing

Figure C.13 Grips of the 220-kip MTS Four-pole Servo-Hydraulic Testing Machine

Figure C.14 Controller and Function Generator of the 220-kip MTS Four-pole Servo-Hydraulic Testing Machine Along With the Data Acquisition Center (Scanners and Computer)

Figure C.15 Tensile Coupon from Bell Ford Bridge in Grips of MTS Testing Machine before Testing

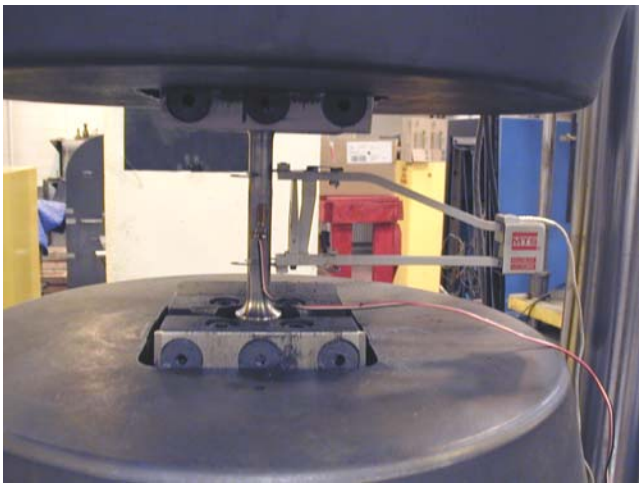

Figure C.16 Tensile Coupon from Adams Mill Bridge in Grips of MTS Testing Machine before Testing

Figure C.17 SATEC Impact Testing Machine Along with Cooling Bath Used in Charpy Impact Testing

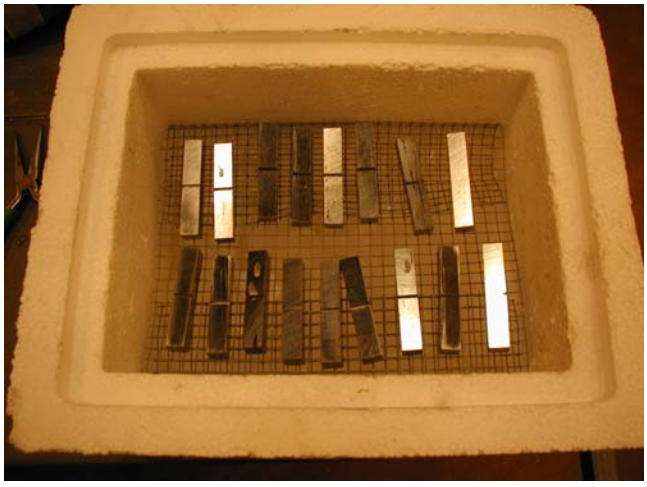

Figure C.18 Charpy Impact Specimens Suspended in Cooling Container Before Water, Ice, Dry Ice, and/or Alcohol is Added.

Figure C.19 Cooling Bath with Suspended Charpy Impact Specimens after Water and Ice is Added

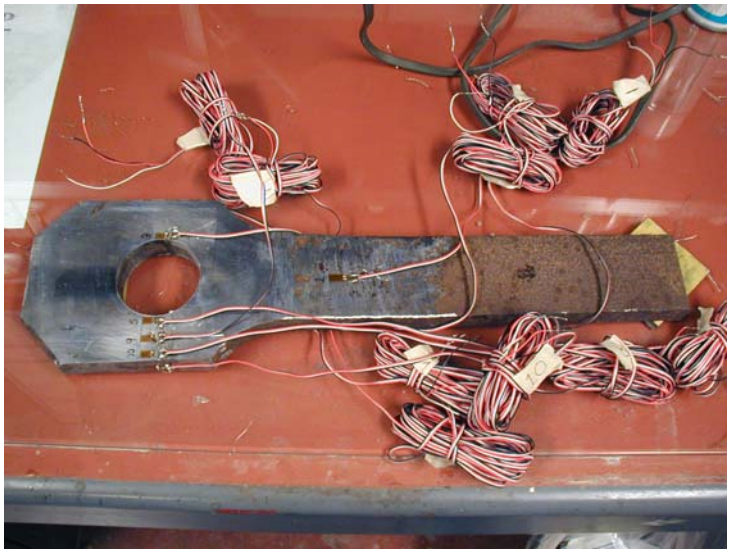

Figure C.20 Eyebar End Connection after Strain Gages were Attached

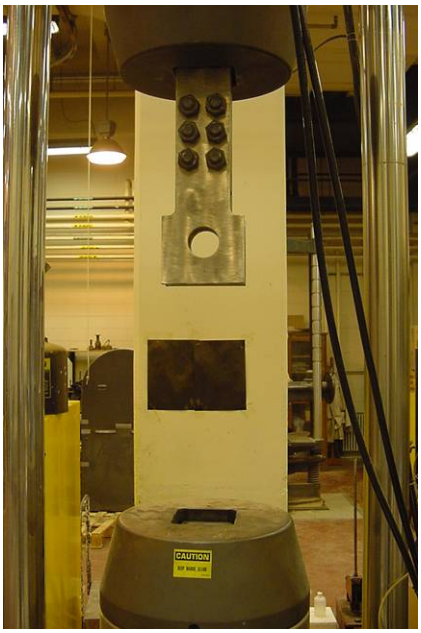

Figure C.21 Photograph of Attachment Utilized in Testing Eyebar End Connections in the 220-kip MTS Servo-Hydraulic Testing Machine

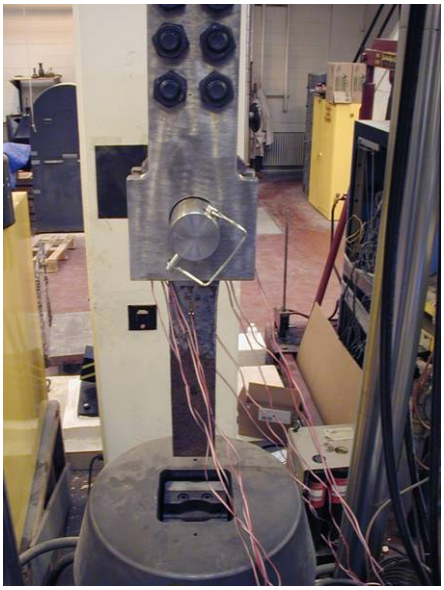

Figure C.22 View of Eyebar End Connection with Pin Inserted through the Testing Attachment.

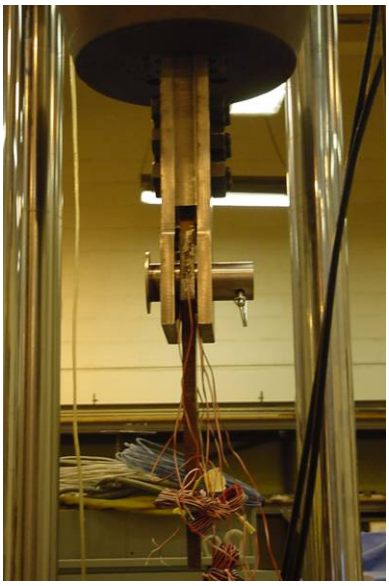

Figure C.23 Side View of Eyebar End Connection, Pin, and Test Attachment

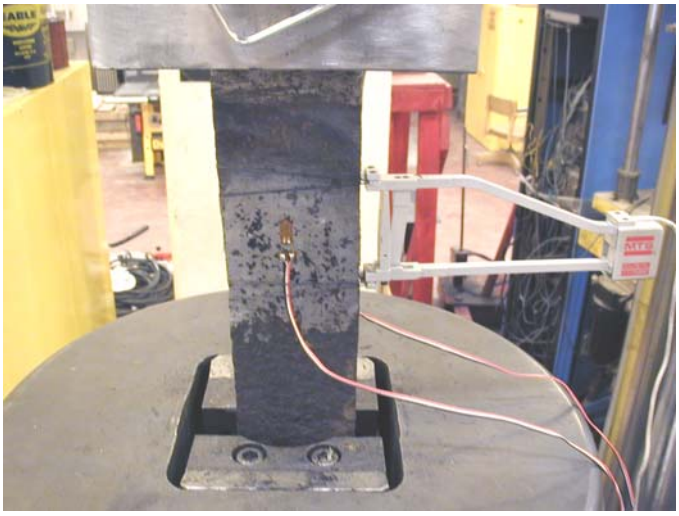

Figure C. 24 Shank of Eyebar End Connection Placed in Bottom Grip of MTS Machine with Extensometer and Strain Gages in Place

Figure C.25 Chisel Hammer to Remove Surface Slag of Filler Weld in Eyebar End Connection Repair

Figure C.26 Eyebar End Connection A after Half of Filler Weld Repair Completed

Figure C.27 Eyebar End Connection B after Half of Filler Weld Repair Completed

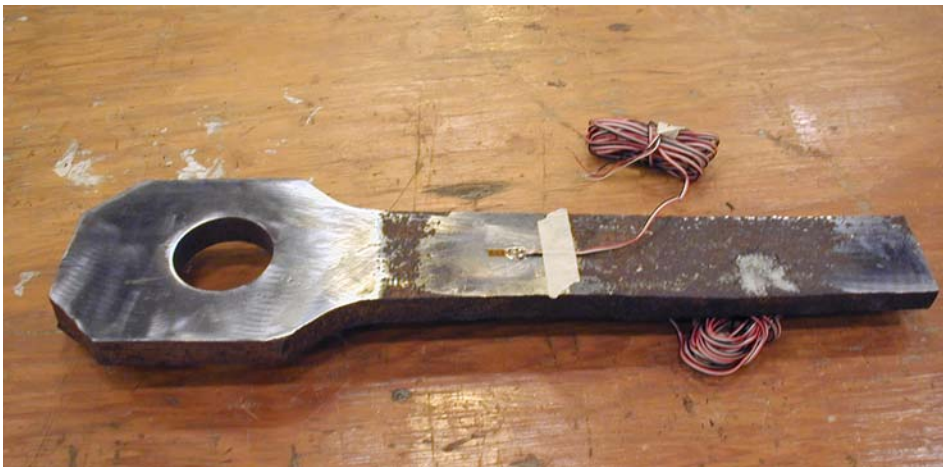

Figure C.28 Eyebar End Connection A after Filler Weld Repair and Surface Grinding Completed

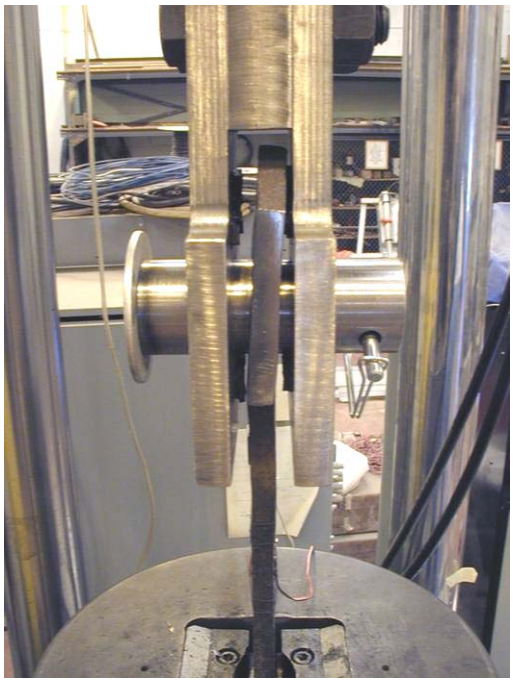

Figure C.29 Eyebar End Connection B After Being Placed in MTS Testing Machine

Appendix D. Welding Procedure for Wrought Iron Tension Members

D.1 Groove Weld with Double-V Connection Butt Joint

The following describes the step-by-step procedure for a full-penetration groove weld with a double-V butt joint to join two wrought iron plates:

1- A chemical analysis was completed to determine the weldability of the wrought iron.

2- The edges of the pieces to be welded together were ground and cleaned of all surface corrosion. A grinding wheel was used to form the double v butt joint shown in Figure D.1.

3- The wrought iron pieces were preheated to about 200 ^{o}F prior to welding.

4- An E6010 or E7018 SMAW 1/8” diameter welding rod was used to place an initial pass on the land of the joint. This was done with a current of 100 to 105 Amps for E6010 and 110-115 Amps for E7018 welding rods. The root welds were placed at a rate of approximately 3 inches per minute using a DC Reverse Polarity Miller Arc Welding Machine set on medium, which corresponded to 17-19 volts. A view of the joint after the initial weld pass can be seen in Figure D.2.

5- After the initial root pass was placed, surface slag and impurities that rose to the top of the weld, as seen in Figure D.3, were chipped off and cleaned with a chisel hammer and wire brush. A grinder was then used on the other side of the weld to grind back to the root pass, as shown in Figure D.4. This was done to ensure that full penetration was acquired in the following weld pass.

6- Passes were then added with the same E6010 or E7018 SMAW 1/8” diameter welding rod at an average rate of 3.8 in/min using the same machine, amperage and voltage as the initial pass. These passes were alternated on either side until the final pass was above the original surface of the wrought iron being welded together, as seen in Figure D.5. In between each pass the chisel hammer, wire brush and sometimes the grinder were used to remove slag that had risen to the surface of the weld.

7- The metal was also left to cool slightly in between each pass to ensure that the temperature was not too high. (This would correlate to having a maximum inter-pass temperature of 250^{o}F similar to the Filler Weld Repair.)

8- Figure D.6 shows the number and sequence of weld passes placed in each tensile test coupon.

9- After the welding was completed, the specimens were left to cool in air slowly to room temperature.

10- The specimens were then surface ground smooth until the faces were flush.

D.2 Filler Weld for Eyebar Connection Corrosion Repair

The following describes the step-by-step procedure for a filler weld repair of an eyebar member:

1- A chemical analysis was completed to determine the weldability of the wrought iron.

2- Material was removed from the eyebar connection to resemble the corrosion repair pattern being modeled. (For actual corrosion repair, the plate should be ground to solid metal remove corrosion present.)

3- The wrought iron pieces were preheated to about 200 ^{o}F prior to welding.

4- E7024 SMAW 1/8” diameter welding rod was used to place an initial pass at various locations on the eye connection. This was done with a current of around 120 to 130 Amps using a DC Reverse Polarity Miller Arc Welding Machine set on medium, which corresponded to 17-19 volts. For the eyebar with corrosion around the hole and free edge (Eyebar B), passes were initially placed around all of the edges to create a dam effect for the rest of the filler weld. For the edge corrosion repair (Eyebar A), the initial pass was placed along the edge in the long direction of the removed area. Photographs of the initial pass patterns can be seen in Figure D.7 and Figure D.8.

5- Passes were added with E7024 SMAW 1/8” diameter welding rods until the surface of the weld was above the original surface of the eyebar. In between each weld pass a chisel hammer and wire brush were used to remove the slag on the surface of the welds. The temperature was also checked using a pyrometer to ensure the base metal temperature did not exceed 250 ^{o}F, to reduce heat distortion and ease in welding.

6- Once the filler weld was completed, the eyebars were checked for heat distortion. Figure D.9 demonstrates the resulting heat distortion from the welding in Eyebar B. This eyebar was then heated using a torch until the metal reached a cherry red color (approx 1200 ^{o}F) as seen in Figure D.10. Once the eyebar was red hot, it was hammered against a hard surface to achieve the desired straightness.

7- Both eyebars were allowed to completely cool in air slowly to room temperature.

8- The weld surface was ground smooth until the faces were flush with the eyebar.

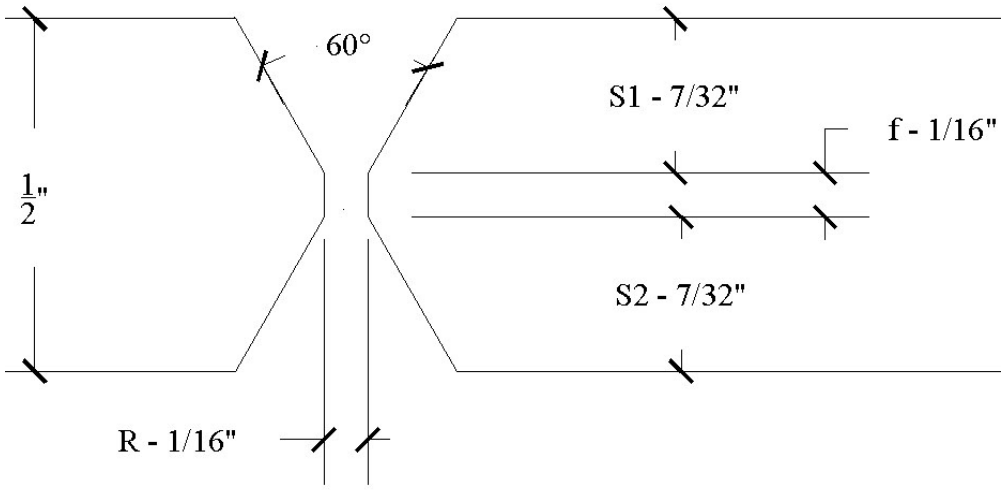

Figure D.1 Weld Joint Detail Used During Testing

Figure D.2 Weld Joint After Initial Root Pass

Figure D.3 Surface Impurities or Scale on Surface of Weld

Figure D.4 Back Grinding of the Root Weld

Figure D.5 Completed Weld Before Surface Grinding

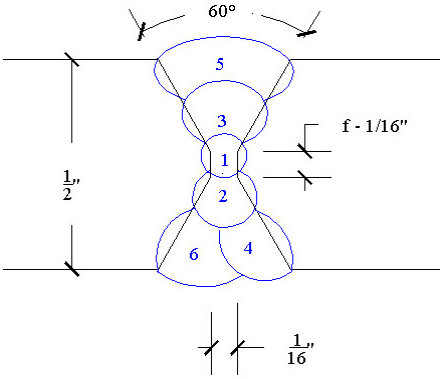

BF-E5-NH1,T
E7018 SMAW

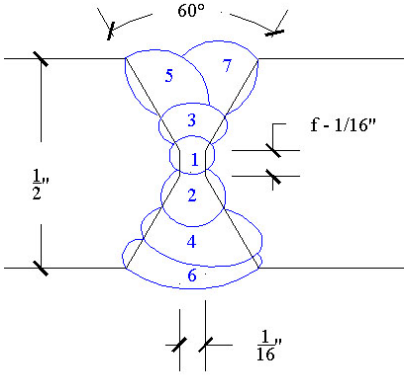

BF-E5-NH2,T
E6010 SMAW

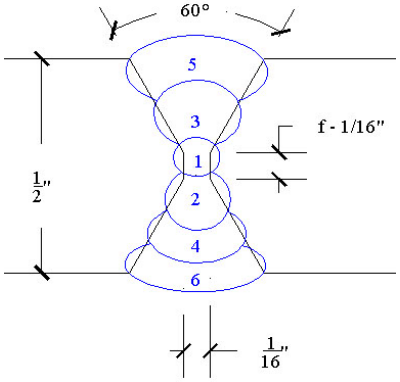

BF-E5-NH3,T
E6010 SMAW

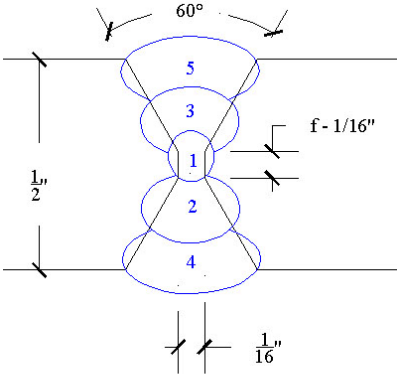

BF-E5-NH4,T
E7018 SMAW

All Electrode Size: 1/8 inch

Current: 100-105 Amps (E6010)

110-115 Amps (E7018)

Voltage: 17-19 Volts

Polarity : D.C. Reversed

Preheat: 200°F

All Welding in Flat Position

Backside of Pass 1 Ground Before Placing Pass 2

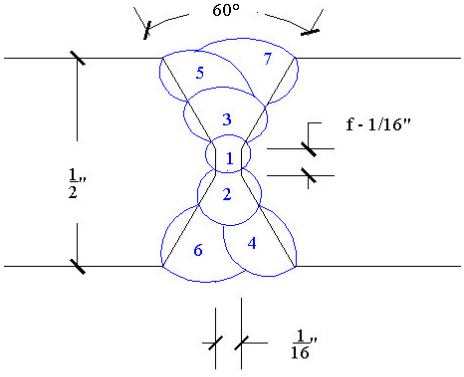

BF-E5-NH5,T
E6010 SMAW

Figure D.6 Weld Passes and Procedure Summary for Each Test Specimen

Figure D.7 Initial Pass Pattern on Eyebar B

Figure D.8 Initial Pass Pattern on Eyebar A

Figure D.9 Resulting Heat Distortion From Welding in Eyebar B

Figure D.10 Heating of Eyebar Connection B to Cherry Red Color before Straightening